



Universidade Estadual de Campinas  
Faculdade de Engenharia Química

**Tiago Albertini Balbino**

**SISTEMAS MICROFLUÍDICOS PARA A FORMAÇÃO DE NANOESTRUTURAS  
LIPOSSOMAS PARA O CARREAMENTO DE GENES**

***MICROFLUIDIC SYSTEMS FOR THE FORMATION OF LIPOSOMAL  
NANOSTRUCTURES FOR GENE CARRIER***

Campinas  
2016



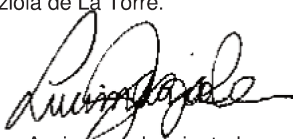
Universidade Estadual de Campinas  
Faculdade de Engenharia Química

**Tiago Albertini Balbino**

**SISTEMAS MICROFLUÍDICOS PARA A FORMAÇÃO DE NANOESTRUTURAS  
LIPOSSOMAIS PARA O CARREAMENTO DE GENES**

***MICROFLUIDIC SYSTEMS FOR THE FORMATION OF LIPOSOMAL  
NANOSTRUCTURES FOR GENE CARRIER***

Este exemplar corresponde à versão final da tese de doutorado defendida por Tiago Albertini Balbino e orientada pela Profa. Dra. Lucimara Gaziola de La Torre.



Assinatura da orientadora

Tese de Doutorado apresentada ao Programa de Pós-Graduação em Engenharia Química da Universidade Estadual de Campinas, para o btenção do título de Doutor em Engenharia Química.

*Thesis presented to the School of Chemical Engineering of the University of Campinas in partial fulfillment of the requirements for the degree of Doctor in Chemical Engineering.*

**Orientadora:** Profa. Dra. Lucimara Gaziola de La Torre

Campinas  
2016

# Ficha Catalográfica

**Agência(s) de fomento e nº(s) de processo(s):** FAPESP, 2012/23143-9 e 2013/14925-6;  
CAPES

Ficha catalográfica  
Universidade Estadual de Campinas  
Biblioteca da Área de Engenharia e Arquitetura  
Luciana Pietrosanto Milla - CRB 8/8129

B185s Balbino, Tiago Albertini, 1987-  
Sistemas microfluídicos para a formação de nanoestruturas lipossomais para o carreamento de genes / Tiago Albertini Balbino. – Campinas, SP : [s.n.], 2016.

Orientador: Lucimara Gaziola de La Torre.  
Tese (doutorado) – Universidade Estadual de Campinas, Faculdade de Engenharia Química.

1. Microfluídica. 2. Nanotecnologia. 3. Lipossomas. 4. DNA. 5. Terapia gênica. I. Torre, Lucimara Gaziola de La, 1971-. II. Universidade Estadual de Campinas. Faculdade de Engenharia Química. III. Título.

## Informações para Biblioteca Digital

**Título em outro idioma:** Microfluidic systems for the formation of liposomal nanostructures for gene carrier

### **Palavras-chave em inglês:**

Microfluidics

Nanotechnology

Liposomes

DNA

Gene therapy

**Área de concentração:** Engenharia Química

**Titulação:** Doutor em Engenharia Química

### **Banca examinadora:**

Lucimara Gaziola de La Torre [Orientador]

Eneida de Paula

Rosiane Lopes da Cunha

Antonio Augusto Malfatti Gasperini

Adriano Rodrigues Azzoni

**Data de defesa:** 29-02-2016

**Programa de Pós-Graduação:** Engenharia Química

# Folha de Aprovação

Tese de Doutorado defendida por Tiago Albertini Balbino e aprovada em 29 de Fevereiro de 2016 pela banca examinadora constituída pelos doutores:

Profa. Dra. Lucimara Gaziola de La Torre

Profa. Dra. Eneida de Paula

Profa. Dra. Rosiane Lopes da Cunha

Dr. Antonio Augusto Malfatti Gasperini

Prof. Dr. Adriano Rodrigues Azzoni

\* A Ata de Defesa, assinada pelos membros da Comissão Examinadora, consta no processo de vida acadêmica do aluno.

*À minha família*

# Agradecimentos

Agradeço à professora Lucimara Gaziola de La Torre, por quem tenho grande admiração, pela orientação sempre atenciosa ao longo desses 6 anos. Seu entusiasmo pela pesquisa e docência são inspiradores. Agradeço aos professores e pesquisadores Adriano Azzoni, Rosiane Cunha, Eneida de Paula e Antônio Gasperini, por aceitarem compor a banca avaliadora. Também aos colaboradores e colegas que contribuíram enormemente para o enriquecimento desse trabalho tornando-o tão interdisciplinar: Marcelo Bispo de Jesus, Leide Cavalcanti, Juliana Serafin, Wyattt Vreeland, Abraham Abouzeid, Antônio Gasperini, Allan Radaic e Cristiano de Oliveira.

Agradeço aos órgãos de fomento, CAPES e FAPESP (Processos 2012/23143-9 e 2013/14925-6), pelo financiamento. Ao Laboratório de Microfabricação (LMF, LNNANO, CNPEM) e aos professores Marcelo Bispo de Jesus, Rosiane Cunha, Eneida de Paula, Maria Helena Santana, Cristiano de Oliveira e Liliane Lona por terem cedido gentilmente o uso de seus laboratórios. Agradeço também aos professores do Departamento de Engenharia de Materiais e Bioprocessos, da Faculdade de Engenharia Química da Unicamp, pelo conhecimento compartilhado dentro e fora de sala de aula.

Aos meus queridos amigos, agradeço de coração tanto pelos momentos de risada quanto pelo apoio e incentivo nos momentos mais difíceis. Vocês tornam meus dias muito mais felizes e estarão sempre nas minhas lembranças. Agradeço ainda aos familiares pela torcida e por todo o carinho quando volto para casa.

Finalmente, agradeço à minha família por todos os laços de amor que nos une: meus pais, Tania e João, e minhas irmãs, Marcela e Danúbia. O apoio incondicional de vocês foi parte essencial para a realização dessa tese. Agradeço a compreensão pela distância tão grande, por todos os abraços nos aniversários que não foram dados, por não estar do lado quando alguém ficava doente, pelas ligações ruins e chamadas que acabaram com um “te amo” falhado... Eu sei que a falta pesa aí, mas queria que soubessem que a saudade por vocês é o que mais me dói aqui. Vocês sempre serão meus exemplos de vida e a fonte da minha inspiração.

A todos vocês, agradeço humildemente por terem contribuído para a concretização desse projeto.

*Porque no fundo, por mais que você leia,  
estude, pense, crie e tenha lucidez, você  
olha o mundo com os olhos de um cão,  
com o mesmo olhar assim apalermado,  
meio aguado, como os animais te olham.*

*(Hilda Hilst)*

## Resumo

A microfluídica permite a formação de diversas nanopartículas e sistemas nanocarreadores por meio da mistura controlada de correntes que escoam em canais micrométricos. Lipossomas catiônicos têm sido empregados como uma alternativa eficaz para o carregamento de material genético e diversos fármacos para aplicações biomédicas. O uso de processos microfluídicos para a formação de lipossomas e seus complexos com DNA (lipoplexos) possibilita uma redução do número de etapas em comparação a processos convencionais, permitindo ainda o desenvolvimento de processos passíveis a ampliação de escala. O presente trabalho teve como objetivo o desenvolvimento de plataformas microfluídicas de fluxo contínuo para a obtenção de vetores não-virais baseados em lipossomas catiônicos e DNA plasmidial (pDNA) e suas aplicações em terapia gênica. Inicialmente, um dispositivo microfluídico de focalização hidrodinâmica foi empregado na complexação entre pDNA e lipossomas para a formação de lipoplexos. Em condições de alto carregamento de pDNA, as propriedades físico-químicas e estruturais de lipoplexos obtidos pelo processo microfluídico resultaram em respostas biológicas mais eficientes que aqueles obtidos pelo processo convencional “bulk”. Em seguida, regiões de focalização hidrodinâmica foram associadas em série e em pseudo-paralelo para a formação de lipossomas com maior produtividade por dispositivo. Em ambas configurações, foi possível preparar lipossomas protegidos estericamente pelo polímero polietilenoglicol (PEG), os quais apresentaram propriedades adequadas para aplicações em terapia gênica. Por fim, utilizando focalizações hidrodinâmicas consecutivas, foi possível desenvolver um dispositivo microfluídico com duas regiões distintas para a formação de lipossomas e a posterior complexação com pDNA em dispositivo único. Assim, com este trabalho foi possível aprimorar e desenvolver processos microfluídicos para a formação de lipossomas e de lipoplexos com redução significativa do número de etapas, contribuindo para a viabilização de nanocarreadores de material genético destinados a aplicações na área biomédica.

**Palavras chave:** microfluídica, nanotecnologia, lipossomas, DNA, terapia gênica.

# Abstract

Microfluidics allows the formation of a variety of nanoparticles and nanocarriers systems via controlled mixing of streams that flow within micro-sized channels. Cationic liposomes have been employed as an efficient alternative for the delivery of genetic material and therapeutic drugs for biomedical applications. The use of microfluidic processes for the formation of liposomes and their complexes with DNA (lipoplexes) enables the reduction of the number of steps compared to conventional processes, allowing the development of processes liable to scale amplification. The present work aimed at the development of continuous-flow microfluidic platforms to generate nonviral vectors based on cationic liposomes and plasmid DNA (pDNA) and their applications in gene therapy. Firstly, a microfluidic device based on the hydrodynamic flow-focusing technique was employed to form electrostatic complexes between pDNA and liposomes for the formation of lipoplexes. Under high pDNA loading conditions, physicochemical and structural properties of lipoplexes obtained in the microfluidic process resulted in more efficient biological assays than those obtained via conventional bulk process. Next, flow-focusing regions were associated in series and pseudo-parallel architectures for the formation of liposomes with higher productivity per device. In both architectures, it was possible to obtain liposomes with a protective and steric shield provided by poly(ethylene glycol) (PEG), whose properties were appropriate for gene therapy applications. Lastly, using consecutives flow-focusing regions, a microfluidic device was developed with two distinct regions for the formation of liposomes and lipoplexes with significantly reduced number of steps, contributing to the advances of gene nanocarriers for biomedical applications.

**Keywords:** microfluidics, nanotechnology, liposomes, DNA, gene therapy.

# Lista de Ilustrações

## Capítulo 2

Figura 2.1. Esquema hipotético da formação de lipossomas em microcanais através da técnica da focalização hidrodinâmica (adaptado de Balbino *et al.* (34)). ..... 30

Figura 2.2. Dispositivo microfluídico simples (A) e com barreiras nos microcanais (B). Diagrama esquemático do aparato experimental utilizando o dispositivo com barreiras nos microcanais (C), e do mecanismo hipotético de formação dos complexos pDNA/lipossomas catiônicos utilizando processo microfluídico (D) (adaptado de Balbino *et al.* (41)). ..... 32

## Capítulo 3

Figure 3.1. Schematic of the microfluidic device for continuous lipoplex assembly ..... 39

Figure 3.2. Physicochemical properties of plasmid DNA (pDNA)/cationic liposome (CL) lipoplexes prepared by bulk-mixing (BM) and microfluidic processes..... 45

Figure 3.3. Plasmid DNA (pDNA) incorporation into liposomal structure. (a) Gel retardation assay, (b) resistance to DNase I at  $R_{\pm} 1.5$ , and (c) accessibility to the fluorescence probe for pDNA/cationic liposome lipoplexes assembled by bulk-mixing and microfluidic methods..... 46

Figure 3.4. Nanostructural SAXS scattering intensities of liposomes and lipoplexes assembled by microfluidic and bulk-mixing processes for systems with a varying molar charge ratio ( $R_{\pm}$ )..... 48

Figure 3.5. Parameters obtained from a simultaneous fitting of the SAXS scattering intensities. (a) Average number of correlated bilayers (N) as a function of the molar charge ratio ( $R_{\pm}$ ). (b) Multilamellar phase fraction and bilayer thickness of lipoplexes assembled by bulk-mixing and microfluidic processes..... 49

Figure 3.6. Schematic representation of the electrostatic assembly of plasmid DNA and cationic liposomes via bulk-mixing (BM) and microfluidic processes. .... 51

Figure 3.7. *In vitro* gene delivery evaluation of lipoplexes. Transfection of plasmid DNA (pDNA)/cationic liposome lipoplexes assembled by microfluidic and bulk-mixing processes into PC3 cancer cells ..... 53

## Capítulo 4

Figure 4.1. Schematic illustration of “stealth” liposome sterically functionalized with hydrophilic polymer (surrounding green area) for targeted delivery..... 56

Figure 4.2. Microfluidic geometries used for liposome synthesis. (a) single, (b) series and (c) pseudo-parallel hydrodynamic focusing configurations ..... **59**

Figure 4.3. (a) Schematic representation of the asymmetric flow field-flow fractionation (AF4) theory. (b) Schematic representation of particle size distribution along the separation channel, during the sample fractionation according to the flow velocity profile. (c) Equipment apparatus of the AF4 system coupled to the MALLS instrument (Images Copyright: Wyatt Technology Europe GmbH). ..... **61**

Figure 4.4. Single hydrodynamic flow-focusing microfluidic device (a) PEGylated-liposome size distributions at varying flow rate ratios (FRRs). (b) Geometric radius of PEGylated liposomes formed in the absence of ethanol and with the addition of ethanol in the aqueous phase, and non-PEGylated liposomes. (c) Size polydispersity of PEGylated liposomes with and with no ethanol, at a lipid concentration of 25 mM..... **63**

Figure 4.5. Intensity chromatograms of fractionated particles using AF4-MALS techniques. PEGylated liposomes produced at varying FRR conditions, in the absence of ethanol (a) and in the presence of ethanol as additive in the aqueous phase (b), using the single microfluidic arrangement ..... **65**

Figure 4.6. Intensity chromatograms of fractionated particles using AF4-MALS techniques. PEG-conjugated liposomes produced using the series configuration at varying FRR conditions at lipid concentration in the lipid stream of (a) 5 mM and (b) 25 mM..... **67**

Figure 4.7. Series hydrodynamic flow-focusing microfluidic device. Geometric radius of PEGylated-liposome using the series configuration at lipid concentration in the ethanol stream ( $C_{LIP}$ ) of (a) 5 mM, and (b) 25 mM. .... **69**

Figure 4.8. Intensity chromatograms of fractionated particles using asymmetric flow-field flow fractionation (AF4) and multiangle laser light scattering techniques. PEG-conjugated liposomes produced using the parallel configuration at varying FRR conditions at lipid concentration in the lipid stream of (a) 5 mM and (b) 25 mM..... **70**

Figure 4.9. Parallel hydrodynamic flow-focusing microfluidic device. Geometric radius distribution of PEGylated-liposome using the series configuration at lipid concentration in the ethanol streams ( $C_{LIP}$ ) of (a) 5 mM, and (b) 25 mM. .... **71**

Figure 4.10. Comparison of microfluidic devices with Single, Series and Pseudo-Parallel arrangements. (a) Geometric radius and (b) Polydispersity of PEGylated-liposome as a function of flow-rate ratio (FRR) at lipid concentration in the ethanol streams ( $C_{LIP}$ ) of 25 mM. **73**

## Capítulo 5

Figure 5.1. Schematic representation of the microfluidic devices for one-step formation of plasmid DNA (pDNA)/cationic liposome (CL) lipoplexes ..... **78**

Figure 5.2. (a) Hydrodynamic diameter weighted by intensity and (b) polydispersity index of liposomes (CL) and lipoplexes obtained by the microfluidic device as a function of the flow rate ratio (FRR).....	85
Figure 5.4. Effects of molar charge ratio ( $R_{\pm}$ ) on hydrodynamic diameter of lipoplexes generated by the two-stage microfluidic configuration.....	86
Figure 5.5. Electrophoretic mobility retardation assay. Lipoplexes were generated by the microfluidic device with two-stage configuration.....	87
Figure 5.6. Transmission electron microscopy (TEM) images of (a and b) “pure” liposomes and (c and d) lipoplexes prepared by the two-stage microfluidic device .....	88
Figure 5.7. Cell viability assay on (a) prostate cancer cells (PC3) and (b) human cervical cancer (HeLa) cells of lipoplexes obtained by bulk and microfluidic processes .....	89
Figure 5.1S. (a) Representation of the one-stage microfluidic device for the formation of lipoplexes with a single hydrodynamic flow-focusing region, at lipid concentration in the central stream of (b) 6.5 mM and (c) 12 mM. ....	91
Figure 5.2S. Hydrodynamic diameter (square symbols) and polydispersity index (circle symbols) of lipoplexes generated by the one-stage microfluidic device as a functions of (a) Flow Rate Ratio (FRR) and (b) Total volumetric rate ( $Q_T$ ) .....	92

## Capítulo 7

Figura 7.1. Figura ilustrativa dos lipossomas funcionalizados com lipídeos contendo o polímero polietilenoglicol e peptídeos com sequência RGD.....	97
---	----

## Lista de Abreviaturas e Siglas

AF4	Fracionamento por campo de fluxo assimétrico (do inglês, <i>asymmetric flow field-flow fractionation</i> )
BM	Mistura tipo batelada (do inglês, <i>bulk mixing</i> )
C <sub>DNA</sub>	Concentração da solução plasmidial
CL	Lipossomas Catiônicos
C <sub>LIP</sub>	Concentração lipídica na dispersão em etanol
CMC	Concentração micelar crítica
DLS	Espalhamento Dinâmico de Luz (do inglês, <i>Dynamic Light Scattering</i> )
DNA	Ácido desoxirribonucleico
DOPE	L- $\alpha$ -dioleoil fosfatidiletanolamina
DOTAP	1,2-dioleoil -3-trimetilamônio-propano
dspDNA	DNA plasmidial de fita dupla
EGFP	Proteína verde fluorescente melhorada (do inglês, <i>enhanced green fluorescent protein</i> )
EPC	L- $\alpha$ -fosfatidilcolina de ovo
EtBr	Brometo de etídio
FACS	Avaliação da emissão de fluorescência das células (do inglês, <i>Fluorescence-Activated Cell Sorting</i> )
f <sub>mb</sub>	Fração de bicamadas múltiplas
FRR	Razão entre vazões (do inglês, <i>Flow Rate Ratio</i> )
FRR <sub>1</sub> ou 2	FRR da primeira ou segunda região do dispositivo de dois estágios
f <sub>sb</sub>	Fração de bicamadas únicas
HeLa	Do inglês, <i>Human ephitelial carcinoma</i>
HFF	Focalização hidrodinâmica (do inglês, <i>hydrodynamic flow-focusing</i> )
I	Intensidade de Espalhamento
LC	Lipossoma catiônicos
LF2K	Lipofectamina 2000
MALS	Espalhamento de luz multiângulos
N	Número de bicamadas

P	Fator de forma
PC3	Do inglês, <i>prostate cancer cell line</i>
PdI	Índice de polidispersidade (do inglês, <i>polydispersity index</i> )
PDMS	Polidimetilsiloxano
pDNA	DNA plasmidial
PE	Fosfatidiletanolamina
PEG	Polietilenoglicol
PEG-PE	<i>1,2-dimyristoyl-sn-glycero-3-phosphoethanolamine-N-[methoxy (polyethylene glycol)-5000] (PEG-PE)</i>
q	Módulo do vetor de espalhamento
Q <sub>DNA</sub>	Vazão volumétrica da corrente contendo o pDNA
QELS	Espalhamento quase elástico de luz (do inglês, <i>quasi elastic light scattering</i> )
Q <sub>T</sub>	Vazão volumétrica total
Q <sub>T1</sub>	Q <sub>T</sub> da primeira região do dispositivo de dois estágios
Q <sub>Total</sub>	Soma das vazões de todas as correntes da primeira região com a vazão de DNA na segunda região
Q <sub>w</sub>	Vazão volumétrica da corrente de água ultrapura
R	Raio geométrico
R <sub>±</sub>	Razão molar de cargas. Relação entre moles de cargas positivas de lipídios catiônicos e cargas negativas do material genético
RNA	Ácido ribonucleico
SAXS	Espalhamento de raio X a baixo ângulo (do inglês, <i>small angle X-ray scattering</i> )
SD	Desvio padrão
S <sub>eff</sub>	Fator de estrutura efetivo
S <sub>MCT</sub>	Fator de estrutura modificado de <i>Caillé</i>
TEM	Microscopia de transmissão eletrônica
ζ	Potencial Zeta.

# Sumário

<b>1. Introdução Geral .....</b>	<b>18</b>
1.1. Introdução.....	18
1.2. Objetivos.....	19
1.3. Apresentação da Tese .....	21
 <b>2. Revisão Bibliográfica .....</b>	<b>24</b>
2.1. Terapia Gênica .....	24
2.2. Lipossomas catiônicos.....	25
2.3. Complexação eletrostática entre carreadores catiônicos e pDNA .....	27
2.4. Microfluídica.....	27
2.5. Microfluidica e a formação de lipossomas.....	29
2.6. Sistemas microfluídicos para complexação eletrostática entre carreador catiônico e material genético .....	30
 <b>3. Microfluidic assembly of pDNA/cationic liposome lipoplexes with high pDNA loading for gene delivery.....</b>	<b>34</b>
3.1. Abstract .....	34
3.2. Introduction .....	35
3.3. Experimental Procedure.....	38
3.3.1. Microfluidic device .....	38
3.3.2. Preparation of liposomes .....	39
3.3.3. Plasmid amplification .....	40
3.3.4. pDNA/CL lipoplex formation.....	40
3.3.5. Zeta potential ( $\xi$ ) and size measurements.....	41
3.3.6. pDNA accessibility .....	41
3.3.7. Agarose gel electrophoresis .....	41
3.3.8. DNase I protection assay.....	41
3.3.9. SAXS studies.....	42
3.3.10. Transfection Protocol.....	42
3.3.11. Statistical analysis .....	43
3.4. Results and Discussion.....	43
3.4.1. Microfluidic process provided the assembly of lipoplexes with better physicochemical properties than bulk mixing .....	43
3.4.2. Nanostructural analysis by SAXS .....	47
3.4.3. Microfluidic-assembled lipoplexes achieved higher gene delivery efficiency under high pDNA loading conditions.....	51

3.5. Conclusion .....	54
3.6. Acknowledgments .....	54

#### **4. Effects of series and pseudo-parallel microfluidic arrangements for the synthesis of long-circulating liposomes decorated with PEG .....**

4.1. Abstract .....	55
4.2. Introduction .....	56
4.3. Experimental .....	58
4.3.1. Microfluidic Device Fabrication .....	58
4.3.2. Liposome preparation .....	59
4.3.3. Asymmetric Flow Field-Flow Fractionation (AF4) with Multi-Angle Laser Light Scattering (MALLS) and Quasi-Elastic Light Scattering (QELS) .....	60
4.4. Results and Discussion .....	62
4.4.1. Effects of FRR, PEG-PE lipid and ethanol using the single MHF architecture .....	62
4.4.2. Formation of liposomes using the series configuration .....	65
4.4.3. Formation of liposomes using the parallel configuration .....	69
4.4.4. Comparison of Series and Pseudo-Parallel configurations .....	71
4.5. Conclusion .....	73

#### **5. One-step formation of nanoscale liposomes and lipoplexes using microfluidic devices .....**

5.1. Abstract .....	74
5.2. Introduction .....	75
5.3. Experimental .....	77
5.3.1. Microfluidic Device .....	77
5.3.2 Plasmid Amplification and Purification .....	77
5.3.3. Preparation of liposomes .....	78
5.3.4. Preparation of lipoplexes .....	79
5.3.5. Zeta potential and size measurements .....	80
5.3.6. Agarose gel electrophoresis .....	81
5.3.7. Transmission Electron Microscopy .....	81
5.3.8. Transfection Protocol and Cytotoxicity .....	81
5.3.9. Statistical analysis .....	82
5.4. Results and Discussion .....	82
5.4.1. Mixing behavior of the two-stage microfluidic configuration .....	83
5.4.2. Effects of Flow Rate-Ratio ( $FRR_1$ ) and Volumetric Flow Rate ( $Q_{T1}$ ) in the first region on Liposome and Lipoplex Size .....	84
5.4.3. Effects of pDNA Content on Lipoplex Size .....	85
5.4.4. pDNA-retaining ability and morphology of lipoplexes .....	87
5.4.5. In vitro evaluation of cytotoxicity and transfection efficacy of lipoplexes .....	88

5.5. Conclusions .....	90
5.6. Acknowledgments .....	90
5.7. Supplementary information .....	91
 <b>6. Conclusões .....</b>	 <b>94</b>
 <b>7. Perspectivas de Trabalhos Futuros.....</b>	 <b>96</b>
7.1. Formação de complexos pseudo-ternários multifuncionais .....	96
7.2. Formação de lipossomas com peptídeos ancorados na superfície .....	97
7.3. Estudos biológicos de lipoplexos obtidos por dispositivos microfluídicos .....	98
7.4. Estudos de fluidodinâmica computacional de configurações microfluídicas .....	99
 <b>8. Referências .....</b>	 <b>101</b>
 <b>Anexo I. Licença de publicação de artigo na tese .....</b>	 <b>109</b>

# 1. Introdução Geral

## 1.1. Introdução

A ideia de se realizar o tratamento de determinadas doenças através da inserção de um gene terapêutico no organismo de indivíduos foi reportada pela primeira vez no começo da década de 70 (1). Desde então, estudos na área de terapia gênica têm recebido grande atenção principalmente no que tange ao desenvolvimento de sistemas carreadores de material genético através da nanotecnologia (2). Estima-se que o mercado multidisciplinar de terapia gênica movimente mais de 10 bilhões de dólares até o ano de 2025 (3).

A terapia gênica se baseia na introdução de material genético em células alvo a fim de substituir genes defeituosos, inserir genes específicos ou silenciar determinadas expressões gênicas (4). Entretanto, é necessário que o material genético seja transportado por veículos de entrega, uma vez que, por si só, não é capaz de adentrar as células de forma eficiente. Para isso, diversos carreadores não-virais têm sido empregados como alternativas mais seguras, simples e de menor custo em comparação aos vetores virais. Dentre os carreadores nanoestruturados não-virais, os lipossomas catiônicos (LCs) se tornaram uma das estratégias mais populares para o carregamento de genes (5).

Lipossomas são estruturas lipídicas de dimensões coloidais com cerne aquoso circundado por uma ou mais bicamadas lamelares. Devido às suas características intrínsecas, os lipossomas podem encapsular agentes hidrofílicos em seu cerne aquoso e reter compostos hidrofóbicos dentro de suas bicamadas. Ainda possibilitam a formação de complexos eletrostáticos com material genético e podem sofrer modificações superficiais para entregas sítio-específica, ancorando moléculas de caráter anfifílico (6). Comumente, processos convencionais para a produção de lipossomas formam primeiramente vesículas de grandes diâmetros, multilamelares e alta polidispersidade que requerem etapas posteriores para a redução e homogeneização de tamanho. Por exemplo, o processo *bulk* mais utilizado para aplicações em terapia gênica, que se baseia na hidratação de filme lipídico seguido por extrusões múltiplas em membranas, requer uma série de operações manuais descontínuas e laboriosas.

Para aplicações em terapia gênica, o uso de lipídeos catiônicos permite a formação de LCs e posteriormente lipoplexos, obtidos através de interações eletrostáticas com o material genético negativamente carregado, que, por sua vez, permite a condensação e o

carreamento de genes às células (7). Os lipoplexos podem apresentar diferentes características físico-químicas, estruturais e biológicas dependendo de diversos fatores, como a composição lipídica, a força iônica do meio de complexação, a ordem e o tipo de mistura, concentrações das soluções e proporção entre carreador e material genético. A formação dos lipoplexos pelo processo convencional *bulk* se dá através da mistura manual entre os LCs e o material genético por simples pipetagem ou sistema de vórtice, através da interação eletrostática entre cargas positivas e negativas. Entretanto, sob determinadas condições, esses processos podem gerar lipoplexos com características inadequadas para ensaios biológicos, principalmente devido à mistura heterogênea e sem controle das linhas de fluxo, além de não permitirem que a produção volumétrica seja amplificada e automatizada.

Recentemente, em virtude dos avanços na microfabricação, plataformas microfluídicas têm recebido crescente atenção para a formação de lipossomas e complexação de lipoplexos. Sistemas microfluídicos operam pequenas quantidades de fluidos dentro de canais micrométricos, onde a mistura das correntes ocorre sob escoamento laminar por difusão molecular, proporcionando ambientes em que os fenômenos de transferência de massa ocorrem de forma constante e reproduzível (8,9). Para o preparo de lipossomas e lipoplexos, os processos microfluídicos não só permitem a formação de nanocarreadores monodispersos, como também possibilitam que diversas etapas sequenciais sejam integradas, reduzindo drasticamente o número de etapas normalmente necessárias em processos convencionais. Neste contexto, essas plataformas de tamanhos miniaturizados se apresentam como estratégias promissoras para o desenvolvimento de processos que incorporem diversas etapas em dispositivo microfluídico único e que possam contribuir para a viabilização de produtos farmacêuticos destinados a aplicações biomédicas.

## **1.2. Objetivos**

Com esse trabalho, pretende-se contribuir na área da nanotecnologia, mais especificamente para o desenvolvimento de processos destinados a aplicações biomédicas, e na área de microfluídica, para produção de sistemas nanocarreadores de material genético. Para isso, o objetivo principal foi desenvolver processos microfluídicos para a produção de nanocarreadores de genes baseados em lipossomas catiônicos, a fim de obter processos com reduzido número de etapas e passíveis de amplificação de escala ou aplicações futuras para medicina personalizada. Para alcançar estes resultados, intentou-se

investigar processos de formação de lipossomas e de lipoplexos em dispositivos microfluídicos de fluxo contínuo baseados na técnica de focalização hidrodinâmica e compará-los ao processo convencional *bulk* (modelo reator batelada). Dessa forma, a pesquisa foi estruturada a partir de três metas principais:

- Complexação entre lipossomas catiônicos e pDNA em dispositivo microfluídico: Os lipoplexos de pDNA/LC foram formados em dispositivo de focalização hidrodinâmica única e comparados aos obtidos pelo processo “bulk”. Os lipoplexos foram caracterizados quanto às propriedades mesoscópicas a fim de embasar discussões sobre os fenômenos coloidais envolvidos na complexação eletrostática, quando realizada em diferentes processos de mistura, e seus efeitos em ensaios biológicos *in vitro*.
- Desenvolvimento de dispositivos microfluídicos de focalização hidrodinâmica para a formação de lipossomas: Diferentes arranjos microfluídicos foram explorados para a formação de lipossomas com características adequadas para aplicações em terapia gênica. Para tal, regiões de focalização hidrodinâmica foram associadas em série e em paralelo afim de aumentar a eficiência de produção por dispositivo. De forma complementar, avaliou-se a formação de lipossomas com a incorporação de lipídeos derivatizados contendo em sua estrutura polietilenoglicol (PEG), formando lipossomas com tempos prolongados de circulação. Esses lipossomas permitirão estudos futuros de acoplamento de moléculas para o direcionamento a células específicas.
- Dispositivos microfluídicos para a formação de lipossomas e lipoplexos em etapa única: A fim de otimizar a produção de lipoplexos reduzindo substancialmente o número de etapas, foi desenvolvido um dispositivo com duas regiões distintas de focalização hidrodinâmica associadas em série. Assim, os lipossomas catiônicos são formados numa primeira região para posteriormente serem complexados com pDNA numa segunda região.

### 1.3. Apresentação da Tese

Neste trabalho, os estudos decorrentes das pesquisas realizadas em cada uma das etapas estabelecidas são estruturados na forma de capítulos. Os avanços nas áreas de microfluídica e nanobiotecnologia são apresentados a seguir na forma de artigos que foram publicados ou serão submetidos a periódicos internacionais, selecionados quanto ao impacto das descobertas e contribuições obtidas, bem como quanto à afinidade do conteúdo abordado. Dessa forma, os itens introdução, metodologia, resultados, discussão e conclusões de cada parte constam nos artigos em seus respectivos capítulos. É importante ressaltar que os capítulos com resultados inéditos apresentam ainda uma revisão mais breve, porém mais detalhada e específica, de acordo com o contexto em que os artigos elaborados se inserem.

No Capítulo 2, *Revisão Bibliográfica*, são abordados os aspectos teóricos quanto ao Estado da Arte no âmbito em que essa pesquisa se insere. De modo geral, os avanços referentes aos estudos de sistemas lipossomais para a aplicações em terapia gênica tem possibilitado o tratamento de diversas doenças. Entretanto, processos convencionais podem apresentar limitações na transposição desses estudos em escala laboratorial para testes *in vivo* e ensaios clínicos. Neste contexto, as alternativas possíveis encontradas na literatura que utilizam plataformas microfluídicas para contornar tais adversidades são apresentadas e discutidas.

No Capítulo 3, intitulado *Microfluidic assembly of pDNA/cationic liposome lipoplexes with high pDNA loading for gene delivery*, a formação de lipoplexos formados entre lipossomas catiônicos e pDNA foi realizada em dispositivos de focalização hidrodinâmica e comparados aos obtidos pelo processo convencional *bulk*. Ambos processos geraram lipoplexos eficientes em reter o pDNA nas estruturas lipossomais e protegê-lo contra a degradação enzimática, nas condições estudadas. A caracterização físico-química, realizada por espalhamento dinâmico de luz (DLS), aliada à estrutural, realizada por espalhamento de raios-x a baixo ângulo (SAXS), mostrou que os lipoplexos obtidos por dispositivos microfluídicos apresentaram propriedades significativamente distintas somente em condições de alto carregamento de pDNA. Utilizando um modelo otimizado com número de variáveis reduzido para o tratamento dos dados de SAXS, foi identificado que altas proporções de pDNA induzem a formação de lipoplexos com maior número de bicamadas sobrepostas (aproximadamente 5) utilizando o método *bulk*, enquanto lipoplexos obtidos

pelo dispositivo microfluídico apresentaram  $N$  médio de 2,5. Ensaio de internalização celular e transfecção *in vitro* mostraram que os dispositivos microfluídicos produziram lipoplexos com características mais adequadas para entrega gênica em altas proporções de pDNA, com transfecções mais eficientes em células de câncer de próstata. De modo geral, nessa etapa, a correlação encontrada entre as características mesoscópicas e a performance *in vitro* dos lipoplexos contribui para a elucidação dos fenômenos coloidais envolvidos na formação dos complexos eletrostáticos e seus efeitos no comportamento biológico *in vitro*, empregando diferentes métodos de mistura. O manuscrito foi publicado na revista *Langmuir* e os direitos são reservados a *American Chemical Society*, com permissão para publicação integral na presente tese de doutorado.

O Capítulo 4, por sua vez, sob o título de *Effects of series and pseudo-parallel microfluidic arrangements for the synthesis of long-circulating liposomes decorated with PEG*, explorou o emprego de associações em série e pseudo-paralelo de regiões de focalização hidrodinâmica para a produção de lipossomas conjugados ou não com polietilenoglicol (PEG). O uso de fosfolipídios derivatizados com PEG confere aos lipossomas uma proteção estérica que prolonga o tempo de circulação quando administrados sistemicamente. As arquiteturas microfluídicas com associações em série e pseudo-paralelo foram investigadas a fim de elucidar fenomenologicamente os efeitos das geometrias na formação de lipossomas derivatizados com PEG, visando aumentar a concentração das formulações finais para futuros estudos de melhoria de produtividade. Ambas configurações foram capazes de produzir lipossomas com diâmetros e polidispersidade apropriados para futuras aplicações em terapia gênica. Entretanto, a associação em pseudo-paralelo gerou lipossomas com características físico-químicas mais adequadas e menor polidispersidade, minimizando os efeitos ocasionados pela presença do etanol na autoagregação dos lipídeos.

Já o Capítulo 5, *One-step formation of nanoscale liposomes and their lipoplexes via microfluidic devices for gene delivery*, versa sobre o desenvolvimento de plataformas microfluídicas para a formação de lipoplexos formados entre lipossomas catiônicos e pDNA em dispositivo único. Um dispositivo microfluídico com duas regiões distintas foi investigado para a formação de lipossomas e a subsequente complexação com pDNA, formando então lipoplexos. Os lipoplexos obtidos exibiram características físico-químicas apropriadas para aplicações em terapia gênica e capazes de reter e condensar o material genético nas estruturas. Os experimentos biológicos realizados em diferentes linhagens celulares evidenciaram a viabilidade do dispositivo em produzir lipoplexos de forma satisfatória, cujos

níveis de transfecção foram similares aqueles obtidos por lipoplexos produzidos em processos convencionais, os quais requerem diversas operações manuais consecutivas. A plataforma microfluídica integrada permite o preparo de lipoplexos através da formação de lipossomas combinada sequencialmente à complexação com material genético, reduzindo significativamente o número de etapas necessárias para se produzir sistemas carreadores de genes.

Por fim, a tese se encerra com as *Conclusões Gerais e Sugestões para Trabalhos Futuros*, em que são discutidas as principais conclusões decorrentes dos avanços proporcionados com os resultados obtidos, assim como as perspectivas que surgiram durante os estudos da pesquisa de doutorado e que são propostas como continuação de trabalhos futuros.

## 2. Revisão Bibliográfica

### 2.1. Terapia Gênica

A terapia gênica é uma técnica baseada na introdução de material genético às células, que visa a correção ou inativação dos genes responsáveis por uma doença específica ou ainda a produção de determinada proteína pela própria célula (1,10). Para que se viabilize o efeito projetado neste material genético, como, por exemplo, em um DNA plasmidial (pDNA) que codifica uma proteína terapêutica, este DNA deve vencer várias barreiras intra e extracelulares para alcançar o núcleo celular e utilizar a própria célula para a síntese da molécula de interesse. Este processo é denominado de transfecção. Entretanto, a instabilidade química do material genético, a rápida degradação enzimática nos fluidos corpóreos e seu tamanho elevado geram uma grande dificuldade nas aplicações *in vitro* e *in vivo*, dificultando o processo de transfecção (11).

Nesse sentido, vários grupos de pesquisa têm estudado o efeito de diferentes tipos de carreadores, intentando obter proteção para o pDNA e aumentar sua eficiência de transfecção. Sistemas virais de entrega gênica, tais como adenovírus, são uma importante alternativa que promove altos níveis de transfecção; porém, além de serem dispendiosos e de alto custo, em casos raros, os vetores virais podem apresentar efeitos oncogênicos (12). Outra alternativa potencial é o uso de sistemas não-virais, baseados, por exemplo, no emprego de proteínas, polímeros catiônicos ou lipídeos de natureza catiônica para formarem um complexo com o ácido nucleico e permitirem a proteção e entrada destes nas células. Estes sistemas apresentam menores níveis de transfecção quando comparados com os sistemas virais, por não possuírem a mesma especialização, porém são mais seguros, de fácil manuseio e passíveis de aumento de escala (13).

Com o emprego de sistemas não-virais, diversos fatores físico-químicos e de condições de cultura, no caso de estudos *in vitro*, podem influenciar na eficiência de transfecção. Dentre os parâmetros físico-químicos, podem-se citar o diâmetro dos complexos e distribuição de tamanhos, densidade de carga da superfície, razão molar de cargas entre carreador e material genético e a condensação do material genético nas estruturas. Já nas condições de transfecção, podem-se citar a natureza e citotoxicidade do carreador, condições de cultura *in vitro*, tempo de transfecção, linhagem celular empregada (14,15), e forma de administração, nos casos de estudos *in vivo* (16). Dentre os sistemas

não-virais utilizados em terapia e entrega gênica, os lipossomas catiônicos (LCs), têm se mostrado promissores para o tratamento de diversas doenças.

## **2.2. Lipossomas catiônicos**

Lipossomas são estruturas aproximadamente esféricas de dimensões coloidais com cerne aquoso circundado por uma ou mais bicamadas lamelares lipídicas separadas por água. São formados quando lipídios se autoagregam espontaneamente em vesículas na presença de água, atingindo formas mais favoráveis entropicamente de estado de energia livre. Pelo fato das lamelas mimetizarem membranas celulares, os lipossomas possuem diversas características interessantes, que incluem interações com biomembranas e com diversas células. O uso de lipídeos catiônicos permite a obtenção de LCs que podem formar complexos com material genético por interações eletrostáticas (6). Os LCs se apresentam como uma alternativa para a veiculação de material genético, pois permitem a sua proteção contra a degradação enzimática. Além disso, a facilidade de interação com as células é uma característica intrínseca das estruturas lipídicas catiônicas, devido à sua semelhança com a membrana celular de característica aniônica (11).

Apesar das várias formas possíveis de aplicação e dos grandes estudos na área, apenas uma pequena quantidade de produtos lipossomais é aprovada para aplicações farmacêuticas em humanos. Isto provavelmente ocorre devido à falta de técnicas eficientes de produção de lipossomas, com baixo custo e passíveis de transposição para escala industrial. Além disso, é necessário que as formulações lipossomais atendam às especificações farmacêuticas industriais, como esterilização, concentrações apropriadas e estabilidade coloidal (17).

Os LCs, como a maioria dos carreadores de genes não-virais, utilizam apenas de sua natureza catiônica para fazer o transporte do material genético até as células. No processo de transporte para o interior das células, os nucleotídeos associados aos LC são inicialmente internalizados, preferencialmente através do mecanismo de endocitose. A força motriz para esta internalização é a natureza catiônica dos complexos pDNA/LC frente à natureza aniônica das membranas celulares. Em uma segunda etapa, após a internalização dos complexos pelo compartimento endossomal, é necessário que o material genético realize o escape da membrana endossomal para o citoplasma, possivelmente por ruptura da membrana. Uma alternativa para superar a barreira do compartimento endossomal é a utilização de lipídeos específicos nas formulações lipossomais. Sabe-se que a presença de

fosfatidiletanolaminas (PEs), também designadas como *helpers*, intensifica o processo de liberação do material genético no citoplasma por possuírem características fusogênicas, que facilitam a desestabilização da membrana endossomal (18).

A experiência prévia do grupo de pesquisadores deste projeto iniciou-se com o desenvolvimento da nanoestrutura lipossomal incorporando o DNA-hsp65, com pesquisas utilizando LCs compostos por fosfatidilcolina natural de ovo (EPC), 1,2-dioleil-sn-glicero-3-fosfatidiletanolamina (DOPE) e 1,2-dioleil-3-trimetilamônio-propano (DOTAP), que possuem funcionalidades de incorporação ao pDNA e ligação eletrostática com a superfície das células, intensificação da liberação do pDNA no citoplasma celular e estruturação em nanopartículas, utilizando a composição lipídica previamente otimizada (19). Os lipossomas foram preparados pelo método da desidratação-rehidratação, gerando agregados multilamelares. O controle das condições operacionais de temperatura e intensidade de agitação possibilitou a obtenção de estruturas com diâmetro médio da ordem de 200 a 600 nm, que podem ser consideradas como nanoestruturas ou na interface nano/microestruturas (16,20), de tamanho apropriado para aplicação como vacinas para ativação do sistema imunológico contra a tuberculose.

Recentemente, em continuação as pesquisas iniciadas anteriormente, pode-se correlacionar as propriedades físico-químicas e estruturais com o fenômeno de transfecção *in vitro* em células HeLa (*Human epitheloid carcinoma*) dos complexos formados entre LC (EPC/DOTAP/DOPE, lipossomas extrudados e unilamelares) e o pDNA modelo pVAX-Luc, que codifica a luciferase (21). Neste trabalho, uma vez que a caracterização físico-química dos complexos não foi suficiente para elucidar os diferentes níveis de transfecção obtidos para diferentes razões molares de cargas, foram conduzidas investigações de espalhamento de raios X a baixo ângulo (SAXS) a fim de avaliar as modificações estruturais. As análises de SAXS mostraram que a população de vesículas com dupla bicamada lipídica cresce gradativamente com o aumento da razão molar de cargas, assim como observado na transfecção *in vitro*. Próxima à região de isoneutralidade de cargas, a queda nos níveis de transfecção foi explicada pelo aparecimento de outra população de partículas, com uma média de 5 bicamadas lipídicas, o que, provavelmente, interferiu na liberação do pDNA às células. Desta forma, os LCs formados por EPC/DOTAP/DOPE de diâmetro de 100 nm se mostraram eficientes e viáveis para transfecção *in vitro* em células HeLa.

### **2.3. Complexação eletrostática entre carreadores catiônicos e pDNA**

Embora muitos estudos comprovem a eficácia dos lipossomas para aplicações em terapia e vacinação gênica, o modo de formação desses complexos é pouco explorado. O processo espontâneo de complexação influencia diretamente na condensação do material genético nas estruturas carreadoras. Dependendo de diversos fatores, como os citados anteriormente, e ainda outros (como concentração das soluções, força iônica do meio, ordem de mistura, temperatura de complexação e tipo de carreador), partículas com diferentes propriedades físico-químicas, estruturais e morfológicas podem ser obtidas (15,22,23). Tais diferenças podem resultar em diferentes respostas biológicas.

Atualmente, o método convencional para a formação de complexos de sistemas não-virais é através do processo *bulk*, no qual as duas soluções, plasmídeo e de carreador, são misturadas via breve agitação em sistema de vórtice ou, mais comumente, por simples pipetagem manual (15,24). Entretanto, devido aos diversos fatores que influenciam na formação dos complexos, o processo de complexação convencional “bulk” pode resultar em transfeções inconsistentes e muitas vezes pouco reprodutíveis (24,25). Neste contexto, o desenvolvimento de diferentes processos que promovam o controle da complexação eletrostática entre os carreadores catiônicos e o pDNA, e que permitam a formação de partículas uniformes e de forma reprodutiva, resultará, conseqüentemente, em testes biológicos mais reprodutíveis. Estes resultados são fundamentais para o desenvolvimento de produtos farmacêuticos que veiculam materiais genéticos destinados à terapia gênica.

Outro fato importante é a futura demanda por quantidades maiores de complexos para testes clínicos. Considerando as dificuldades no controle da formação dos complexos utilizando processos convencionais “bulk”, cujo modo de operação é em batelada, a microfluídica emerge como uma estratégia promissora que pode ser explorada para aumentar a produtividade e, conseqüentemente, o desenvolvimento de processos inovadores e que operem de modo contínuo.

### **2.4. Microfluídica**

A Microfluídica é um campo multidisciplinar que manipula pequenas quantidades de fluidos. Ela utiliza características hidrodinâmicas para controlar concentrações de diferentes moléculas no espaço e no tempo (8). Os sistemas microfluídicos operam em regime de escoamento laminar e possuem uma razão área/volume muitas vezes maior que outros sistemas, o que lhes conferem propriedades únicas de transporte. Dentre as vantagens dos

sistemas microfluídicos com relação a seus análogos de sistemas convencionais se destacam: reações muito mais rápidas; tamanho mínimo de dispositivos; menor consumo de amostra e reagente; controle preciso de fenômenos de transferência térmico e mássico; escoamento estritamente laminar; baixo consumo e dissipação de energia; e baixo custo relativo de produção por dispositivo (26). Em aplicações na área de biotecnologia, o uso de dispositivos microfluídicos permite a manipulação de diferentes biomateriais, com investigações em diversas áreas, desde o desenvolvimento de biorreatores enzimáticos e microbianos, processos de separação, até a obtenção de nanopartículas (27).

No campo da engenharia química moderna, a microfluídica tem se destacado pois se insere na perspectiva de Intensificação de Processos, em que as inovações buscam reduzir o tamanho da planta e consumo de energia em várias ordens de grandeza para determinados fins. A intensificação de processos visa desenvolver tecnologias que também reduzam substancialmente a produção de resíduos, a razão tamanho de equipamento/capacidade de produção, e que sejam mais eficientes energeticamente, o que resultará em tecnologias sustentáveis e mais baratas (28). A estratégia de aumento de produção (*scale-up*) dos sistemas microfluídicos se dá de forma diferente dos processos fluídicos convencionais em macroescala, uma vez que estes requerem aumento do tamanho dos equipamentos. O aumento de produção dos processos microfluídicos ocorre em termos de amplificação de processos, isto é, os dispositivos não são alterados em suas dimensões, mas sim, montados em paralelo de forma a se elevar a produção por réplica (29).

Devido à flexibilidade desses dispositivos para operar com uma variedade de materiais, vários tipos de nanopartículas obtidas por síntese, formação ou auto-agregação em microcanais são reportadas na literatura, uma vez que, frequentemente, são capazes de superar obstáculos existentes nos métodos convencionais de obtenção, como o controle da polidispersidade e do tamanho de partícula, e ainda em processos com maior reprodutibilidade (22,30). Ademais, a obtenção de nanopartículas pelo método microfluídico muitas vezes dispensa uma etapa posterior de processamento para a redução e homogeneização de tamanho, o que resulta em processos mais simples e que podem ser utilizados de acordo com novas perspectivas de medicina personalizada (que atende características individuais dos pacientes), como terapia e vacinação gênica. Para estas aplicações, a utilização no “point-of-care” pode facilitar o tratamento terapêutico, reduzindo a quantidade de compostos oxidados e degradados.

## 2.5. Microfluidica e a formação de lipossomas

A utilização de dispositivos microfluídicos para a produção de lipossomas foi idealizada empregando um dispositivo baseado na técnica da focalização hidrodinâmica (*hydrodynamic flow-focusing*) (31). Com esta técnica, a formação dos lipossomas ocorre através do contato de duas fases de fluidos solúveis entre si, uma aquosa e outra orgânica (solúvel na fase aquosa). A fase orgânica é aquela na qual os lipídeos estão dispersos em um solvente (solúvel em água), como etanol ou isopropanol. Dessa forma, à medida que ocorre o escoamento entre as correntes (orgânica e aquosa), ocorre a difusão entre essas fases. Conforme ocorre a difusão na região de contato entre as fases, os lipídeos se tornam cada vez menos solúveis no meio aquoso, e começam a se autoagregar, formando discos de bicamadas lipídicas planares. À medida que essas bicamadas lipídicas planares crescem, elas começam a se ligar, a fim de diminuir a área superficial das cadeias hidrofóbicas dos lipídeos expostas pelas extremidades ao meio aquoso. Dessa forma, os discos se fecham em vesículas esféricas com uma bicamada separando um meio aquoso no cerne do meio externo, conforme ilustra a Figura 2.1 (29,32–34).

Embora o estudo da produção de lipossomas em microcanais tenha recebido atenção, os estudos reportados na literatura estudaram a formação das vesículas em baixas concentrações lipídicas, uma vez que partem da solubilidade dos lipídeos no solvente orgânico, etanol ou isopropanol, que é de aproximadamente 5 mM. Porém, as soluções lipossomais obtidas podem, muitas vezes, não ser viáveis para aplicações em terapia e vacinação gênica, pois requerem concentrações lipídicas dos lipossomas mais altas. Dessa forma, nosso grupo de pesquisa investigou recentemente, no âmbito da dissertação de mestrado do autor dessa tese, a produção de lipossomas catiônicos compostos pelos lipídeos EPC, DOTAP e DOPE, destinados a terapia e vacinação gênica (34). Ainda, pelo nosso conhecimento, foi a primeira vez que um estudo sistemático da produção de lipossomas de caráter catiônico foi realizado. Nesse trabalho, foi estudada a produção de LCs em sistema contínuo em altas concentrações com o emprego de dois dispositivos microfluídicos. O primeiro com única focalização hidrodinâmica e o segundo com duas focalizações hidrodinâmicas paralelas, objetivando o aumento da área de contato entre os fluxos aquosos e orgânicos, e assim a área de difusão. Verificou-se que o dispositivo com dupla focalização hidrodinâmica é capaz de operar a vazões mais altas que o de focalização única. Os estudos de SAXS revelaram a predominância de lipossomas unilamelares produzidos por ambos os dispositivos, como já haviam sugerido as microscopias de

transmissão eletrônica. Estudos biológicos *in vitro* mostraram a potencialidade dos LCs produzidos em ambos dispositivos investigados (foco simples e duplo).

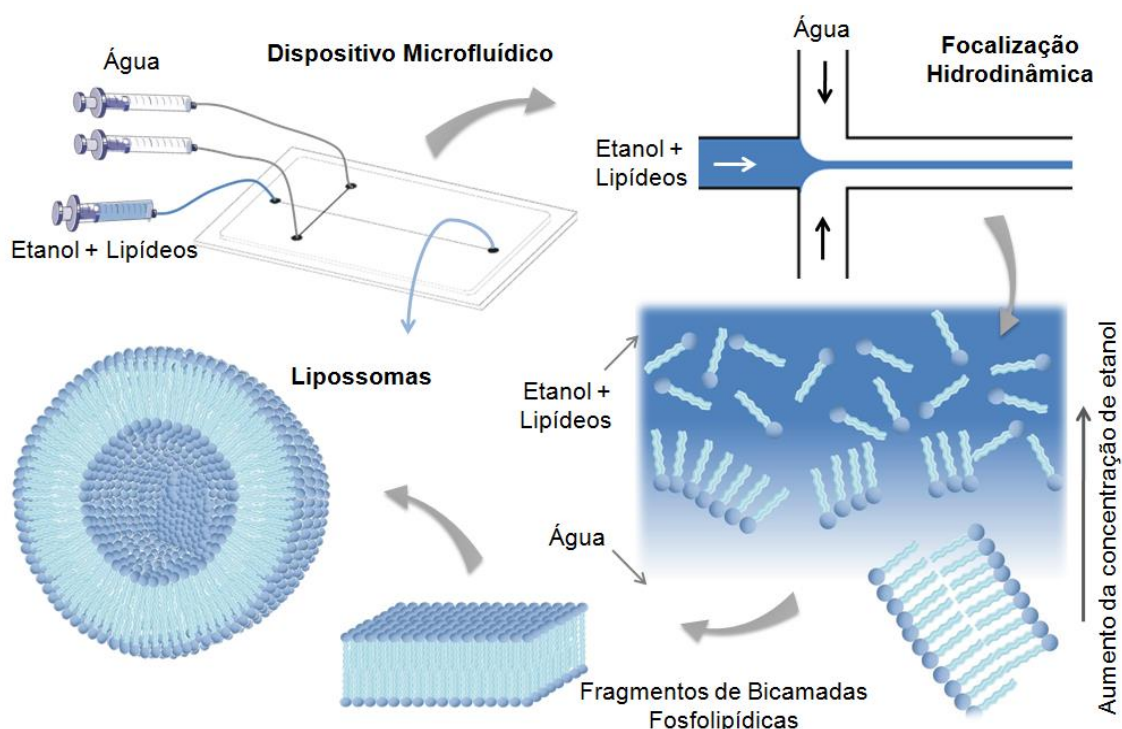


**Figura 2.1.** Esquema hipotético da formação de lipossomas em microcanais através da técnica da focalização hidrodinâmica (adaptado de Balbino *et al.*, (34)).

## 2.6. Sistemas microfluídicos para complexação eletrostática entre carreador catiônico e material genético

Devido às dificuldades relacionadas à formação dos complexos carreadores de material genético mencionadas anteriormente, a microfluídica emerge como uma ferramenta para superar tais desafios. Os sistemas microfluídicos permitem a realização da complexação eletrostática em fluxo contínuo, com o controle do cisalhamento e das condições difusionais, permitindo a orientação de macromoléculas.

Estudos reportados na literatura puderam comprovar a eficiência do método microfluídico para a formação de sistemas não-virais. Esses estudos se dividem basicamente em duas abordagens: (i) a mais estudada se baseia na técnica de focalização hidrodinâmica, em que o fluxo central, que contém o material genético, é hidrodinamicamente focalizado por duas correntes adjacentes, com o carreador catiônico (22,35–39); (ii) a segunda se baseia na formação de incubadores na ordem de tamanho de picolitros, no qual o material genético e o carreador catiônico são confinados em gotas

formadas por emulsão água em óleo obtidas nos microcanais, com uma etapa adicional de pós-processamento para a separação do solvente orgânico (24,40).

O primeiro estudo reportado na literatura demonstrando a viabilidade da formação de complexos entre pDNA e lipossomas compostos por DOTAP e DOPC (1,2-dioleoil-*sn*-glicero-*sn*-3-fosfatidilcolina) foi realizado através da técnica de focalização hidrodinâmica, em que foi feita uma caracterização estrutural *in situ* por análises de SAXS (35). Os autores verificaram que, para a razão molar de cargas e composição lipídica utilizadas, houve um aumento de vesículas lipossomais multilamelares conforme a posição de incidência do feixe de luz, o qual percorreu o microcanal principal a partir do foco, onde as correntes se cruzam, até próximo à saída. Também foi possível verificar que o processo de formação dos complexos ocorria em duas etapas: na primeira, a formação do complexo multilamelar e, em seguida, o rearranjo do pDNA dentro das lamelas lipídicas.

Nosso grupo de pesquisa investigou a utilização de sistemas microfluídicos para a formação de complexos pDNA/LC em modo contínuo, como ilustra a Figura 2.2 (41). Com o emprego de dois dispositivos e tendo o método de complexação convencional “bulk” como referência, os complexos obtidos através de os ambos dispositivos estudados – um de paredes dos microcanais com blocos padronizados, Figura 2.2b, e outro de parede simples, sem restrições de escoamento, Figura 2.2a – foram capazes de transfectar *in vitro* células humanas do tipo HeLa. Diferentemente do estudo que será apresentado no Capítulo 3, neste trabalho a razão molar de cargas foi mantida em 6, condição identificada anteriormente como mais eficiente em ensaios *in vitro* (21). O dispositivo simples atingiu níveis de transfecção similares ao alcançados pelos complexos obtidos pelo método “bulk”, enquanto o dispositivo com blocos nos microcanais apresentou menores níveis de transfecção. Isso provavelmente ocorreu devido à diferença de condensação do pDNA nas estruturas lipossomais, conforme demonstrado a partir dos ensaios de sonda de fluorescência (acessibilidade). De modo geral, ambos os dispositivos foram capazes de produzir complexos de tamanho e polidispersidade controlados para aplicações em terapia e vacinação gênicas.

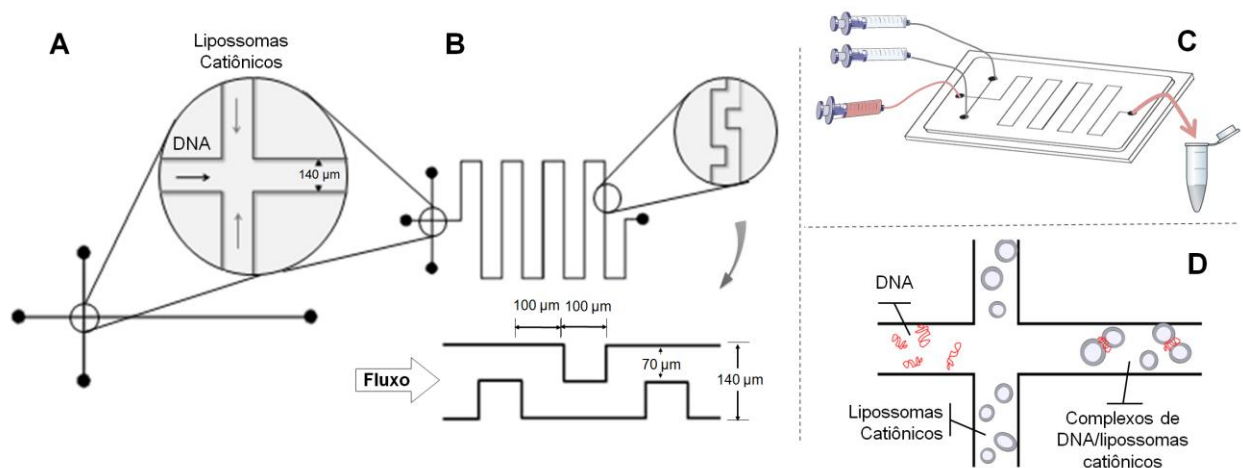


**Figura 2.2.** Dispositivo microfluídico simples (A) e com barreiras nos microcanais (B). Diagrama esquemático do aparato experimental utilizando o dispositivo com barreiras nos microcanais (C), e do mecanismo hipotético de formação dos complexos pDNA/lipossomas catiônicos utilizando processo microfluídico (D) (Adaptado de Balbino *et al.*, (41)).

A formação de complexos de polietilenoimina (PEI) e pDNA com tamanhos menores e mais uniformes também foi alcançada com o emprego da técnica de focalização hidrodinâmica (36). Os complexos obtidos por processo microfluídico apresentaram maior viabilidade celular e uma melhora significativa da expressão do gene exógeno. O mesmo grupo de pesquisa estudou, posteriormente, um dispositivo multientradas com duas focalizações hidrodinâmicas consecutivas, para a formação de complexos de mRNA, protamina e lipídeos (38). Os melhores resultados foram obtidos utilizando uma configuração mais simples de 3 canais: no canal central, a solução de mRNA era injetada, enquanto nas entradas laterais, eram injetadas as correntes que continham os lipídeos e a protamina, que haviam sido pré-misturados. O diâmetro hidrodinâmico das partículas variou entre 100 e 300 nm. Comparado ao método “bulk”, as nanopartículas obtidas pelo sistema microfluídico apresentaram menores tamanho e polidispersidade, além de propiciarem a produção de estruturas mais uniformes. Esses complexos também se mostraram eficientes em estudos biológicos *in vitro*. Apesar da tentativa de formação dos complexos multifuncionais em uma única etapa com a utilização da geometria de 5 entradas, os autores só puderam obter complexos mais homogêneos quando realizaram uma mistura “bulk” dos carreadores (protamina e lipídeos) numa etapa anterior à complexação, para então fazer o processamento no microdispositivo com 3 entradas.

Por meio de dispositivos microfluídicos de diferentes geometrias, a formação de complexos de pDNA/PEI também foi otimizada em termos das variáveis microfluídicas (22). Estes autores investigaram sistematicamente a influência de variáveis gerais para a

preparação dos complexos (concentrações individuais das soluções, concentração final dos complexos, razão molar de cargas e força iônica do solvente) e também de variáveis microfluídicas (fluxo individual das soluções, razão entre os fluxos e velocidade total de escoamento). Os autores também realizaram a otimização da produção de complexos pDNA/PEI, e observaram a variável razão molar de cargas entre PEI e pDNA sendo a mais significativa frente às variações das propriedades físico-químicas e respostas biológicas. Em comparação ao método clássico de complexação de mistura por pipetagem manual, o tamanho das nanopartículas preparadas pelo processo microfluídico variou numa faixa menor e foi mais uniforme, confirmando a superioridade da microfluídica frente ao método *bulk* para a obtenção desses complexos.

A preparação de complexos em dispositivos microfluídicos foi realizada para a entrega de RNA *in vitro* às células do tipo SKOV3 (39). Os parâmetros para a formação dos complexos foram avaliados pelo método *bulk* e, então, as melhores condições foram transportadas para o estudo de complexação pelo método microfluídico, através de um delineamento composto central rotacional. Como observado em estudos anteriores, os complexos obtidos pelo método microfluídico quando comparados àqueles obtidos pelo método *bulk* apresentaram menores tamanho e polidispersidade e aumentaram a proteção ao material genético e a eficiência de transfecção. Entretanto, os diferentes adjuvantes utilizados para a formação dos complexos multifuncionais foram preparados pelo método *bulk*, numa etapa anterior à complexação nos microcanais.

Neste contexto, o desenvolvimento de processos que promovam o controle da complexação eletrostática entre pDNA e LC, que permitam a formação de partículas uniformes e de forma reprodutiva, resultará consequentemente em transfecções mais eficientes. Além disso, o desenvolvimento de dispositivos para a formação de complexos em uma única etapa, sem a etapa *bulk* anterior e de preparação dos adjuvantes, continua sendo um desafio. Estes estudos permitirão o desenvolvimento de novos produtos farmacêuticos que veiculam DNA para aplicação em vacinação e terapia gênica.

### 3. Microfluidic assembly of pDNA/cationic liposome lipoplexes with high pDNA loading for gene delivery<sup>§</sup>

Tiago A. Balbino<sup>a</sup>, Juliana M. Serafin<sup>a</sup>, Antonio A. M. Gasperini<sup>b</sup>, Cristiano L. P. de Oliveira<sup>c</sup>,  
Leide P. Cavalcanti<sup>a</sup>, Marcelo B. de Jesus<sup>d</sup>, Lucimara G. de La Torre<sup>a, \*</sup>

<sup>a</sup>School of Chemical Engineering, University of Campinas, UNICAMP, Campinas, SP, Brazil;

<sup>b</sup>Brazilian Synchrotron Light Laboratory, CNPEM, Campinas, São Paulo, Brazil

<sup>c</sup>Institute of Physics, University of São Paulo, USP, São Paulo, SP, Brazil

<sup>d</sup>Department of Biochemistry and Tissue Biology, Institute of Biology, University of Campinas, SP, Brazil

\*Corresponding author: [latorre@feq.unicamp.br](mailto:latorre@feq.unicamp.br)

#### 3.1. Abstract

Microfluidics offers unique characteristics to control the mixing of liquids under laminar flow. Its use for the assembly of lipoplexes represents an attractive alternative for the translation of gene delivery studies into clinical trials on a sufficient throughput scale. Here, it was shown that the microfluidic assembly of pDNA/cationic liposome (CL) lipoplexes allows the formation of nanocarriers with enhanced transfection efficiencies compared with the conventional bulk-mixing (BM) process under high pDNA loading conditions. Lipoplexes generated by microfluidic devices exhibit smaller and more homogeneous structures at a molar charge ratio ( $R_{\pm}$ ) of 1.5, representing the ratio of lipid to pDNA content. Using an optimized model to fit small-angle X-ray scattering (SAXS) curves, it was observed that large amounts of pDNA induces the formation of aggregates with a higher number of stacked bilayers ( $N \sim 5$ ) when was used the BM process, whereas microfluidic lipoplexes presented smaller structures with a lower number of stacked bilayers ( $N \sim 2.5$ ). *In vitro* studies further confirmed that microfluidic lipoplexes achieved higher *in vitro* transfection efficiencies in prostate cancer cells at  $R_{\pm} 1.5$ , employing a reduced amount of cationic lipid. The correlation

---

<sup>§</sup> Manuscript published in *Langmuir*, 2016, 32 (7), p 1799–1807. Reprinted with permission from *Langmuir*. Copyright 2016 American Chemical Society (*Anexo I*).

of mesoscopic characteristics with *in vitro* performance provides insights for the elucidation of the colloidal arrangement and biological behavior of pDNA/CL lipoplexes obtained by different processes, highlighting the feasibility of applying microfluidics to gene delivery.

**Keywords:** gene delivery, microfluidics, nanomedicine, lipoplex, liposomes, pDNA

### 3.2. Introduction

Since it was first reported in 1972, gene therapy has been pursued as a promising strategy for the treatment of several diseases, with ongoing clinical trials. As an example, this technology has been shown to be a safe and effective treatment for 1.5 years after vector administration in Leber congenital amaurosis, the most severe inherited retinal dystrophy, which causes blindness or visual impairment (42,43). DNA-based gene therapy relies upon the insertion of a functional plasmid DNA (pDNA) into the nucleus of cells, which in turn enables the expression of therapeutic proteins; this phenomenon is called transfection (44). For systematic gene delivery to be effective, the pDNA requires appropriate protection due to its poor cellular internalization and fast enzymatic degradation. Many materials, such as chitosan (45), cationic lipids (46) and proteins (47), have been employed as nonviral gene carriers. Such carriers are capable of electrostatically binding and condensing pDNA into cationic nano-sized particles with optimal characteristics to be internalized and processed by cells (48). Among nonviral cationic carriers, liposomes have long been explored for the delivery of nucleic acids (49).

Liposomes are self-assembled polar lipid vesicles of colloidal dimensions whose bilayer structure is similar to that of human cell membranes (11). The use of cationic lipids in the lipid blend allows the formation of cationic liposomes (CLs) that can electrostatically interact with the negatively charged pDNA, forming lipoplexes. The spontaneous interactions between CLs and pDNA can lead to the formation of lipoplexes with different characteristics. Several factors, such as the individual concentrations of the species, the ionic strength of the media, the characteristics and composition of the lipid mixture, and the lipid/DNA charge ratio ( $R_{\pm}$ ), can affect the physicochemical, structural and biological properties of lipoplexes (15,41). In a given  $R_{\pm}$  condition, when positive charges from the cationic lipid balance negative charges from the DNA's phosphate groups, lipoplexes are considered to be at the isoneutrality ratio (50). At this point, the surface net charge of the lipoplexes shifts from positive to negative values as  $R_{\pm}$  decreases. Additionally, close to the isoneutrality ratio, lipoplexes tend to form agglomerates with larger particle sizes and high polydispersity

indexes (Pdl)s and can also exhibit structures with a higher number of stacked bilayers (21,51,52).

During lipoplex assembly, when the macroionic pDNA and cationic lipid interact with each other, the DNA can trigger the aggregation and/or fusion of vesicles, causing a complete reorganization of the vesicle structure (46). This reorganization can result in several structures, including (i) a lamellar structure, in which the pDNA is sandwiched between lipid bilayers; (ii) an inverted hexagonal structure, in which the pDNA is coated with a lipid monolayer on a hexagonal matrix; and (iii) an intercalated hexagonal structure, in which the pDNA is covered by lipid micelles disposed on a hexagonal matrix (15,53). These arrangements strongly rely upon the different characteristics of the lipids used, such as the degree of saturation, the phospholipid chemical structures and the colloidal self-assembly of the lipid mixture (11,54).

The current process for lipoplex formation comprises the bulk mixing (BM) of DNA and CLs by pipetting or vortexing, with a final volume usually on the order of hundreds of microliters. Due to the variables involved, employing conventional BM processes would compromise lipoplex formation at higher volumetric throughputs, likely causing inconsistent and poorly reproducible results from batch to batch (24). Thus, the development of robust and automatized processes to form lipoplexes is an essential step toward industrial application of gene delivery.

Microfluidic systems offer particular characteristics to control minute amounts of liquids. Microfluidics is a technology that studies and manipulates fluids at the submillimeter length scale (9). As a consequence, the mixing of species inside microchannels is mainly driven by molecular diffusion under laminar flow conditions. In contrast to macroscale systems, microfluidic devices have increased surface-to-volume ratios and fast mixing times, enhancing heat and mass transfer. Due to their flexibility in handling different materials, microfluidic systems have been used to address issues in biomedical research (9). Taking advantage of these features, one promising application of microfluidics technologies is the formation of nanoscale gene delivery systems. The assembly of poly(ethylene imine) (PEI)/DNA polyplexes was studied in a plastic microfluidic device (36). Polyplexes presented larger particle sizes at lower nitrogen/phosphate (N/P) ratios, i.e., higher DNA loading conditions. The *in vitro* results showed improved exogenous gene expression in fibroblast cells in comparison with complexes assembled via a BM procedure. Most likely due to the enhanced and better-controlled mass transfer between species, complexes formed by the microfluidic method presented more compact and ordered condensates. By exploring the microfluidic assembly of PEI/DNA polyplexes as well, Debus et al (22) performed an

optimization study of the process. Different microchannel architectures were arranged onto a modular lab-on-a-chip baseboard. The authors investigated variables related to microfluidic processes and intrinsic general parameters for polyplex preparation. Particle size was shown to be dependent mostly on the  $R_{\pm}$  of complexes, whereas other parameters seemed to be of minor influence on the process (22).

Lipid-based nanoparticles are currently the leading systems for the delivery of small interfering RNA (siRNA) (55). The synthesis of siRNA-loaded lipid nanoparticles in a micromixer exhibited equivalent or better gene silencing in mice compared with the conventional BM process (55). A mixing microchannel with staggered herringbone structures was able to produce highly potent limited-size nanoparticles with low polydispersity. In addition to demonstrating the improved scalability of the process, which is a requirement for clinical purposes, the study showed feasible microfluidic parallelization through the vertical and horizontal replication of mixers in a single microfluidic chip.

Our research group explored the continuous formation of pDNA/CL lipoplexes using microfluidic devices with two different architectures (41). The first geometry comprised a hydrodynamic focusing device with a straight mixing channel, whereas the second comprised a longer mixing channel with uniform barriers, which were used to accelerate the mixing between streams through swirling regions. Compared with the hydrodynamic focusing device, the device with barriers presented lower transfection efficiency, which was associated with more limited pDNA accessibility in the liposomal structure. All of the pDNA/CL complexes were formed at a fixed  $R_{\pm}$  value of 6. In contrast, compared with the BM method, complexes assembled in the hydrodynamic focusing geometry had significantly similar physicochemical and *in vitro* characteristics.

For many lipid compositions, pDNA/CL lipoplex sizes present a Gaussian-shaped function for  $R_{\pm}$ , with a peak achieved at the isoneutrality ratio (51,52,56,57). The isoneutrality point, or electroneutrality ratio, occurs when cationic charges from cationic lipid balance anionic charges from pDNA. Theoretically, by assuming the same values of nominal and effective charges for cationic lipid and the pDNA's phosphate group, the isoneutrality ratio occurs at the equimolarity of charges present in the system ( $R_{\pm} = 1$ ). This implies that all cationic and anionic charges are involved in the electrostatic interaction. Once the zeta potential reflects the net charge of the outer region of aggregates, it can be used as a major physicochemical characteristic to obtain information about the electrostatic association between CLs and pDNA. Thus, the effective isoneutrality ratio ( $R_{\pm, \text{eff}} = 1$ ) can be experimentally determined based on the typical sigmoidal curves of zeta potential vs.  $R_{\pm}$  at the inversion of sign (neutral charge,  $\zeta \sim 0$ ) (50,58).

Previously, it has been studied the influence of  $R_{\pm}$  on the physicochemical, structural and *in vitro* properties of pDNA/CL lipoplexes in a bulk system (21). The transfection efficiency of HeLa cells as a function of  $R_{\pm}$  presented a Gaussian shape whose peak occurred at  $R_{\pm}$  values of 3 and 6 (significantly equal). Small-angle x-ray scattering (SAXS) studies showed that large lipoplexes at  $R_{\pm}$  1.8 had a multiple-bilayer phase with an average bilayer number of 5.2, in contrast to the structures observed under other studied  $R_{\pm}$  conditions with a bilayer number of 2. The results showed that the presence of larger and multiple-bilayer aggregates at  $R_{\pm}$  1.8 impaired the release of pDNA into the nucleus, resulting in a lower transfection efficiency. Therefore, it was hypothesized that the characteristics of complexes assembled by both mixing processes would be affected by varying  $R_{\pm}$  conditions, i.e., varying pDNA-loading capacities. This assumption is based on intrinsic differences in fluid flow mixing between microfluidic and bulk methods that can affect the pDNA/CL assembly process, mainly under high pDNA loading conditions.

Thus, in the present work, the assembly of pDNA/CL lipoplexes was investigated using a hydrodynamic flow-focusing microfluidic device under high pDNA loading conditions, i.e., at a low  $R_{\pm}$ . Lipoplexes assembled via the BM process were used for comparison. Lipoplexes have been evaluated in terms of their physicochemical, nanostructural and biological characteristics in an effort to elucidate key parameters involved in the *in vitro* transfection of lipid-based nonviral carriers.

### **3.3. Experimental Procedure**

#### **3.3.1. Microfluidic device**

A hydrodynamic flow-focusing microfluidic device fabricated as previously described elsewhere was used in order to form the pDNA/CL lipoplexes (34). Briefly, UV photolithographic methods were employed to pattern the replication masters using SU-8 photoresist (Newton, MA, USA). The layout geometry was projected using AutoCAD 2008 software (Autodesk) that presents 1 outlet-channel and 3 inlet-channels, all of them with a 140- $\mu$ m-wide and 100- $\mu$ m-deep rectangular cross section; being the mixing channel at 3-cm-long from the cross junction. The poly(dimethylsiloxane) (PDMS) microchannels were constructed by means of soft-lithography with Sylgard 184 Silicone Elastomer Kit (Dow Corning, MI, USA) as material precursor. The PDMS layer was irreversibly sealed to a glass slide by chemically activating both surfaces through oxygen plasma.

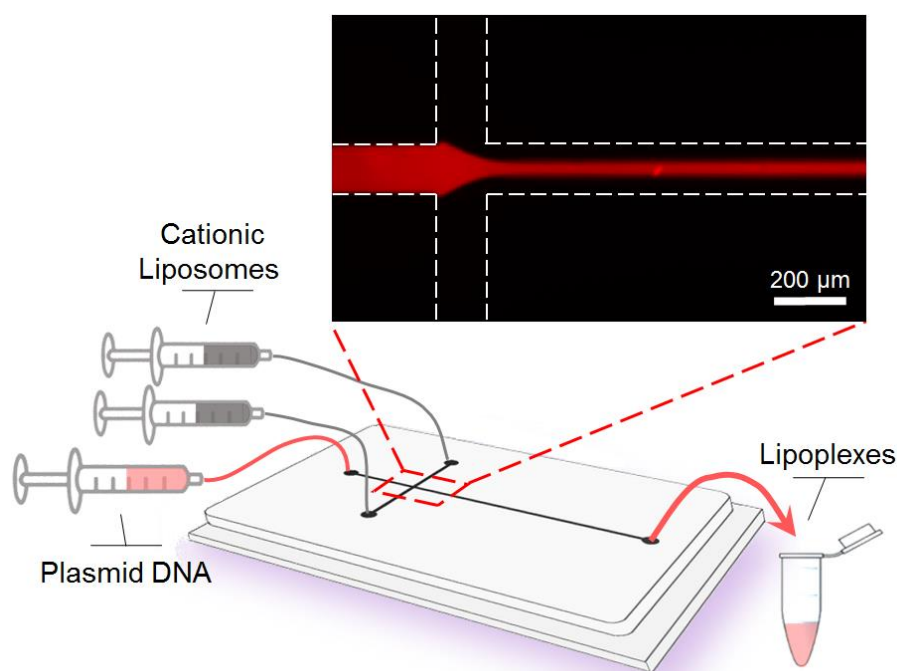


**Figure 3.1. Schematic of the microfluidic device for continuous lipoplex assembly.** The hydrodynamic flow-focusing device consists of three inlets and one outlet. Two programmable pumps controls the fluid flow rates of the syringes. Cationic liposomes (CLs) were introduced via side streams that hydrodynamically focused the central stream containing the plasmid DNA (pDNA). The microfluidic-assisted assembly of pDNA/CL lipoplexes gradually occurred with the diffusion between stream flows along the main channel. The inset shows a fluorescence micrograph of the flow pattern at the cross-junction, obtained using rhodamine in the central stream. The microchannels were 140- $\mu\text{m}$  wide and 100- $\mu\text{m}$  deep. The white dotted lines indicate the borders of the microchannels. The volumetric flow rates used for the side and central streams were 160  $\mu\text{L}/\text{min}$  and 88  $\mu\text{L}/\text{min}$ , respectively. The scale bar denotes 200  $\mu\text{m}$ .

### 3.3.2. Preparation of liposomes

In this work, it has been used egg phosphatidylcholine (EPC) (96% of purity), 1,2-dioleoyl-sn-glycero-3-phosphoethanolamine (DOPE) (99.8% of purity) and 1,2-dioleoyl-3-trimethylammonium-propane (DOTAP) (98% of purity) (Lipoid) lipids to form cationic liposomes via standard dried film method followed by extrusion (21). The lipids EPC, DOPE and DOTAP, at a molar ratio of 2:1:1, were mixed in chloroform (Sigma-Aldrich) and placed in a round-bottom flask. The solvent was removed under vacuum by rotary evaporation to form an evenly distributed film. The lipids were hydrated for  $\sim 1$  h with sterile water for injection. The liposomal dispersion obtained was then physically extruded 15 times under pressure through double-stacked 100-nm polycarbonate membranes. CL dispersion was prepared at a nominal lipid concentration of 16 mM and diluted to 2 mM before experiments. For *in vitro* particle internalization assays, fluorescently labeled CLs were prepared by adding a trace amount of the headgroup labeled lipid 1,2-dipalmitoyl-sn-glycero-3-

phosphoethanolamine-N-(lissamine rhodamine B sulfonyl) (Avanti Polar Lipids, Alabaster, AL) at 0.4 mol% to the extruded CL dispersion.

### **3.3.3. Plasmid amplification**

The plasmid pEGFP-N1 (BD Biosciences Clontech, Palo Alto, USA) was used as vector model and amplified in *Escherichia coli*. The pDNA was purified using PureLink™ HiPure Plasmid pDNA Purification Kit-Maxiprep K2100-07 (Invitrogen), according to manufacturer's instructions and resuspended in sterile water for injection. The evaluation of quality and quantity of the purified pDNA was carried out through a ND-1000 NanoDrop UV-vis spectrophotometer (PeqLab, Erlangen, Germany).

### **3.3.4. pDNA/CL lipoplex formation**

The pDNA/CL lipoplexes were prepared via microfluidic and BM processes at varying positive/negative molar charge ratios ( $R_{\pm}$ ).  $R_{\pm}$  is defined as the molar ratio of positive charges from DOTAP to negative charges from the phosphate groups in pDNA. For lipoplexes formed by the BM process, pDNA solution (200  $\mu\text{g/mL}$ ) was added to the CL dispersion (2 mM), followed by pipette mixing in an ice bath.

For lipoplexes formed by the microfluidic process, the pDNA solution (1 mL) and CL dispersion (2.5 mL) were loaded into gastight glass syringes (Hamilton Co.), similar to what has been described elsewhere (41). Two programmable infusion syringe pumps (KD200, KD Scientific) were then used for fluidic injection and control according to the desired flow-rate ratio (FRR) of the side streams to the central stream. The pDNA stream was injected into the central inlet channel, which was hydrodynamically focused by the two CL side streams (Figure 3.1). For all microfluidics experiments, the microfluidic device was placed over a Peltier thermoelectric system (Watronix, Inc.) to keep the temperature controlled at  $\sim 4^{\circ}\text{C}$ . To prepare pDNA/CL lipoplexes at  $R_{\pm}$  values lower than 1.5, larger amounts of pDNA are required, implying low FRR conditions and consequently poor microfluidic mixing (59). Because the concentrations of the solutions and the mixing quality might be considered as important parameters for lipoplex formation, to achieve a more proper comparison of the assembly processes, it has been evaluated the FRRs of liposomal to DNA streams varying from 2 to 7 for  $R_{\pm}$  1.5 to 6, respectively. Therefore, the species concentrations and the total volumetric flow rate of the liposomal streams remained constant, whereas the flow rate of the pDNA stream varied according to the desired amount of pDNA in the lipoplexes.

### **3.3.5. Zeta potential ( $\xi$ ) and size measurements**

Electrophoretic mobility and dynamic light scattering (DLS) were measured at 25°C using a Malvern Zetasizer Nano ZS (Malvern Instrument, UK) in order to determine the zeta potential, size, polydispersity and size distribution of CL and pDNA/CL lipoplexes. Zeta potential was obtained from the electrophoretic mobility data using the Smoluchowski relation. Dispersion Technology Software (Malvern Instruments Ltd.) version 4.00 was used to obtain number-weighted size distributions and polydispersity index (Pdl) from correlation functions with multiple narrow mode data processing. All the samples were diluted to a lipid concentration of 0.2 mM before analysis and measurements were performed three times for each replicate in water.

### **3.3.6. pDNA accessibility**

PicoGreen fluorescence probe (Quant-iT PicoGreen dsDNA assay, Invitrogen) was employed according to the protocol from the supplier to evaluate the pDNA accessibility in the lipoplexes. The PicoGreen solution was prepared in TE buffer (10 mM Tris-HCl/1 mM EDTA, pH 7.5). The assay was carried out by adding 100  $\mu$ L of the fluorescence solution to 100  $\mu$ L of samples containing 0.1  $\mu$ g of pDNA, in a black 96-well microplate. The absolute fluorescence was measured after ~3 min of incubation using a microplate reader (Gemini XS, Molecular Device), at excitation and emission wavelengths of 485 nm and 525 nm, respectively.

### **3.3.7. Agarose gel electrophoresis**

To check pDNA binding, gel retardation assay was conducted on 0.8% agarose gel containing ethidium bromide (0.5  $\mu$ g/mL). Free pDNA and pDNA/CL lipoplexes (1  $\mu$ g of pDNA) were subjected to the electrophoresis gel under a constant electric field (50 V, 2 h) at room temperature, and were then visualized using a UV transilluminator.

### **3.3.8. DNase I protection assay**

pDNA/CL lipoplexes (1  $\mu$ g of pDNA) were prepared as described above. After, DNase I was added (1 U/2.5  $\mu$ g of DNA) to the pDNA/CL lipoplexes and the suspension was incubated at 37 °C for 30 min to degrade the free DNA (i.e., non-associated with the CL). 1% SDS (final concentration) was used to stop the enzymatic action and to release the DNA from the CL. The samples were subjected to electrophoresis on ethidium bromide-stained 1.3% agarose gels (50 V for 90 minutes) and analyzed under UV light; the images were processed with Image-J software.

### 3.3.9. SAXS studies

The structure of the formed lipoplexes was analyzed by SAXS. The experiments were performed using a laboratory SAXS instrument (Bruker Nanostar) at the Institute of Physics of the University of São Paulo. This equipment is improved by the use of the microfocus source GeniX3D coupled with Fox3D multilayer optics and two sets of scatterless slits for beam definition, all provided by Xenocs. The samples were kept on a quartz capillary glued to a homemade stainless steel case, which enabled proper rinsing and reuse of the sample holder, allowing accurate background subtraction. CuK $\alpha$  beam energy (wavelength  $\lambda=1.54$  Å) and a sample-to-detector distance of 670 mm were used. The 2D scattering data were recorded by a Vantec-2000 detector, and integration of the SAXS patterns were performed using the Bruker SAXS software. The measured profiles are reported as a function of the scattering vector modulus  $q$  ( $q=4\pi \sin(\theta)/\lambda$ ), where  $2\theta$  is the scattering angle. The typical range of  $q$  values was from 0.008 to 0.35 Å<sup>-1</sup>. Several 900 s frames were measured for each sample to check the sample stability and possible radiation damage effects. Background subtraction, data treatment and averaging were performed using the SuperSAXS program package (60).

Liposome dispersions exhibit a liquid-crystalline character: they have both a form factor, which is related to the electron density profile (EDP) across the lipid bilayer, and a structure factor, which is related to the lipid bilayer stacking. The model used in this work for the lipid bilayer form factor is described in previous studies by our group (21,61,62). It is assumed that the system is composed of two phases: a fraction ( $f_{sb}$ ) of single-bilayer structures, where there is no correlation in the position of stacked bilayers or where they are nonexistent, and a fraction ( $f_{mb}$ ) of multi-bilayer structures, where there is a clear correlation among the stacked bilayers' positions. Therefore, the scattering intensity  $I(q)$  can be written as

$$I(q) = P(q) S_{eff}(q) \quad (\text{Equation 1})$$

with

$$S_{eff}(q)=f_{sb}+f_{mb} S_{MCT}(q) \quad (\text{Equation 2})$$

where  $P(q)$  is the bilayer form factor,  $S_{eff}(q)$  is the effective structure factor (with the constraint  $f_{sb}+f_{mb} = 1$ ), and  $S_{MCT}(q)$  is the modified Caillé structure factor (63,64).

### 3.3.10. Transfection Protocol

The biological activity (i.e. transfection efficiency) of pDNA/CL lipoplexes produced by BM and microfluidic processes were assessed in prostate cancer cell line PC3. For transfection, the PC3 cells were seeded on 12-well plates at a density of 100,000 cells per

well. After 24 h, the cells were semi-confluent (70–90%), they were washed once with PBS, followed by the addition (400  $\mu$ l per well) of serum- and antibiotic-free medium. Next, it was added 100  $\mu$ l of the lipoplexes formed by 1  $\mu$ g of the pDNA and CL or Lipofectamine 2000 (LF2k) (Invitrogen, Breda, The Netherlands); after, the cells were incubated for 4 h at 37 °C. After this incubation, the transfection medium was replaced with complete medium. The percentages of EGFP-positive cells were determined after 24 h by flow cytometry (FACS/Calibur Flow Cytometer, Becton Dickinson, Mansfield, MA).

### **3.3.11. Statistical analysis**

The statistical significance of experiments was determined by Student's t-test. The differences were considered significant for  $*p < 0.05$ . All experiments were performed at least three times and data are presented as mean  $\pm$  standard deviation (SD).

## **3.4. Results and Discussion**

Usually, when using the conventional BM method to form lipoplexes, high pDNA loading conditions result in highly polydispersed systems with lower transfection efficiencies (21,51,52). Previously, it has been demonstrated the influence of  $R_{\pm}$  on the colloidal and biological characteristics of lipoplexes obtained by the BM method (21) and that when using a hydrodynamic flow-focusing microfluidic device, lipoplexes at  $R_{\pm} 6$  exhibited characteristics significantly similar to those of lipoplexes assembled using the BM method (41). Here, it was studied the microfluidic formation of pDNA/CL lipoplexes under high pDNA loading conditions. It has been therefore investigated a few different  $R_{\pm}$  conditions for lipoplex assembly by both processes (bulk and microfluidic mixing) in terms of physicochemical, structural and biological properties.

### **3.4.1. Microfluidic process provided the assembly of lipoplexes with better physicochemical properties than bulk mixing**

To rationally design gene delivery systems, it is crucial to identify the best  $R_{\pm}$  conditions. It is known that gene nanocarriers should be positively charged to favor interaction with cell surfaces and small in size to be more efficiently internalized and processed by cells (65). The investigation was initiated by comparing the physicochemical properties of lipoplexes prepared by microfluidic and BM processes. The pDNA/CL lipoplexes were characterized through number-weighted hydrodynamic diameter, Pdl and zeta potential measurements (Figure 3.2). Extruded pure liposomes had a hydrodynamic

diameter of  $88.7 \pm 4.7$  nm, a Pdl of  $0.21 \pm 0.03$ , and a zeta potential of  $+61.3 \pm 3.3$  mV. Both processes formed lipoplexes with the greatest sizes and highest Pdl values at  $R_{\pm} 1.5$  (Figures 3.2a and b). At  $R_{\pm} 1.5$ , samples of lipoplexes assembled via BM were highly polydispersed (Figure 2b) and thus not suitable for proper dynamic light scattering analysis.(66,67) At  $R_{\pm} \geq 3$ , the physicochemical properties of lipoplexes were significantly similar using the bulk and microfluidic processes under the same  $R_{\pm}$  conditions. The zeta potential values of lipoplexes decreased with decreasing  $R_{\pm}$  (Figure 3.2c). The decrease in zeta potential was more evident for the lipoplexes assembled via the BM process than for the microfluidic lipoplexes ( $p < 0.05$ ). The size and zeta potential results are in good agreement with previous works, which have shown the isoneutrality ratio for this lipid composition occurred in the range of  $R_{\pm} \sim 1$  (21,68). Thus, based on size and zeta potential characteristics, at  $R_{\pm} 1.5$ , the microfluidic process was more efficient in incorporating the pDNA into the liposomal structure than the BM process was. Furthermore, the difference in the zeta potential values of lipoplexes at  $R_{\pm} 1.5$  (Figure 2c) shows that effective isoneutrality ratios also depend on the assembly process employed.

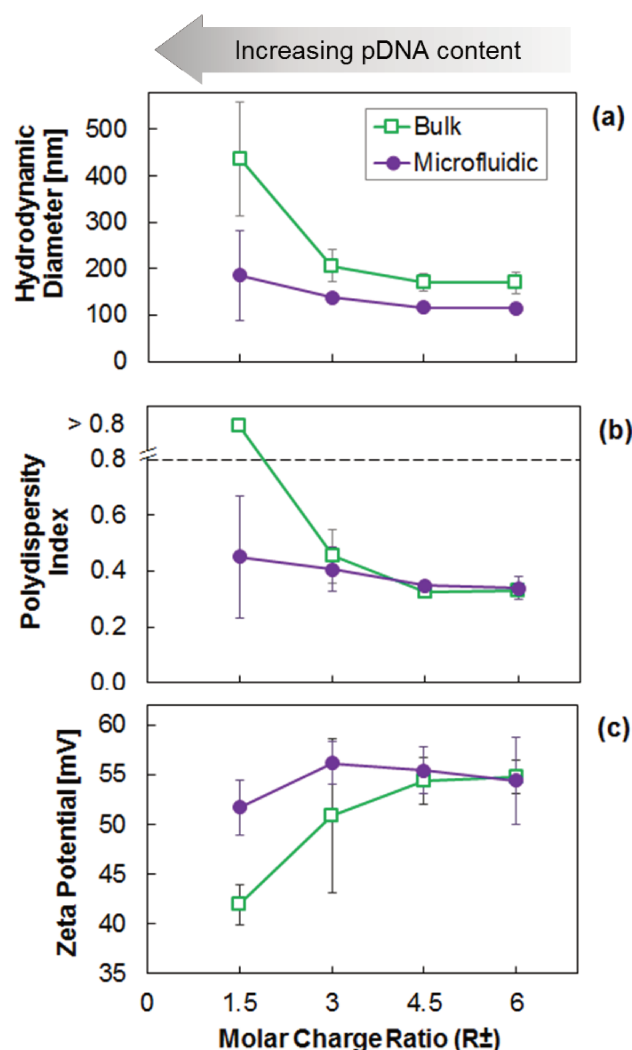


**Figure 3.2.** Physicochemical properties of plasmid DNA (pDNA)/cationic liposome (CL) lipoplexes prepared by bulk-mixing (BM) and microfluidic processes. **(a)** Number-weighted hydrodynamic diameter, **(b)** polydispersity index (Pdl), and **(c)** zeta potential ( $\zeta$ ) of pDNA/CL lipoplexes assembled via bulk-mixing and microfluidic processes as a function of the molar charge ratio ( $R_{\pm}$ ). The flow rate of the liposomal streams was maintained at 160  $\mu\text{L}/\text{min}$ , and the flow rate of the pDNA stream varied from 22  $\mu\text{L}/\text{min}$  to 89  $\mu\text{L}/\text{min}$ . The Pdl above 0.8 was considered as an inappropriate measurement and is separated from the other values by a horizontal dotted line. The error bars correspond to the standard deviation of three independent experiments.

After the physicochemical studies of the lipoplexes, it has been assessed the pDNA incorporation into the liposomal structure (Figure 3.3) via assays of gel retardation and resistance to DNase I, as well as by assessing the accessibility of the pDNA to the PicoGreen® fluorescence probe. The ability of CLs to incorporate and retain the pDNA in their structure was evaluated via gel retardation assay (Figure 3.3a). As can be observed, only the free pDNA migrated out of the well, giving rise to characteristic bands. All lipoplexes tested were able to retard the pDNA inside the wells, which indicates that the pDNA was successfully incorporated into the lipoplexes using both assembly processes. In addition, to

investigate the degree to which the liposomal carriers mediate pDNA protection from nucleases degradation *in vivo*, an *in vitro* DNase I protection assay was performed (Figure 3.3b). Agarose gel electrophoresis demonstrated that free pDNA treated with DNase I, used as a negative control, was fully degraded, whereas free pDNA that was not incubated with DNase I, used as a positive control, migrated out of the well. Because it is possible to observe other bands than the one related to the supercoiled form, lipoplexes assembled by both processes at  $R_{\pm} 1.5$  exhibited some degradation induced by DNase I.

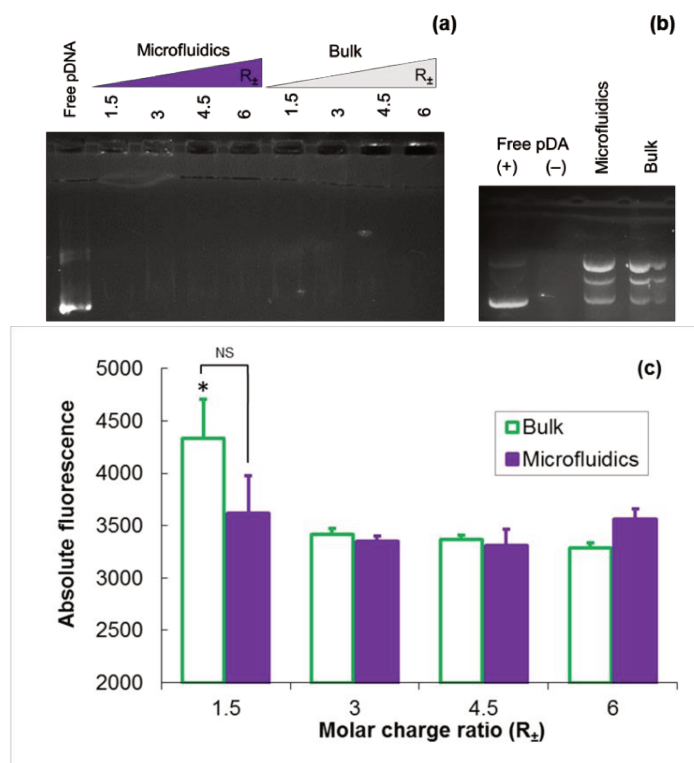


**Figure 3.3. Plasmid DNA (pDNA) incorporation into liposomal structure.** (a) Gel retardation assay, (b) resistance to DNase I at  $R_{\pm} 1.5$ , and (c) accessibility to the fluorescence probe for pDNA/cationic liposome lipoplexes assembled by bulk-mixing and microfluidic methods. For the DNase I assay, lipoplexes were prepared at  $R_{\pm} 1.5$ , and free pDNA was used as positive and negative controls via incubation with or without DNase I, respectively. \*  $p < 0.05$ , significantly different compared with other samples, except at  $R_{\pm} 1.5$  for microfluidic method. NS, not significant.

The pDNA accessibility of the lipoplexes was quantified under varying  $R_{\pm}$  conditions (Figure 3.3c). The probe becomes fluorescent upon binding double-stranded DNA that is accessible or loosely associated with the CL structure. As can be observed in Figure 3.3c, lipoplexes assembled by the microfluidic process did not show significant differences ( $p > 0.3$ ) from one another within the studied  $R_{\pm}$  range, whereas lipoplexes assembled by the BM process presented significantly higher relative fluorescence only at  $R_{\pm} 1.5$ . The higher pDNA accessibility of BM lipoplexes is in accordance with the zeta potential results (Figure 3.2c), in which increasing pDNA content reduced the superficial net charge of lipoplexes, likely due to

the influence of available negative charges from the phosphate group of the pDNA. Based on a comparative analysis, lipoplexes at the same  $R_{\pm}$  presented similar fluorescence values for both assembly processes, agreeing with a previous report of lipoplexes at  $R_{\pm} 6$  (41).

### 3.4.2. Nanostructural analysis by SAXS

The SAXS intensity profiles of the bulk and microfluidic series at different  $R_{\pm}$  values ( $R_{\pm} 1.5, 3, 4.5$  and  $6$ ) were measured and compared with those of pure CLs. Figure 3.4 shows the scattering curves for all systems. The pure CLs presented a typical scattering profile for a unilamellar vesicle system, whereas lipoplexes assembled by the BM and microfluidic processes showed a very broad correlation peak corresponding to a periodicity that varied from  $65$  to  $67 \text{ \AA}$ , depending on the system. This correlation peak was associated with the fraction of the system exhibiting multilamellar order. As expected for this lipid composition,(21) inverse hexagonal phases were not observed for any studied samples. As the  $R_{\pm}$  decreased to  $1.5$ , the correlation peak became more pronounced, and a second diffraction peak appeared, indicating a higher ordering of the bilayer stacking. Through proper modelling of the scattering curve, it is possible to obtain information about the membrane structure and the long-range ordering. The model used here is described in terms of Equation 1 and is detailed elsewhere.(21,61,62) Briefly,  $P(q)$ , or the form factor, carries information about the shape of the bilayer and its electronic contrast, and it is described mathematically as the square modulus of the Fourier transform of a sum of equally spaced Gaussian functions, which simulates the EDP.  $S(q)$ , or the structure factor, carries information about the system periodicity, membrane rigidity and average number of correlated bilayers; the modified Caillé structure factor was used to simulate the bilayer stacking.

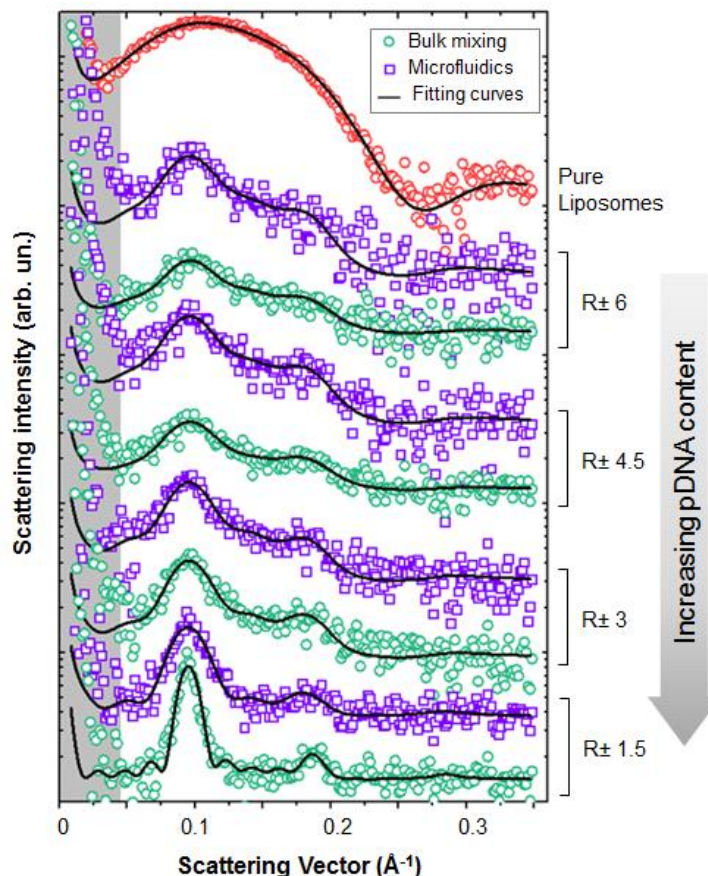


**Figure 3.4.** Nanostructural SAXS scattering intensities of liposomes and lipoplexes assembled by microfluidic and bulk-mixing processes for systems with a varying molar charge ratio ( $R_{\pm}$ ). The model does not consider  $q$  values smaller than  $0.05 \text{ \AA}^{-1}$ , which are in the gray shadowed area.

As a first attempt to fit the scattering intensity, it was considered a model in which each of the pDNA/CL lipoplexes ( $R_{\pm} 1.5, 3, 4.5$  and  $6$  for BM and microfluidic mixing, with pure CLs for comparison) had its own form and structure factors. However, due to the low scattering intensity of the system, the statistics for the experimental data were poor, and therefore, it was not possible to obtain a stable solution for the model parameters. To achieve more stable fitting, a second attempt was based on previous results obtained by our group for pDNA/CL lipoplexes (21). In this model, additional constraints were included, and the following was assumed: (i) The form factor of the bilayers of lipoplexes does not change significantly relative to that of pure liposomes, even when high amounts of pDNA are present. In fact, it was observed that the bilayer thickness slightly increased proportionally to the pDNA content (Figure 3.5b), likely due to rearrangement of the lipid heads near the DNA. In this sense, the form factor of all systems could be approximated as the form factor of the pure CL curve (Figure 3.4a) where the bilayer thickness is scaled by a parameter which takes into account this increase. According to our data, the rearrangement of the lipid heads

increased the mean bilayer thickness by less than 5% compared with what was observed for pure CLs (Figure 3.5b). (ii) When the number of correlated bilayers is approximately 2, the value of the Caillé parameter is lower than 0.05, and the periodicity is near 66 Å (Table I(21)). When the number of correlated bilayers (N) is higher than 2, the value of the Caillé parameter increases (to approximately 0.08 for  $N = 5.2 \pm 0.5$ ), and the periodicity also has a slight increase (to  $66.6 \pm 0.2$  Å, according to the same reference). Based on this information, the value of the Caillé parameter was fixed at 0.05 and the value of the periodicity at 66.0 Å for all systems. The reason to fix these parameter values was to obtain accuracy in the multilamellar phase fraction, which has a strong correlation with the Caillé parameter, and the form factor parameters, which have a strong correlation with the periodicity parameter when the number of stacking bilayers is near 2 (as in our case).

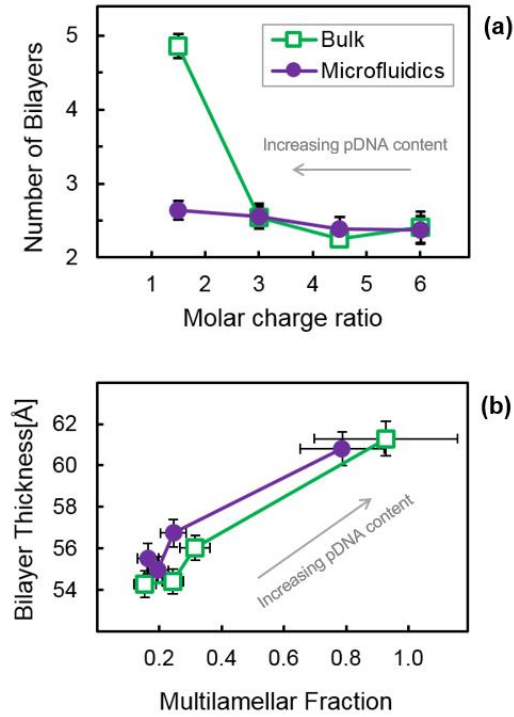


**Figure 3.5. Parameters obtained from a simultaneous fitting of the SAXS scattering intensities.** (a) Average number of correlated bilayers (N) as a function of the molar charge ratio ( $R_{\pm}$ ). (b) Multilamellar phase fraction and bilayer thickness of lipoplexes assembled by bulk-mixing and microfluidic processes. The solid lines are a visual guide to better demonstrate the trend of the variations. The error bars correspond to different fitting procedures.

Under the assumption that the overall bilayer shape is the same for the pure CLs and the lipoplexes, one can describe the system by using only 5 model parameters: (i) the fraction of multi-bilayer structures ( $f_{mb}$  in Equation 1), (ii) the number of correlated bilayers (N), (iii) the scaling parameter that takes into account the increase in the bilayer thickness with the inclusion of the pDNA, (iv) an overall scaling factor, and (v) a constant background.

Using this approach, it was possible to closely monitor the influence of  $R_{\pm}$  on the first three parameters (the fraction of multilamellar structures, the number of correlated layers and the bilayer thickness), which are of great interest when comparing the bulk and microfluidic processes used to produce the lipoplexes.

In Figure 3.5, the results of the fitting of the SAXS intensity profiles are shown for the number of correlated bilayers ( $N$ ), the multilamellar phase fraction ( $f_{mb}$ ) and the bilayer thickness. The presence of pDNA in the liposomal system induced the formation of a multilamellar phase with an average number of stacking bilayers higher than 2 (Figure 3.5a). The value of the number of correlated bilayers ( $N$ ) for lipoplexes assembled by both processes was  $\sim 2.5$ , except at  $R_{\pm} 1.5$ , at which lipoplexes assembled by the BM process exhibited a higher number of stacking bilayers ( $N = 4.9 \pm 0.2$ ). This is in good agreement with our previous finding that lipoplexes prepared by the BM process exhibited fractions of multilamellar populations with  $N \sim 5.2$ , which was only observed near the isoelectric ratio ( $R_{\pm} 1.8$ ) (21). Interestingly, microfluidic-assembled lipoplexes presented a lower value for  $N$  than those from BM did, although similar multilamellar phase fractions were presented at  $R_{\pm} 1.5$ . This shows that lipoplexes close to the isoelectric ratio can present very distinct bilayer stacking orders according to the assembly process. As can be observed in Figure 3.5b, the multilamellar phase fraction and the average bilayer thickness increased with the pDNA content in lipoplexes assembled in both processes, i.e., decreasing  $R_{\pm}$ . For the multilamellar phase fraction, one would expect the observed behavior because the pDNA plays the role of an electrostatic adhesion between two consecutive bilayers, and therefore, increasing the pDNA content would increase the fraction and/or the number of stacking bilayers. The average bilayer thickness increases with the pDNA content because the pDNA adheres to the headgroup region of the lipid bilayer. As the SAXS intensity was related to the EDP across the bilayer in our particular case, the presence of the pDNA increased the bilayer's effective size observed by the technique. As a consequence, the average bilayer thickness was proportional to the multilamellar phase fraction, as can be observed in Figure 3.5b. The differences observed under high pDNA loading conditions are likely due to the mixing characteristics of each process employed.

The microfluidic device employed here utilizes the hydrodynamic flow-focusing technique to control the convective-diffusive mixing of miscible fluids under laminar flow. Under high pDNA loading conditions, the gradual mixing of species along the main channel enabled better and more homogeneous accommodation of the pDNA into the liposomal structure, resulting in smaller lipoplexes with a lower number of stacking bilayers, as illustrated in Figure 3.6. Conversely, due to BM characteristics, when all pDNA is added to

the liposome dispersion in conventional BM processes, the strong and fast interactions between positive/negative charges lead to the formation of larger aggregates with higher polydispersity (Figure 3.2). In addition to differences in the fluid mixing, the accessibility to the pDNA probe, the Caillé parameter and the bilayer thickness of lipoplexes were significantly similar at  $R \pm 1.5$ , whereas the properties of size, size polydispersity, zeta potential and the number of stacking bilayers significantly changed when employing different techniques. This indicates that the intermolecular interactions of noncovalent bonds between cationic lipids and anionic pDNA were unaffected by the assembly processes, although the pDNA arrangement into the bilayer structures of lipoplexes significantly changed.

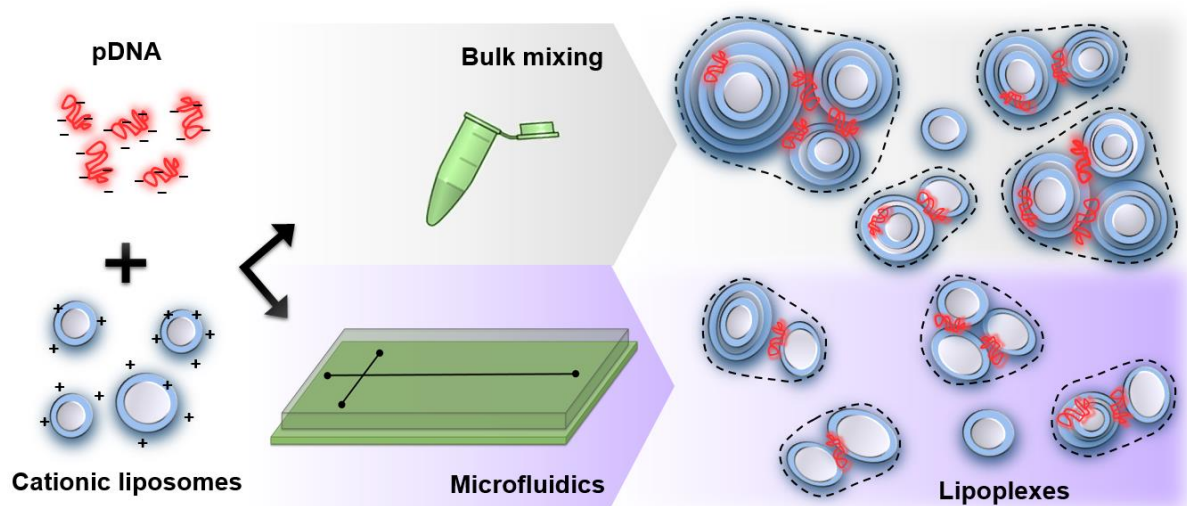


**Figure 3.6.** Schematic representation of the electrostatic assembly of plasmid DNA and cationic liposomes via bulk-mixing (BM) and microfluidic processes. At  $R \pm 1.5$ , microfluidic devices generated smaller lipoplexes with lower polydispersity and a lower number of stacked bilayers than the conventional BM assembly process did.

### 3.4.3. Microfluidic-assembled lipoplexes achieved higher gene delivery efficiency under high pDNA loading conditions

Having determined key differences in the physicochemical and structural properties of pDNA/CL lipoplexes assembled by the microfluidic process, the effects of those differences on the biological role of pDNA/CL lipoplexes assembled by different processes have been investigated (i.e., via transfection studies). Lipoplexes were prepared ~12 h prior to *in vitro* assays in prostate cancer cells, which were then analyzed by flow cytometry. Lipoplex internalization at  $R \pm 1.5$  was followed to evaluate the kinetics of lipoplex internalization by

cells (Figure 3.7a). For this, CLs were fluorescently labeled prior being complexed with pDNA. It is possible to observe that microfluidic lipoplexes exhibited faster kinetics of internalization, with more than 85% of cells having internalized CLs after 30 min, whereas only ~30% of cells had internalized BM lipoplexes. In addition to having distinct internalization kinetics and physicochemical properties, lipoplexes assembled by the two studied processes achieved similar cell internalization levels (~95%) after 2 h. However, microfluidic-assembled lipoplexes achieved a transfection efficiency approximately 2-fold higher than that of BM-assembled lipoplexes (inset graph of Figure 3.7a) at  $R_{\pm} 1.5$ . As a positive control, the commercial transfection reagent Lipofectamine (LF2k) has been employed; Figure 3.7a (inset graph) shows the higher transfection efficiency achieved by the LF2k compared with pDNA/CLs formed by the microfluidic and BM processes at  $R_{\pm} 1.5$ . In addition to the lower transfection efficiency of the lipid composition employed here relative to that of LF2K, it is known that the multivalent cationic lipid DOSPA that is present in LF2K results in cytotoxic effects that reduce cell viability by approximately 30%, limiting *in vivo* studies (21).

The effects of varying  $R_{\pm}$  conditions on transfection efficiency were then evaluated for lipoplexes assembled by both processes. In Figure 7b, it is possible to observe that the pDNA content in the lipoplexes had a strong influence on transfection efficacy, as was expected based on previous work.(21,51) No significant difference was found in the percentage of transfected cells at  $R_{\pm} 3, 4.5$  and 6 when comparing both processes; it can be observed that when  $R_{\pm}$  decreased from 6 to 3, i.e., when the pDNA loading capacity was increased, there was an increase in the transfection efficiency. Surprisingly, at  $R_{\pm} 1.5$ , i.e., under higher pDNA loading conditions, the transfection efficiency increased for the microfluidic-assembled lipoplexes, whereas it was reduced for the BM-assembled lipoplexes. This corroborates the previous physicochemical studies, in which microfluidic-assembled lipoplexes exhibited size and zeta potential properties that were more convenient for gene delivery applications. The *in vitro* results indicate that the presence of larger structures with a higher average number of stacking bilayers impaired pDNA internalization and processing by cells.

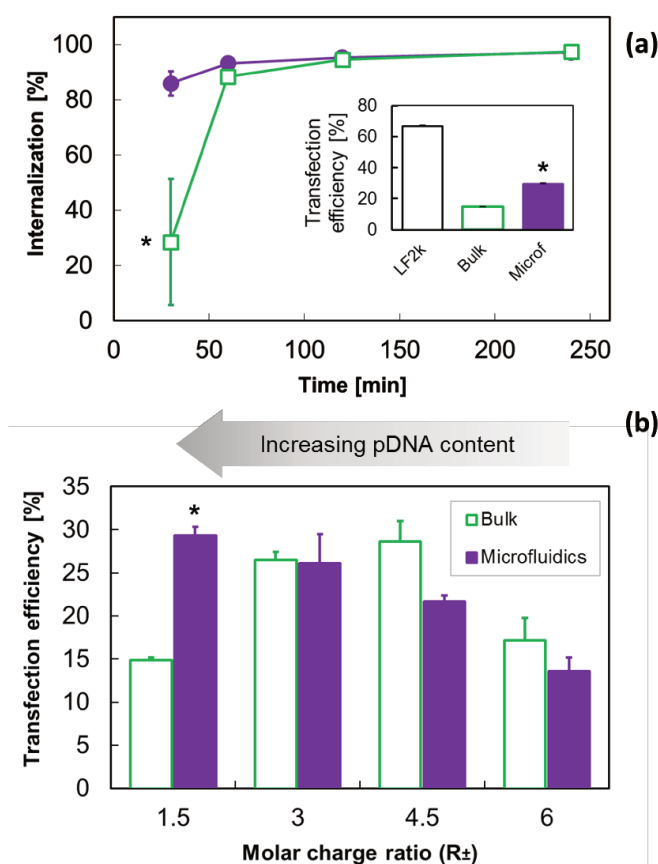


**Figure 3.7. *In vitro* gene delivery evaluation of lipoplexes.** Transfection of plasmid DNA (pDNA)/cationic liposome lipoplexes assembled by microfluidic and bulk-mixing processes into PC3 cancer cells. Cells were transfected with EGFP-encoding pDNA and analyzed by measuring the EGFP-positive cells by flow cytometry. **(a)** Internalization kinetics of lipoplexes at  $R_{\pm} 1.5$ . Lipofectamine (LF2k) was used as a positive control and compared with lipoplexes at  $R_{\pm} 1.5$ , as shown in the inset graph. **(b)** Transfection efficiency of lipoplexes under varying  $R_{\pm}$  conditions. Each value represents the SD of at least three replicates. \*  $p < 0.05$ , significantly different compared between pairs at the same  $R_{\pm}$ .

The microfluidic-assembled lipoplexes achieved significantly equal transfection efficiencies at  $R_{\pm} 1.5$  and 3. This corroborates the physicochemical and structural results that showed significantly similar values for particle size, polydispersity, and zeta potential (Figure 3.2); pDNA accessibility (Figure 3.3); and the number of bilayers (Figure 3.5) for lipoplexes assembled in the microfluidic process. Because lipoplexes achieved similar levels of transfection under such  $R_{\pm}$  conditions, the main advantage of using lipoplexes at  $R_{\pm} 1.5$  relies on the amount of cationic lipid in the formulation. In transfections mediated by lipoplexes, an excess amount of cationic lipid can compromise cell viability, i.e., the lower the amount of cationic lipid employed is, the lower the cytotoxicity is (50,65,69). Lipoplexes assembled by the microfluidic process achieved high transfection efficiency under high pDNA

loading conditions, utilizing less amount of cationic lipids. Overall, the microfluidic-assembled lipoplexes showed unique physicochemical and structural features under high pDNA loading conditions (i.e., smaller size, lower polydispersity and structural arrangements with fewer stacked lipid bilayers), which affected cellular processing and resulted in higher transfection efficiency.

### 3.5. Conclusion

In this work, for the first time, it was found that microfluidic devices generated lipoplexes with increased transfection efficiency compared with lipoplexes generated by the conventional BM process under high pDNA loading conditions. At  $R \pm 1.5$ , i.e., in the presence of high pDNA content, the particle size, polydispersity, nanostructure and biological efficiency of the microfluidic-assembled lipoplexes were significantly different. In addition to the advantages of using miniaturized systems, under such conditions, microfluidics provided more convenient fluid dynamics for the mixing of pDNA and CLs, generating smaller lipoplexes with a lower number of stacked bilayers, which in turn resulted in enhanced *in vitro* transfection efficiency. Lipoplexes prepared with other pDNA contents exhibited similar physicochemical properties and biological results. Although BM processes are easy to employ on the laboratory scale, the need for automatized processes with higher throughputs for lipoplex assembly might be a key challenge for the production of nonviral gene delivery systems. The results presented here may contribute to the development of processes for lipoplex assembly and to the understanding of the influence of mesoscopic properties on *in vitro* gene delivery.

### 3.6. Acknowledgments

The authors gratefully acknowledge the financial support of the São Paulo Research Foundation – FAPESP, Brazil (Grants No. 2012/23143-9 and 2011/19952-6). The microfluidic devices were constructed at the Microfabrication Laboratory (LMF) of the Brazilian Nanotechnology National Laboratory (LNNano). We thank Prof. M. H. Santana for the laboratory infrastructure support at Unicamp.

## 4. Effects of series and pseudo-parallel microfluidic arrangements for the synthesis of long-circulating liposomes decorated with PEG<sup>§</sup>

Tiago A. Balbino<sup>a</sup>, Abraham H. Abouzeid<sup>b</sup>, Wyatt N. Vreeland<sup>b</sup>, Lucimara G. de La Torre<sup>a,\*</sup>

<sup>a</sup> School of Chemical Engineering, University of Campinas, UNICAMP, Campinas, SP, Brazil;

<sup>b</sup> Material Measurement Laboratory, Biomolecular Measurement Division, National Institute of Standards and Technology, Gaithersburg, USA

\*Corresponding author: [latorre@feq.unicamp.br](mailto:latorre@feq.unicamp.br)

### 4.1. Abstract

Continuous-flow fluidic devices with microfluidic hydrodynamic focusing (MHF) areas associated in series and pseudo-parallel configurations are explored for the synthesis of nanoscale, stealth liposomes conjugated with poly(ethylene glycol) (PEG). Microfluidic platforms enable the direct formation of liposomes obviating the need for laborious post-processing steps to reduce and homogenize particle size, which are among the most important characteristics of a liposome preparation). However, these systems produce a low concentration of liposomes which can impair future applications in clinical trials of nanomedicines. In this study, microfluidic geometries were designed with MHF regions in series and pseudo-parallel architectures to generate PEGylated and non-PEGylated liposomes in order to increase the liposome concentration in the final formulation relative to a single MHF. A series architecture of 3 MHF's produced liposome with mean geometric radii in the range of 70 nm to 100 nm and polydispersities in the range of 0.3 and 0.4 as measured by light scattering. Pseudo-parallel architecture generated PEGylated liposomes with narrower geometric radii distributions, with controllable modal sizes by varying the FRR conditions, with mean geometric radii in the range of 70 nm to 100 nm and an average polydispersity of 0.2. Concentrations of liposomal formulations obtained by both series and pseudo-parallel architectures were 3 times higher than those compared to single MHF under similar focusing conditions. Series and pseudo-parallel microfluidic architectures show

---

<sup>§</sup> Manuscript to be submitted to Journal of Colloid and Interface Science

promise for producing liposome preparations at concentrations more suitable for further biomedical applications.

## 4.2. Introduction

Liposomes are vesicular systems with an aqueous core surrounded by one or more phospholipid bilayers. First described by Bangham et al (1965), liposomes are formed when certain lipids are placed in an aqueous phase and spontaneously self-assemble into vesicles to yield more entropically favorable states of free energy (70). With diameters ranging from approximately 20 nm up to several micrometers, they have applications in the biomedical and molecular biology (71) fields but also in food (72) and cosmetic (73) areas. In the biomedical area cationic liposomes show promise for the efficient delivery of genes into cells (74) through the condensation and retention of the negatively charged genetic material on the cationic charges of liposomes. Liposomes are particularly useful in gene delivery systems as they enable different strategies for surface modification to prevent the attachment of serum proteins and subsequent recognition by the mononuclear phagocyte system when administered systemically. Poly(ethylene glycol) (PEG) is perhaps the most widely used surface modification agent to form stealth liposomes; it provides a protective shield on the exterior region of the liposomes, as illustrated in Figure 4.1, which delay clearance from the body, resulting in extended blood-circulation times (75).

Several methods for producing liposomes with different properties have been demonstrated, summarized elsewhere (76,77). Briefly, the thin-lipid film hydration method is one of the most widely used techniques; however, as with most conventional bulk-scale techniques, it requires cumbersome post-formation operations for reduction and homogenization of size; these include sonication or repeated membrane extrusions. Current developments in liposome production have focused on reducing time-consuming and number of

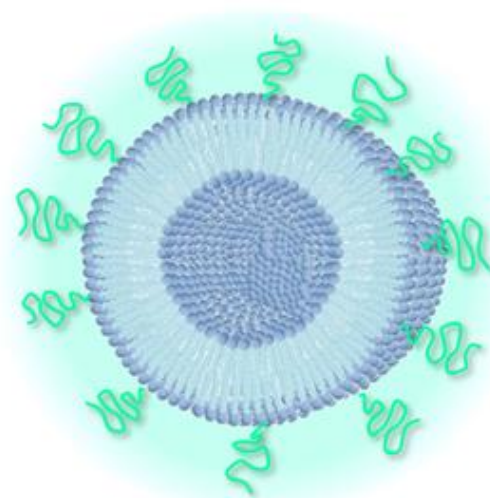


**Figure 4.1.** Schematic illustration of “stealth” liposome sterically functionalized with hydrophilic polymer (surrounding green area) for targeted delivery.

steps by means of high-throughput processes (78,79). In this sense, microfluidic techniques have been employed as alternative tools for the continuous synthesis of monodisperse vesicles with tunable sizes, exempting additional post-processing step for size control (80).

Microfluidics is a versatile technology to manipulate fluid flows in micrometer-sized channels at very low Reynold ( $Re$ ) and Péclet ( $Pe$ ) numbers, where molecular diffusion prevails over advective mixing. For the synthesis of nanoparticles, microfluidic systems can provide controlled, and tunable mixing, resulting constant and reproducible mixing and mass transfer environments and high-throughput processes (81). Mixing in microfluidic devices occurs almost entirely by molecular diffusion (*i.e.* low  $Pe$ ) under laminar flow (*i.e.* low  $Re$ ), which results in a more precise control of particle size and size distributions and therefore enhanced batch-to-batch reproducibility (size and size homogeneity is often among the most important characteristics of a liposome preparation). These advantages are increasingly promising for the development of platforms that enable formation of liposomes of controlled and reproducible size. Among the microfluidic methods, the hydrodynamic flow-focusing (HFF) technique is one of the most explored for liposome formation in continuous flow. This platform comprises a center lipidic-tincture stream that is compressed or focussed by two perpendicular or oblique aqueous streams. The diffusive mixing of water into the alcohol along this focusing region causes increased fluid hydrophilicity where the phospholipids self-assemble into bilayers fragments, which grow by combining with each other until they start to bend and close into spherical vesicles, forming liposomes (33). The use of microfluidic HFF technique for liposome formation has been demonstrated for gene and vaccine therapy (34), modelling of artificial cells (82), passive transdermal drug delivery and also for folate-functionalized target drug delivery (83,84).

Since its first report (31), different microfluidic platforms based on HFF technique have been investigated to improve and optimize the liposome characteristics. As an example, a three-dimensional microfluidic HFF device was designed to produce liposomes in which glass capillaries were concentrically assembled so that the alcohol and water streams could radially diffuse into each other. This device was constructed from low-cost, commercially available components, and could produce nanoscale liposomes at volumetric rates up to four orders of magnitude than single two dimensional planar HFF device (79). Despite the advances to improve the characteristics of microfluidic processes, the development of simple and easy to implement alternatives for production of liposomes using microfluidic platforms remains a challenge, especially for gene delivery applications. Most of these studies have reported an increase in the volumetric throughput of microfluidic

processes for liposome production (78,79,85) but few has attempted to the increase in lipid concentration of the final liposome formulations and the inherent colloidal effects, what can be a limiting factor for gene delivery clinical trials.

In the present work, we explored in-line microfluidic arrangements to synthesize stealth PEG-conjugated liposomes for future applications in gene delivery. Multiple HFF regions were prepared in series and pseudo-parallel arrangements in order to evaluate their effects on the vesicle formation and concentration of obtained liposomes. We have previously employed a microfluidic device with two HFF regions in a pseudo-parallel architecture to generate cationic liposomes capable to delivery plasmid DNA (pDNA) into mammalian cells *in vitro* (34). Here, the performance of series and pseudo-parallel configurations with three HFF regions were evaluated at different volumetric flow-rate ratio (FRR) between aqueous and ethanol streams, at high and low concentration of the lipid concentration in the lipidic tincture, to generate both PEGylated and non-PEGylated liposomes. The results were compared to conventional single HFF geometry. The resultant particles were fractionated with asymmetric flow field-flow fractionation (AF4), for size separation of samples, and coupled to a multiangle light scattering (MALS) detector, for size characterization. At similar focusing conditions, both microfluidic architectures studied were able to generate PEG-conjugated liposomes with higher lipid concentration than those obtained with the single HFF geometry.

## **4.3. Experimental**

### **4.3.1. Microfluidic Device Fabrication**

Polydimethylsiloxane (PDMS)/glass microfluidic devices were obtained employing soft lithography with dry film photoresist techniques (86). The designs of the devices' geometries were projected using AutoCAD (Autodesk). To fabricate the masters, two dry film photoresist layers (Riston MM115i, DuPont, Research Triangle Park, NC) (40  $\mu\text{m}$  nominal thickness each) were sequentially laminated onto a clean glass slide. The lamination process was conducted using a feed rate of 0.02 m/s at 110  $^{\circ}\text{C}$ ; the laminated glass slide was placed on a hot plate at 100  $^{\circ}\text{C}$  for 20 min to promote adhesion between the photoresist and the glass substrate. The laminated glass slide was then exposed through a photomask with a collimated UV flood exposure at a dose of 72  $\text{mJ}/\text{cm}^2$  for a single photoresist layer, with an increase of 20% in UV dose time per additional photoresist layer. The structure was developed using a solution of 1 % (w:v) of sodium carbonate. The master was then placed in

a plastic petri dish and the precursor material of PDMS layers (Sylgard 184, Dow Corning Corp. Midland, MI) was poured on top. PDMS channels and glass substrate were irreversibly bonded by oxidizing the surfaces using a plasma chamber via microwave oxidation (87). All the channels had a rectangular-like cross section with a depth of 70  $\mu\text{m}$  and a width of 80  $\mu\text{m}$ .

#### 4.3.2. Liposome preparation

Three microfluidic geometries with different hydrodynamic flow-focusing (HFF) architectures were investigated for liposome synthesis. Figure 4.2a shows the conventional single hydrodynamic focusing configuration. The second architecture was a series hydrodynamic focusing configuration (Figure 4.2b), the second and third lipid stream inlets are focused by the previous stream containing pre-formed liposomes, which is split into two channels before the crossjunction. The third geometry is a parallel hydrodynamic focusing configuration (Figure 4.2c) with a layout where the focused lipid streams parallelly flow along the main channel.

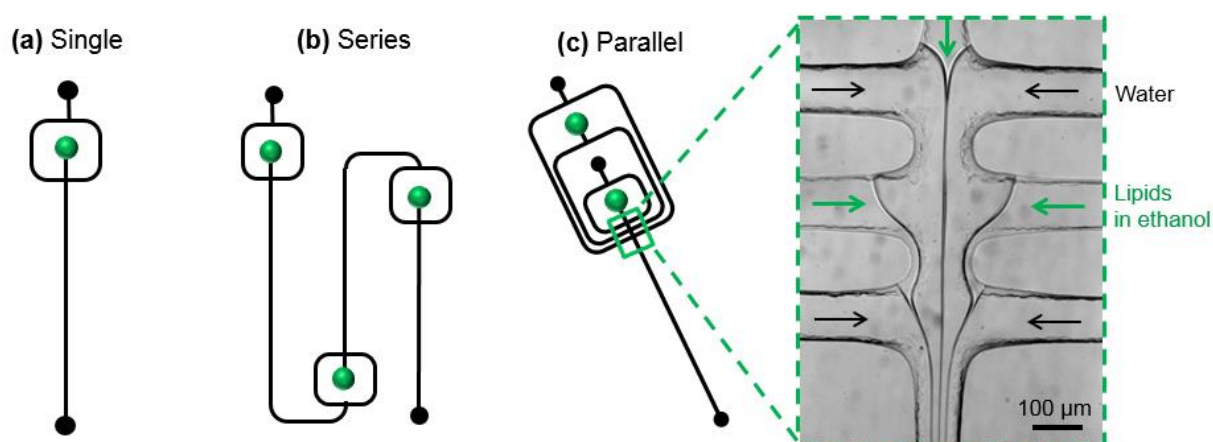


**Figure 4.2.** Microfluidic geometries used for liposome synthesis. (a) single, (b) series and (c) pseudo-parallel hydrodynamic focusing configurations. Inset shows an optical micrograph of the parallel configuration at an aqueous flow rate of 200  $\mu\text{L}/\text{min}$  and a flow rate ratio (FRR) of 50. The green circles represent lipidic tincture inlets, the black circles represent aqueous inlets of solution outlets.

Egg phosphatidylcholine (EPC), 1,2-dioleoyl-sn-glycero-3-phosphoethanolamine (DOPE), 1,2-dioleoyl-3-trimethylammonium-propane (DOTAP), and 1,2-dimyristoyl-sn-glycero-3-phosphoethanolamine-N-[methoxy(polyethylene glycol)-2000] (PEG-PE) were all obtained from Avanti Polar Lipids Inc. For non-PEGylated liposomes, the lipids EPC:DOTAP:DOPE were mixed in chloroform (Mallinckrodt Baker Inc., Phillipsburg, NJ) in the proportion of 50:25:25 %molar, respectively. For PEGylated liposomes, 5% of PEG-PE

was added to the formulation and the final proportion was 50:25:20:5 %molar of EPC:DOTAP:DOPE:PEG-PE, respectively. Lipid mixtures were added in scintillation vials to be dried overnight in a vacuum desiccator. The dried lipid blend were then dispersed in anhydrous ethanol (99.5% Sigma-Aldrich) to lipid concentrations ( $C_{LIP}$ ) of 5 mM and 25 mM. Deionized water and lipids dispersed in ethanol were passed through 0.22  $\mu$ m filter (Millipore Corp., New Bedford, MA) and then loaded into glass gastight syringes (Hamilton Co., Reno, NV). Syringe pumps (model PHD2000, Harvard Apparatus Inc., Holliston, MA) were used to control the flow rate of each stream into the inlet channels. In the experiments, the total aqueous volumetric flow rate was kept constant at 200  $\mu$ L/min and the total lipid volumetric flow rate varied according to the FRR to be studied. FRR is defined as the ratio of the total aqueous volumetric flow rate to the total lipid-ethanol volumetric flow rate. Therefore, at a given FRR value and  $C_{LIP}$ , all three microfluidic arrangements produce liposomes with the same final lipid concentration. Microfluidic-synthesized liposomes were collected in triplicates from the microchannel outlet for subsequent analysis.

#### **4.3.3. Asymmetric Flow Field-Flow Fractionation (AF4) with Multi-Angle Laser Light Scattering (MALLS) and Quasi-Elastic Light Scattering (QELS)**

An Eclipse AF4-MALLS instrument (DAWN EOS and QELS, Wyatt Technology, Santa Barbara, CA) was used for high-resolution size-based separation and characterization of the microfluidic-produced nanoparticles (29). Briefly, AF4 provides the fractionation of particles based on their diffusion coefficients in a flow channel with a perpendicular crossflow, as illustrated in Figure 4.3. The crossflow focuses the sample against the membrane at the bottom of the channel, what creates a parabolic flow profile due to the laminar flow of the fluid. This flow velocity gradient separates particles of different sizes (different diffusion rates) as they flow along the channel. The fractionation occurs with smaller particles eluting first than larger ones. The eluting outlet stream is connected to the MALLS-QELS instrument to obtain the data for size analysis.

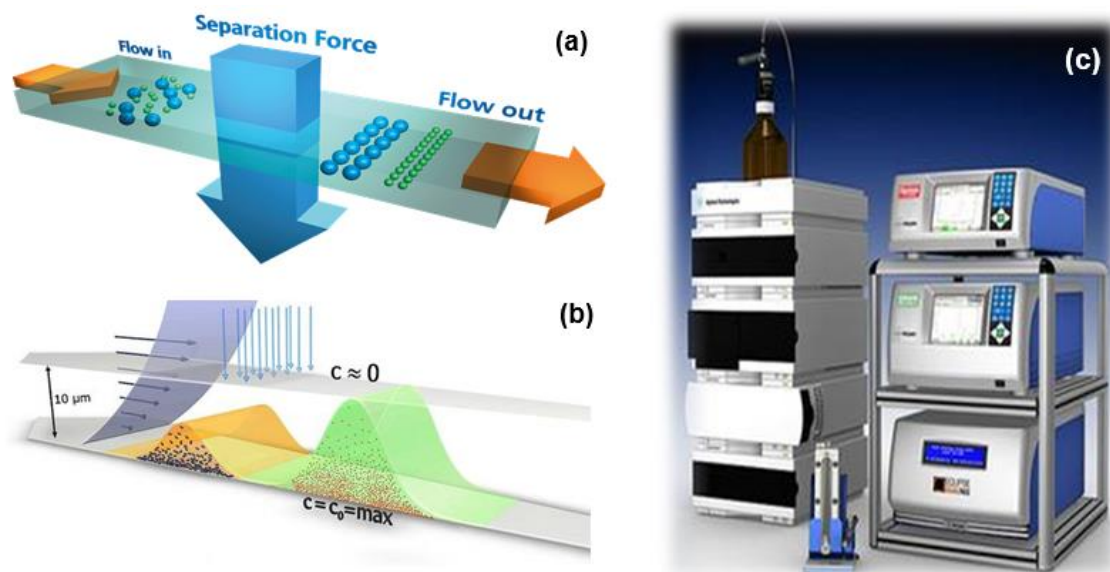


**Figure 4.3.** (a) Schematic representation of the asymmetric flow field-flow fractionation (AF4) theory. (b) Schematic representation of particle size distribution along the separation channel, during the sample fractionation according to the flow velocity profile. (c) Equipment apparatus of the AF4 system coupled to the MALLS instrument (Images Copyright: Wyatt Technology Europe GmbH).

PBS buffer containing 0.1% sodium azide was used as elution buffer for sample fractionation. The AF4 channel used in this study had a  $250\ \mu\text{m}$  thick separation spacer, and a cellulose membrane with the molecular weight cutoff value of 10 kDa was used for the crossflow partition. Flows were automatically controlled with Eclipse 2 software (Wyatt Technology, Santa Barbara, CA). A volume of  $150\ \mu\text{L}$  of samples was injected and the separation was performed with a  $1\ \text{mL/min}$  channel flow rate. After injection and focusing steps, the crossflow was linearly decreased from  $2.0\ \text{mL/min}$  to  $0\ \text{mL/min}$  over a 60 min elution period. Size of fractionated particles was estimated using the MALLS and QELS detectors, and ASTRA 6.1 software (Wyatt technology) was employed for data processing. Static light scattering intensity ( $\lambda=690\ \text{nm}$ ) was simultaneously measured at 15 angles. Samples were measured at 1 s intervals for the MALLS and 5 s intervals for the QELS. As discussed later, according to the characteristics of each elution peak, we applied two different models for size analysis: (i) solid sphere model and (ii) coated sphere model, which considers a spherical structure in which two radial regions have different refractive index (e.g., monolayered vesicles). The models showed good fit with the MALLS data and were used to determine the geometric radii distributions of the fractionated samples. AF4/MALLS evaluation of samples was performed to obtain accurate particle number size distributions with no need of assumptions of form distributions that are usually assumed in dynamic light scattering analysis (e.g. lognormal distribution). Thus, the polydispersity used herein does

not assume form distributions of samples and is defined as  $(R_{75\%} - R_{25\%})/R_{50\%}$ , in which X% of particles has a geometric radius below the radius  $R_{X\%}$  (33).

#### **4.4. Results and Discussion**

Liposome dispersions obtained by microfluidic methods are usually too dilute for direct use in pharmaceutical applications. Two multi-inlet configurations were designed to increase the inlet streams containing lipids in ethanol aiming at the increasing in lipid concentration of liposomes obtained in microfluidic devices. Changes in disposals of microchannels have significant modifications on hydrodynamic fluid flow characteristics and can influence lipids self-aggregation. These changes might affect liposome size and size distribution as prepared in the microfluidic device. Thus, liposomes with varying microfluidic process conditions were synthesized using two microfluidic configurations with series and pseudo-parallel architectures to investigate the influence on liposomes formation. A conventional architecture with a single HFF geometry was used to compare focusing conditions (FRR), the influence of ethanol presence in the aqueous phase on the liposome formation, and the similarities between PEGylated and non-PEGylated liposomes generated by microfluidic processes.

##### **4.4.1. Effects of FRR, PEG-PE lipid and ethanol using the single MHF architecture**

Since the influence of FRR variations can significantly affect particle size in microfluidic liposome formation, we first investigated varying FRR conditions for the lipid composition employed in this work. Figure 4.4a shows the size distribution analysis from AF4/MALS data of PEGylated liposomes generated by the single configuration. With increasing FRR values, the average modal liposome size increased with the size distribution profiles becoming less narrow. The geometric radii of non-PEGylated liposomes presented no significant changes under variations of FRR in range of 20 to 200, whereas PEGylated liposome sizes increased the increase in FRR from 153 to 286. It was previously observed that cationic liposomes composed of EPC/DOPE/DOTAP (2:1:1 molar) and produced using a single HFF microfluidic device exhibited increased sizes with increasing FRR from 8 to 18; whereas, using a double HFF microfluidic device, the sizes of liposomes were significantly independent of the FRR in the same studied range. Studies exploring similar geometries under varying operational conditions (e.g. volumetric throughputs, lipid concentration, temperature, and organic solvent) have shown that, under certain ranges of FRR, the size of liposomes with varying lipid compositions were nearly unaffected (33,34,85,88). In contrast,

under different conditions, studies using single HFF microfluidic devices for the synthesis of liposomes with un-charged and zwitterionic lipids overall liposome sizes increased with decreased FRR (29,33,83). One of the main differences in the experimental procedures of these studies is the lipid compositions utilized. It is expected that lipids that possess distinct properties, such as saturated or unsaturated chains, cationic and anionic phospholipids, cholesterol, surfactants, and a variety of phosphocholines will affect liposome self-assembly mechanisms (76,89) and the resultant liposome characteristics. Since the FRR effect seems to be dependent on lipid composition, these results together show the versatility of microfluidic platforms based on the HFF technique to produce liposomes with varying lipid compositions according to the desired application.

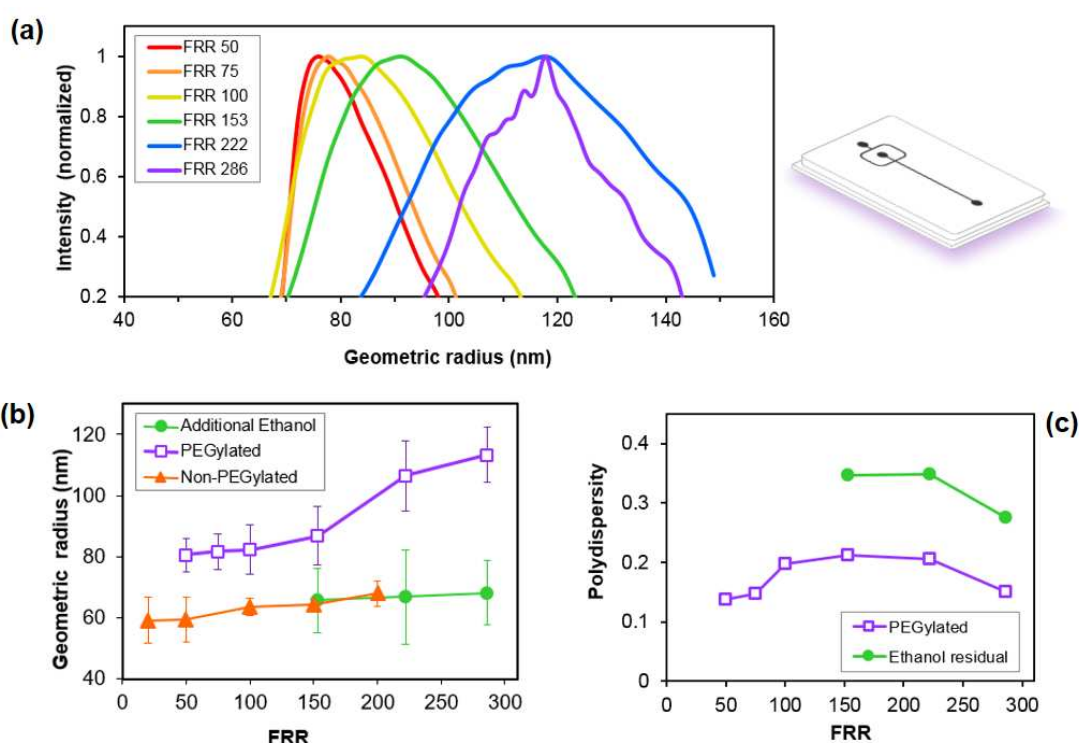


**Figure 4.4. Single hydrodynamic flow-focusing microfluidic device** (a) PEGylated-liposome size distributions at varying flow rate ratios (FRRs). (b) Geometric radius of PEGylated liposomes formed in the absence of ethanol and with the addition of ethanol in the aqueous phase, and non-PEGylated liposomes. (c) Size polydispersity of PEGylated liposomes with and with no ethanol, at a lipid concentration of 25 mM. The ethanol effects experiments were carried out by adding ethanol in the aqueous phase to mimic the amount of ethanol from each FRR condition; thus, FRR of 153, 222 and 286 had an ethanol content of 0.65%, 0.45% and 0.35% (v/v), respectively. Error bars are derived from the distribution of each liposome population, taken as the full width at half maximum divided by the modal diameter.

To evaluate the microfluidic self-assembly process of lipids with or without PEG, the formation of PEGylated and non-PEGylated liposomes was investigated using the single focusing microfluidic device (Figure 4.4b). At the studied FRR range, non-PEGylated

liposomes showed smaller geometric radii when compared to the PEGylated liposomes. This is likely due to the presence of the PEG chains that can reduce the hydrophobicity of the bilayers fragments edges, and thus favor the formation of larger bilayers fragments before they close into larger vesicles. PEG- and folate-conjugated liposomes composed of 1,2-dimyristoyl-sn-glycero-3-phosphocholine (DMPC), cholesterol, and the phospholipids chemically derivatized with PEG and folate were previously generated using a single HFF platform (83); in that case, it was observed that conjugated and non-conjugated liposomes exhibited similar mean sizes.

As discussed below, when using the series configurations, the side streams of the two consecutive focusing regions contain a certain amount of ethanol from the previous lipid inlet (in the series configuration) or from the side lipid streams that diffuse perpendicularly to the stream flow (in the parallel configuration) (Figure 4.2.b). Due to these differences in the geometries arrangements, experiments to explore the effects of the ethanol on liposome self-assembly were carried out to be compared further. It is known that the presence of alcohols can affect physicochemical and structural characteristics of liposomes and bilayers (85,90). Thereby, part of the effects of the presence of the ethanol was examined by pre-mixing ethanol in equivalent amounts to that from the previous lipid inlets to the aqueous streams. Figures 4.4b and c show that PEGylated liposomes obtained in the presence of ethanol in the aqueous phase had larger geometric radii and higher polydispersity than PEGylated liposomes obtained with no addition of ethanol. The mean geometric radii of PEGylated liposomes generated in the absence of ethanol were smaller than that of PEGylated liposomes obtained in the presence of ethanol in the aqueous streams. Figure 4.4c shows the size polydispersity of PEGylated liposomes with and without the presence of ethanol in the aqueous streams. The polydispersity relates the width of the size distribution with the median particle size; it is based on the number-weighted size distributions and can be estimated with no assumptions about the shape of the distribution profiles. It is possible to observe that the polydispersity of PEGylated liposomes is higher with the addition of ethanol in the aqueous phase. In the microfluidic mixing of streams, the driving force for ethanol-water diffusion is reduced in the presence of small amounts of ethanol. The reduction of diffusion velocity in the interface area of lipid and aqueous streams might have impaired a more homogenous lipid self-assembly process, leading to more polydispersed samples.

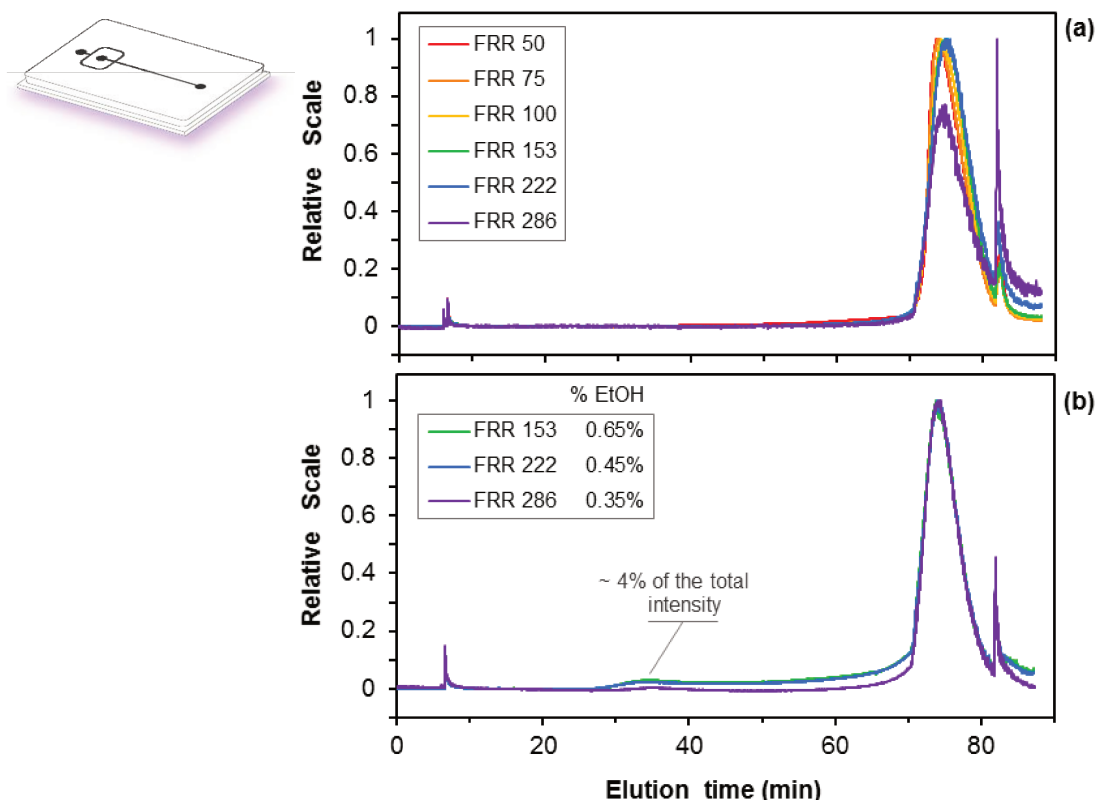


**Figure 4.5.** Intensity chromatograms of fractionated particles using AF4-MALS techniques. PEGylated liposomes produced at varying FRR conditions, in the absence of ethanol **(a)** and in the presence of ethanol as additive in the aqueous phase **(b)**, using the single microfluidic arrangement

The elution chromatograms of PEGylated liposomes from AF4-MALLS in Figure 4.5a shows that, in the region of 10 min to 80 min, there is only one peak between 70 and 80 min for each FRR condition studied. These more intense peaks had good fitting using the coated sphere model, which considers the aqueous core of vesicles surrounded by lipid bilayers (thickness of ~6 nm (34)). The less evident peaks at ~6 min and ~82 min are “system” peaks of the separation method used for the particles fractionation. The intensity chromatograms of the liposomes synthesized in the presence of ethanol (Figure 4.5b) had a low intensity peak at ~35 min, what suggests the presence of smaller structures. The size analysis of these peaks revealed they exhibit similar characteristics of micelles of PEG-PE molecules and they were not observed in any other sample without addition of ethanol in the aqueous phase, as will be in next experiments.

#### 4.4.2. Formation of liposomes using the series configuration

By comparing the single configuration with series and pseudo-parallel designs, the hydrodynamic focusing conditions differ at each FRR value since the total lipid flow rate is

split into 3 streams. By definition, FRR represents the sum of aqueous flow rates to the sum of inlet rates of lipids in ethanol; thereby, the single configuration has a 3-fold higher flow-rate of lipids than series and parallel configurations at a same FRR value. When using the single arrangement, higher focusing conditions (high FRR values) have narrower lipid streams being focused by the aqueous phases. Thus, FRR values of 153, 222 and 286 were examined using the single configuration since they have similar focusing conditions of FRR values of 50, 75 and 100, respectively, using series and pseudo-parallel configurations.

The formation of liposomes using the series configuration (Figure 4.2b) was carried out with all the three lipid inlets having the same lipid flow rate to render similar hydrodynamic focusing conditions (Fig. 4.2.b). Figure 4.6 shows the intensity chromatograms of the fractionated samples at lipid concentrations in the ethanol streams of 5 mM and 25 mM both with 5 mol% of the total lipid being PEG-PE. One can see that the peaks related to liposomes (at around 70 min to 80 min) are more evident at all the studied conditions compared to the peaks related to micellar structures (in the range of 30 min to 50 min). This was expected since it is known that, in colloidal suspensions, vesicular structures are thermodynamically more stable for phospholipids than micellar structures for the type of lipids utilized (89). It has been previously reported that PEG-PE mixtures of certain lipid compositions form micelles upon attempts to produce long-circulating liposomes under varying conditions, in which PEG-derivatized phospholipid can present different levels of incorporation into the lamellar phase (91,92). This phenomenon was considered firstly as a nuisance until it was realized that such micelles could present important features as particulate carriers of therapeutic and diagnostic agents (91).

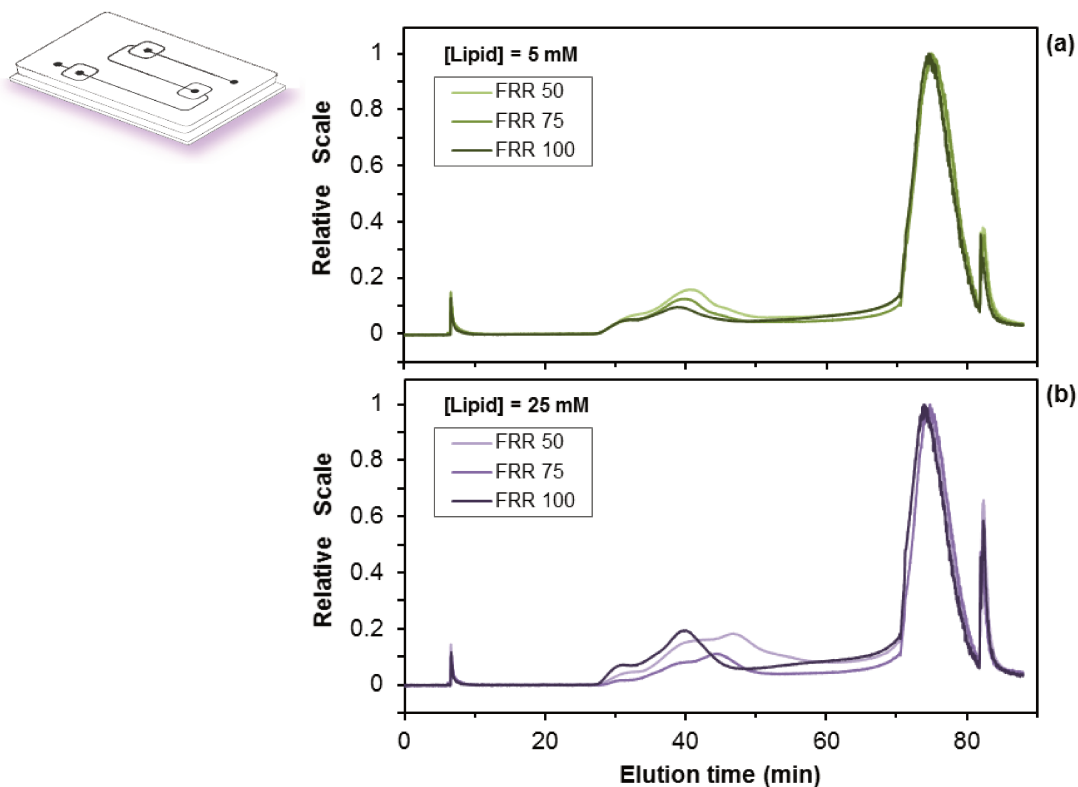


**Figure 4.6.** Intensity chromatograms of fractionated particles using AF4-MALS techniques. PEG-conjugated liposomes produced using the series configuration at varying FRR conditions at lipid concentration in the lipid stream of **(a)** 5 mM and **(b)** 25 mM.

Interestingly, at low lipid concentration, 5 mM, the peaks related to small structures is more pronounced than in samples produced under higher lipid concentration at 25 mM. The peaks of small structures had similar characteristics of the peak of pure PEG-PE micelles (data not shown) and had a better fit using a solid sphere model for the size analysis than the coated sphere model usually utilized for vesicles. The chromatograms show the formation of micelles is favored in the series configuration when using lower  $C_{LIP}$  than when using higher  $C_{LIP}$ . These micelle peaks are in accordance with the effects of the addition of ethanol on the formation of PEGylated liposomes (Figure 4.5b). Because of the presence of ethanol in the second and third HFF regions in the series configuration, the formation of smaller structures was expected since they were not observed in samples obtained in the absence of ethanol.

In micellar suspensions, the relaxation times for monomer exchange (“flip-flop”) and aggregate lifetime involve a diffusion-limited process that depends directly on monomer concentration; whereas in bilayers, monomer exchange is considerably slower as predicted by their much lower monomer solubility (Evans 1999, Patisti 1998). The microfluidic assembly of phospholipid mixtures containing PEG-PE molecules would thus favor the

formation of micelles prior the formation of liposomes according to different concentrations used, as observed in our data. The aggregation pattern of bilayers depends on structural units in a variety of different structural conformations that grow in the lateral direction, while micelles form well-defined aggregate at well-defined CMC (93). Monomers of amphiphiles molecules in aqueous solutions tend to self-assemble into micellar phases at low concentrations, forming other types of liquid crystal phases with the increase in monomer concentration (94). Thereby, with the presence of ethanol in the aqueous phase and at low  $C_{LIP}$ , the gradient of the concentration of monomers (phospholipids and PEG-PE) caused by the ethanol-water mixing favored the formation of micelles that is much faster than the formation of vesicles.

Size distribution profiles of particles produced by the series configuration are presented in Figure 4.7, which were obtained by treating the first elution peak as micelles and the second major peak as vesicles. Liposomes obtained at 5 mM showed narrower and more symmetric size distributions (Figure 4.7a), while liposomes obtained at 25 mM presented skewed and broader distributions (Figure 4.7b). Both lipid concentrations studied showed smaller structures in the geometric radius distributions previously identified as PEG-PE micelles. In general, liposomes produced at low  $C_{LIP}$  showed smaller modal geometric radii than liposomes produced at higher  $C_{LIP}$ , whereas the polydispersity of liposomes generated at low and high  $C_{LIP}$  were significantly similar. This is in agreement with previous reports on the formation of liposomes whose sizes increased with increased lipid concentrations in the alcoholic phase (34,85,95). The formation of phospholipid bilayer fragments (PBFs) theory predicts that the increase in the hydrophobicity promoted by the alcohol-water mixing favors the formation of PBFs that grow until they close into vesicles (33,34). As a result, the increase in  $C_{LIP}$  would cause the self-assembly of a higher quantity of PBFs in the vicinity, that would bind to adjacent PBFs growing in size before they enclose into vesicles with higher curvatures, i.e. larger in size. Another plausible explanation would be based on the formation of pro-liposomes (85); this theory assumes that pro-liposomes are formed when the alcohol is not completely depleted and pro-liposomes grow in size by “recruiting” lipid molecules until a critical hydrophobicity. With the mixing of the water and ethanol+lipids along the main channel, higher lipid concentration would result in larger pro-liposomes and consequently larger vesicles, as more phospholipid molecules would be recruited into the pro-liposomes. Therefore, the increase in size of liposomes with the increase in  $C_{LIP}$  can be further supported by both theories for liposome formation.

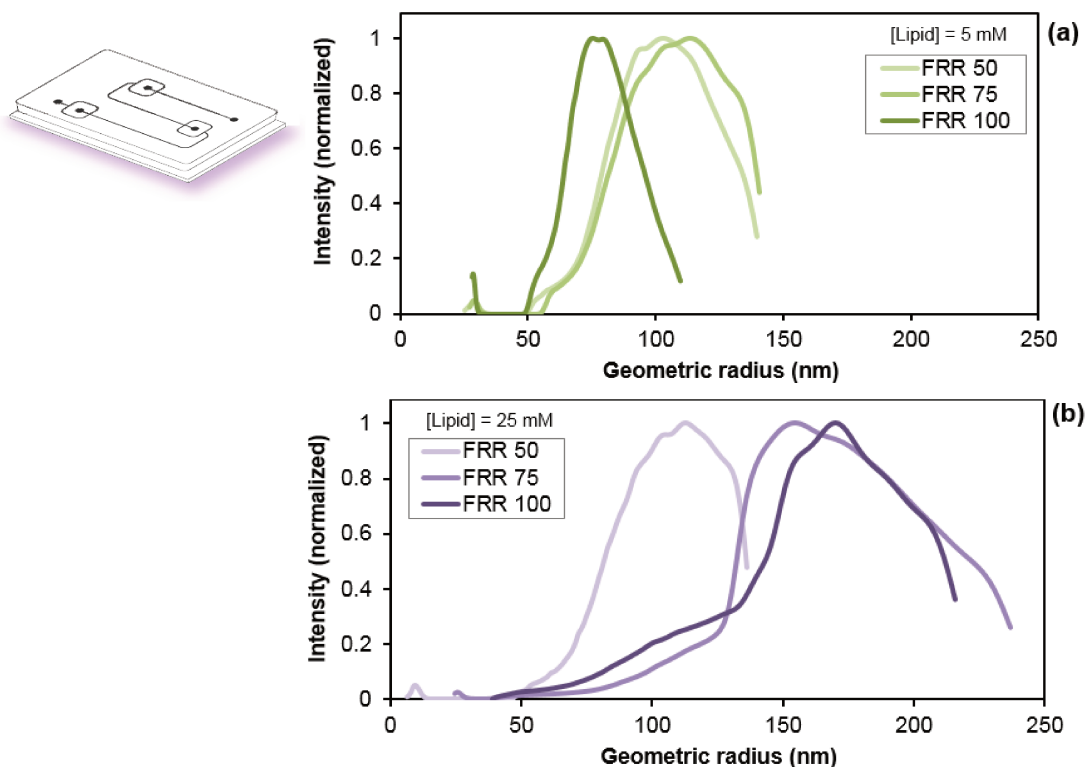


**Figure 4.7. Series hydrodynamic flow-focusing microfluidic device.** Geometric radius of PEGylated-liposome using the series configuration at lipid concentration in the ethanol stream ( $C_{LIP}$ ) of (a) 5 mM, and (b) 25 mM.

#### 4.4.3. Formation of liposomes using the parallel configuration

In our previous work, we investigated the association of two hydrodynamic focusing regions in parallel aiming at increasing the mass productivity of non-PEGylated cationic liposomes (34). Herein, the formation of PEGylated liposomes was investigated using three HFF areas arranged in parallel so that the lipid streams can co-flow in parallel. Figure 4.8 shows the chromatograms of fractionated samples at 5 mM and 25 mM. As one can see, liposomes produced at low lipid concentration (Figure 4.8a) had more pronounced peaks related to the micelle population of the samples, while high lipid concentration did not show micelle intensity peaks (or very low intense). This is in accordance with the series configuration results, where samples presented a more evident micelle population at low  $C_{LIP}$ .

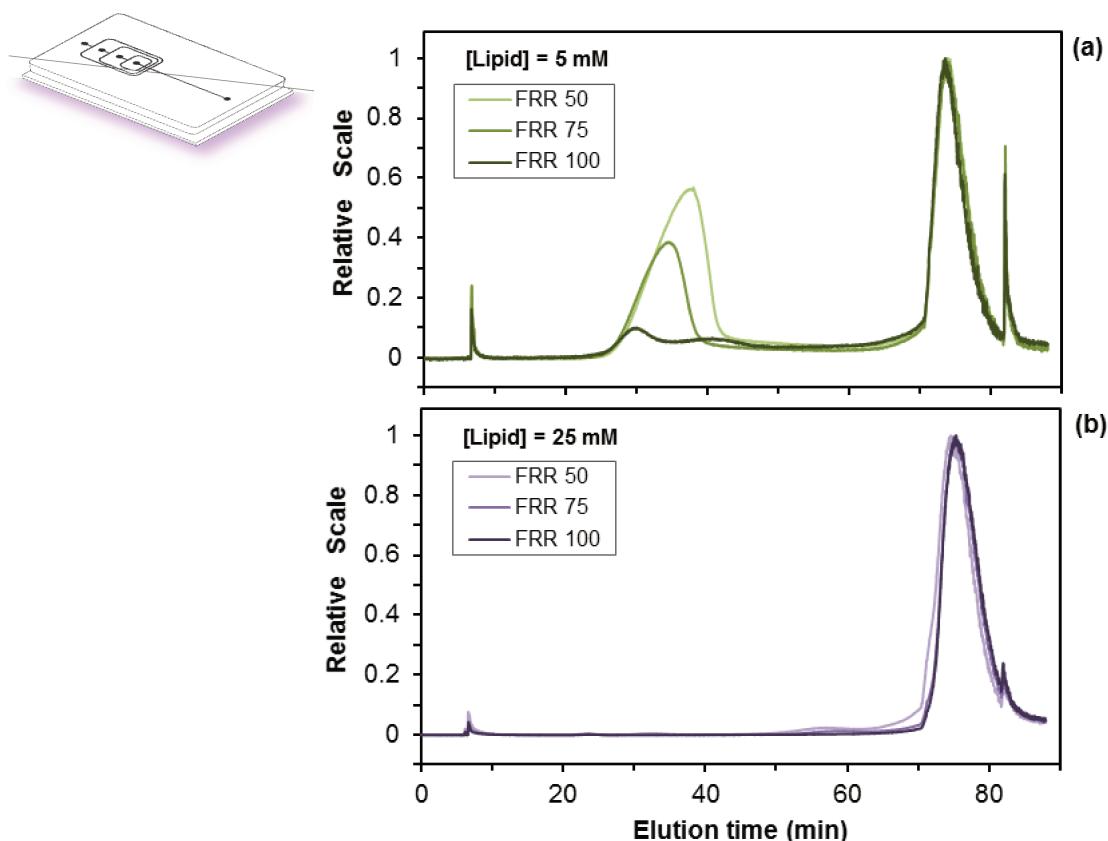


**Figure 4.8.** Intensity chromatograms of fractionated particles using asymmetric flow-field flow fractionation (AF4) and multiangle laser light scattering techniques. PEG-conjugated liposomes produced using the parallel configuration at varying FRR conditions at lipid concentration in the lipid stream of (a) 5 mM and (b) 25 mM.

As can be seen (Figure 4.6 and 4.7), samples obtained using the parallel configuration presented micelle peaks with lower intensity than the samples obtained using the series configuration. Since the formation of liposomes using the parallel arrangement has lower effects of ethanol than the formation of liposomes using the series arrangement, these results agree with the studies of the effects of ethanol in the aqueous phase (Figure 4.5), where we could see that the formation of micelles is favored only in the presence of ethanol. The formation of liposomes using the parallel configuration is affected by the presence of ethanol when the ethanol from the adjacent lipid streams diffuses through the distance between focused lipid streams. Conversely, using the series arrangement, the formation of liposomes occurs in the presence of ethanol in the second and third focusing areas, which would cause stronger effects on liposomes/micelles formation, as corroborated by series arrangement results.

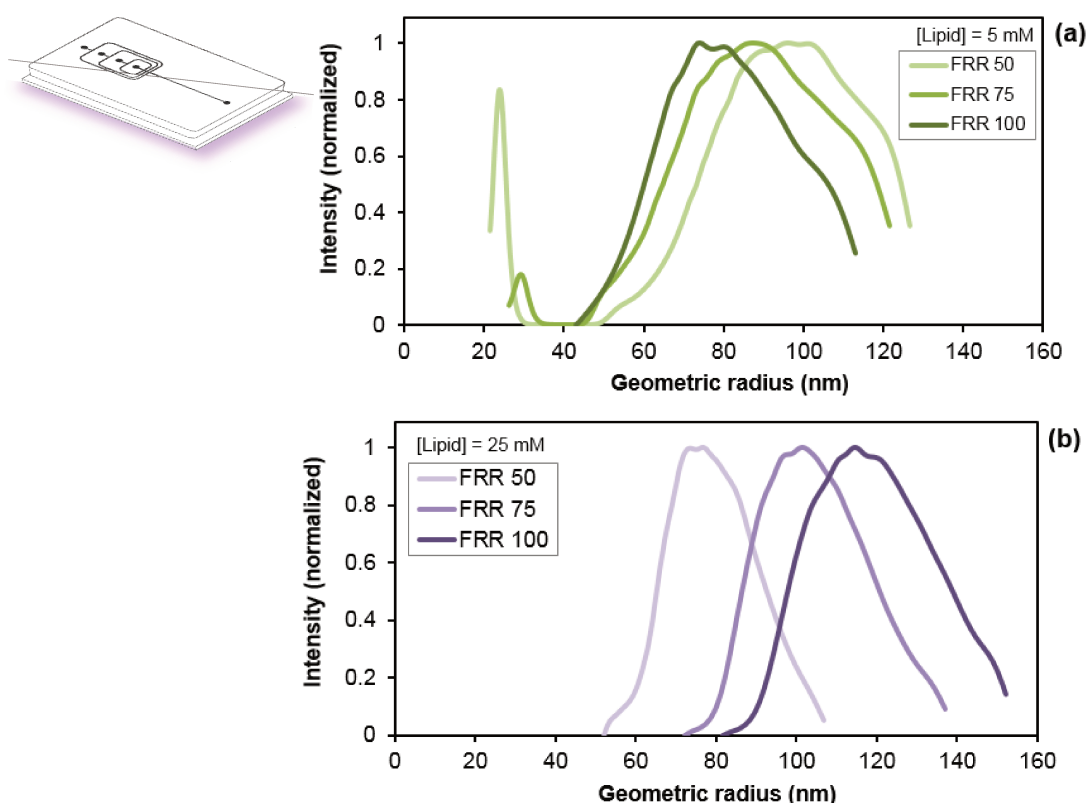


**Figure 4.9. Parallel hydrodynamic flow-focusing microfluidic device.** Geometric radius distribution of PEGylated-liposome using the series configuration at lipid concentration in the ethanol streams ( $C_{LIP}$ ) of (a) 5 mM, and (b) 25 mM.

Size distributions of liposomes produced using the parallel configuration can be seen in Figure 4.9. At low lipid concentration (Figure 4.9a), it is possible to observe a significant micelle peak at FRR of 50 and similar modal geometric radii at the studied FRR conditions. At high lipid concentrations (Figure 4.9b), the geometric radius distributions of liposomes are narrower and more symmetric when compared to low lipid concentration. Liposomes obtained at 25 mM were more easily tuned by varying FRR conditions, with the mode of geometric radii increasing with FRR values. Using a double parallel configuration (34), the increase in FRR from 10 to 16 resulted in larger cationic liposomes that was more evident under increasing  $C_{LIP}$ .

#### 4.4.4. Comparison of Series and Pseudo-Parallel configurations

When comparing the three geometries investigated in the present work, besides the differences in the fluidodynamic of the system, the main modification that would cause a stronger impact on liposome formation is the effects of the ethanol from consecutive or adjacent ethanolic streams of series and pseudo-parallel, respectively. Figure 4.10 shows

the average geometric radius and polydispersity of liposomes synthesized at 25 mM using the microfluidic devices with single, series and parallel HFF arrangements. By comparing both series and pseudo-parallel geometries, it is possible to observe that the parallel configuration produced liposomes with polydispersity similar to liposomes produced in the single configuration, what agrees with the narrower particle size distributions previously observed (Figures 4.7 and 4.8), although the geometric radii were significantly similar to those of liposomes obtained by the single and series configurations. PEGylated liposomes synthesized in the single arrangement under FRR of 153, 222 and 286, which have equivalent focusing conditions to FRR of 50, 75 and 100 using the series and pseudo-parallel arrangements, exhibited a modest overall increase in the mean and modal geometric radii. For both series and pseudo-parallel configurations, the use of lower  $C_{LIP}$  showed to favor the formation of micelles concomitantly with the formation of liposomes. Geometric radii and size polydispersity of liposomes generated using series and pseudo-parallel devices were significantly similar at 5 mM (data now shown). At 25 mM, using the parallel configuration, the polydispersity values of samples were lower ( $\sim 0.2$ ) than samples obtained by the series configuration ( $\sim 0.3$ ). The polydispersity values from the parallel configuration are in agreement with those obtained by the single HFF device with no ethanol as additive in the aqueous phase (Figure 4.4c), whereas the polydispersity of liposomes obtained by the series configuration is similar to liposomes generated in the presence of ethanol (Figure 4.4c).

The formation of liposomes by the parallel configuration with lower polydispersity was expected because of the influence of ethanol on size polydispersity (Figure 4.4c). For both configurations, the liposome synthesis using similar hydrodynamic focusing conditions usually had similar mean and modal geometric radii, although presented distinct size distributions. Thus, the parallel configuration explored here showed to generate liposomes less polydisperse than those from series configurations, with properties suitable for gene therapy applications produced at higher lipid concentration per device.

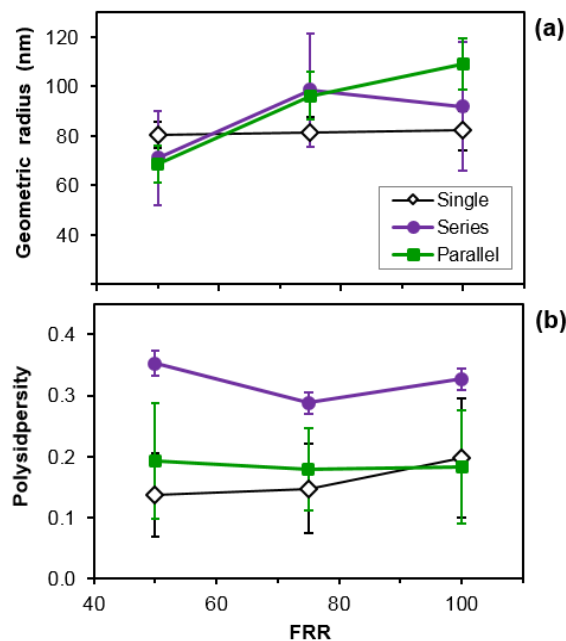


**Figure 4.10. Comparison of microfluidic devices with Single, Series and Pseudo-Parallel arrangements. (a) Geometric radius and (b) Polydispersity of PEGylated-liposome as a function of flow-rate ratio (FRR) at lipid concentration in the ethanol streams ( $C_{LIP}$ ) of 25 mM.**

#### 4.5. Conclusion

In this work, microfluidic devices with series and pseudo-parallel hydrodynamic focusing configurations were employed to synthesize PEGylated and non-PEGylated liposomes with higher final concentrations than conventional single focusing devices. It has been observed that the effects of ethanol in the aqueous phase for the formation of liposomes resulted in the formation of PEG-PE micelles; which was reduced under higher lipid concentration in the ethanolic phase. Since the formation of PEG-decorated liposomes with concomitant formation of PEG-PE micelles is considered as a nuisance, it was found that the development of process exploring the parallelization would be more suitable for the formation of vesicle-based delivery systems in comparison to processes where the effects of series associations of streams is minimized. Additionally, the dry film photoresist technique, used to fabricate the replication masters for the PDMS microchannels, showed to be a convenient alternative to conventional microfabrication approaches requiring limited investment for equipment. Thus, we believe that the studies presented herein might contribute to the development of microfluidic arrangements to form nanoscale particles and functional liposomes for pharmaceutical applications by simply arranging consecutive focusing areas in microfluidic devices.

## 5. One-step formation of nanoscale liposomes and lipoplexes using microfluidic devices<sup>§</sup>

Tiago A. Balbino<sup>1</sup>, Juliana M. Serafin<sup>1</sup>, Allan Radaic<sup>2</sup>, Marcelo B. de Jesus<sup>2</sup>,

Lucimara G. de la Torre<sup>1\*</sup>

<sup>1</sup>Department of Materials Engineering and Bioprocess, School of Chemical Engineering, University of Campinas, UNICAMP, São Paulo, SP, Brazil.

<sup>2</sup>Department of Biochemistry and Tissue Biology, Institute of Biology, University of Campinas, UNICAMP, São Paulo, SP, Brazil.

\*Corresponding author: [latorre@feq.unicamp.br](mailto:latorre@feq.unicamp.br)

### 5.1. Abstract

In this work, pDNA/cationic liposome (CL) lipoplexes for gene delivery were prepared in one-step using multiple hydrodynamic flow-focusing regions. The microfluidic platform was designed with two distinct regions for the synthesis of liposomes and the subsequent assembly with pDNA, forming lipoplexes. The obtained lipoplexes exhibited appropriate physicochemical characteristics for gene therapy applications under varying conditions of flow rate-ratio (FRR), total volumetric flow rate ( $Q_T$ ) and pDNA content (molar charge ratio,  $R_{\pm}$ ). The CLs were able to condense and retain the pDNA into the vesicular structures with sizes ranging from 140 nm to 250 nm. *In vitro* transfection assays showed that the lipoplexes prepared in one-step by the two-stage configuration achieved similar efficiencies than lipoplexes prepared by conventional bulk processes, in which each step comprises a series of manual operations. The integrated microfluidic platform generates lipoplexes with the liposome formation combined in-line with the lipoplex assembly, reducing significantly the number of steps usually required to form gene carrier systems.

**Key-words:** microfluidics, gene delivery, DNA, liposomes, lipoplexes, nanocarriers.

---

<sup>§</sup> Manuscript to be submitted to *Biotechnology and Bioengineering Journal*

## 5.2. Introduction

Gene therapy has long been investigated for curing diverse diseases by introducing nucleic acids into cells to elicit a therapeutic effect. The first studies of gene therapy focused on specific genetic disorders, while now gene delivery has enabled the treatment of different inherited and acquired diseases (96). It is based on the introduction of engineered, foreign genetic material into specific cells to substitute missing genes, replace defective genes, or silencing gene expression (4). However, the naked nucleic acid itself is not able to successfully enter cells; it requires the assistance of suitable vectors. To this end, several engineered nanomaterials have been used as nonviral vectors, which are a safer and simpler alternatives over viral vectors (97). A variety of nanostructured materials, such as biopolymers (98), dendrimers (13), solid lipid nanoparticles (46), and cationic lipids (15) can be used for the condensation of the nucleic acids and its protection against enzymatic degradation when in contact with interstitial fluids (10). Among the nonviral systems, the use of cationic liposomes (CLs) as gene carriers still is a popular strategy (99).

Liposomes are vesicular systems composed of (phospho)lipids containing at least one lipid bilayer surrounding an aqueous core. Because of their intrinsic properties, liposomes possess the ability to encapsulate aqueous solutes within the liposome lumen, retain hydrophobic compounds within the bilayer, and support tailored surface modifications for targeted delivery (11,100). Current processes for the preparation of liposomes generate large, polydisperse vesicles that require a post-processing unit operation step to reduce size and size polydispersity of liposome populations (101). As an example, the conventional bulk process based on the thin-lipid film hydration followed by multiple extrusions through membranes is one of the most used techniques for the formation of liposomes and comprises several discrete manual operations (15,101).

For gene delivery applications, the use of cationic lipids in the lipid mixture enables the formation of CLs and subsequently lipoplexes through electrostatic interactions with negatively charged nucleic acids, allowing the condensation and the delivery of genes into cells (7). Lipoplexes can present different physicochemical, structural and biological characteristics depending on several factors, such as lipid mixture composition, ionic strength of the media, order and type of mixing, solution concentrations, and lipid/genetic material charge ratio. The standard process of lipoplex formation relies on the electrostatic assembly of the pre-formed CLs with the genetic material (DNA or RNA), by mixing the two species via manually up-and-down pipetting or vortexing. Under certain conditions, these methods usually have limited scalability and might generate lipoplexes with inappropriate

characteristics for biological studies, mainly due to the heterogeneous and uncontrolled fluid flows (15,102).

Recently, by virtue of advances in microfabrication, microfluidic platforms have gained substantial attention for their use in liposome synthesis and lipoplex assembly (80,103). Over the past years, microfluidics has been among the most rapidly growing fields of scientific and technological research (104,81,9). Microfluidic devices handle minute volumes of fluid within micro-sized channels, in which the mixing occurs mainly under laminar flow by molecular diffusion, providing constant and reproducible mass transfer environments (8,105). For the preparation of liposomes and lipoplexes, microfluidic platforms not only can generate monodisperse nanocarriers but can also integrate a variety of sequential steps needed for the formation of liposomes and electrostatic complexes with genetic material, reducing significantly the number of steps required in conventional processes. Platforms based on the microfluidic flow-focusing (MFF) technique have previously generated liposomes with tunable sizes and low polydispersity in a one-step, continuous-flow process for different applications (29,83,34,82). Integrated microfluidic devices allow the synthesis of liposomal formulations with minimal reagent waste at or near the point of care. As an example, liposomes containing high concentrations of loaded drug compounds have been prepared by microfluidic platforms, combining in-line regions for liposome synthesis, microdialysis purification and remote drug loading (86). For gene therapy purposes, lipid- and/or polymer-based systems have been prepared by MFF devices for the successful delivery of pDNA and siRNA (36,39,41,55,106), becoming a promising strategy to accelerate the translation of gene therapy studies to clinical trials.

In the present work, an integrated microfluidic platform is employed for the formation of gene nanocarriers by combining in-line regions for liposome synthesis and lipoplexes assembly in continuous flow. Unlike lipoplexes prepared by conventional bulk processes, that usually require a series of laborious and time-consuming operations, lipoplexes with similar physicochemical characteristics and biological behavior were prepared by a single microfluidic device reducing dramatically the number of steps compared to conventional procedures.

## 5.3. Experimental

### 5.3.1. Microfluidic Device

The microfluidic channels were fabricated in polydimethylsiloxane (PDMS) substrates via soft lithography techniques employing dry film photoresist molds, which use simpler experimental procedures and obviates the use of clean room (86). The geometries of the microfluidic devices (Figure 5.1) were designed using AutoCAD (Autodesk). To fabricate the microchannel molds, two layers of the dry film photoresist with 35  $\mu\text{m}$  to 40  $\mu\text{m}$  thick each (Riston MM115i, DuPont, Research Triangle Park, NC) were laminated onto a glass slide. The lamination was carried out at 100 °C using a feed rate of  $\sim 0.02$  m/s and then placed on a hot plate at 110 °C for  $\sim 20$  min to promote adhesion. The glass slide was exposed through a photomask with the microchannel geometries using UV flood equipment at a dose of approximately 90 mJ/cm<sup>2</sup>. After the UV exposure, the dry film substrate was developed with sodium carbonate solution (1 wt%). The final molds were placed in petri dishes and Sylgard 184 Silicone Elastomer Kit (Dow Corning, MI, USA) was poured on the top. The PDMS layers and glass slides were irreversibly sealed via surface plasma oxidization and manually aligned. All the channels had a rectangular-like cross section with a depth of 70  $\mu\text{m}$  and a width of 80  $\mu\text{m}$ . The length of the main mixing channel in the first region was 55 mm, which is longer than previously reported geometries employed for liposome formation (29,34,33), what guarantees proper residence times even for higher FRR<sub>1</sub> conditions. For the lipoplexes assembly in second region, the electrostatic interaction between pDNA and CL is the main driving force to achieve more entropically favorable states of energy in the colloidal dispersion, considering complete mixing of the pDNA and CL streams. Thus, the lipoplexes assembly region was designed with a longer mixing channel of approximately 200 mm to promote a proper pDNA condensation into the structures and the complete mixing of streams at low focusing. In addition, the loops in the mixing channel of the second region shortened the mixing time of the two fluids.

### 5.3.2 Plasmid Amplification and Purification

The plasmid pEGFP-N1 (BD Biosciences Clontech, Palo Alto, USA) (4.7 kbp) was amplified in *Escherichia coli*. The pDNA was purified using PureLink™ HiPure Plasmid pDNA Purification Kit-Maxiprep K2100-07 (Invitrogen), according to manufacturer's instructions and resuspended in sterile water for injection. The quality and quantity of the purified pDNA was evaluated through a ND-1000 NanoDrop UV-vis spectrophotometer (PeqLab, Erlangen, Germany). The A260 nm/A280 nm ratio ( $>1.8$ ) was used as criteria for purity.

### 5.3.3. Preparation of liposomes

Liposomes prepared using the multi-inlet microfluidic device were compared to conventional bulk production. The lipids egg phosphatidylcholine (EPC), 1,2-dioleoyl-sn-glycero-3-phosphoethanolamine (DOPE) and 1,2-dioleoyl-3-trimethylammonium-propane (DOTAP) were used in the previously established molar proportion of 2:1:1, respectively (21). All the lipids were obtained from Lipoid and were not further purified. For the conventional bulk preparation, liposomes were prepared through the dried film technique followed by extrusion. The lipids were dispersed in chloroform (Sigma-Aldrich), placed in a round-bottom flask and removed under vacuum by a rotary evaporation to form a dried lipid film. The lipid film was hydrated with sterile water for injection. To reduce size and polydispersity, the dispersion was passed 15 times through 100-nm polycarbonate membranes, using an Avanti mini-extruder (Avanti Polar Lipids, Inc., Alabaster, AL).

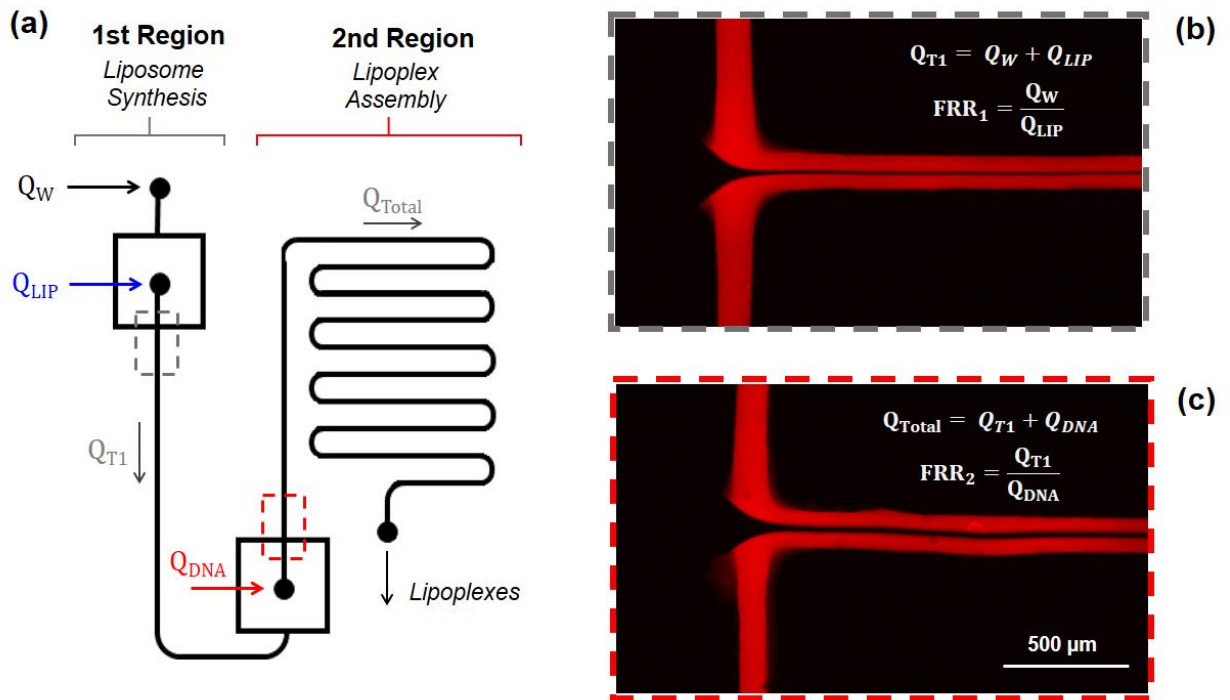


**Figure 5.1.** Schematic representation of the microfluidic devices for one-step formation of plasmid DNA (pDNA)/cationic liposome (CL) lipoplexes. **(a)** Two-stages configuration with two consecutive flow-focusing regions. In the first region, the CL synthesis occurs with the mixing between the aqueous side-streams and the center stream containing the lipid mixture in ethanol. In the second region, the pre-formed liposome streams hydrodynamically focus the pDNA-containing stream, enabling the incubation and stabilization of lipoplexes. Fluorescence micrographs of the flow-focusing of the **(b)** first region for liposome synthesis obtained at  $FRR_1$  10 and  $Q_T$  150  $\mu L/min$ , and of the **(c)** second region for lipoplex assembly at  $FRR_2$  3 and center stream at 47  $\mu L/min$ . Sulforhodamine B was used in the  $Q_{LIP}$  inlet for better visualization. All channels were approximately 80- $\mu m$  wide and 70- $\mu m$  deep.

For the microfluidic process, liposomes were synthesized similarly to (34) in the first region of the two-stage microfluidic device (Figure 5.1). The lipids were dispersed in anhydrous ethanol that was prepared with 4-Å molecular sieves and passed through 0.22 µm filters prior use. Lipid dispersion and water for injection were loaded into glass Gastight® syringes (Hamilton, Reno, NV) and programmable syringe pumps (Harvard Apparatus Inc., Holliston, MA) were used to control flow rates. The focusing region was observed at ~40x magnification under a stereo microscope (Bell Engineering, Italy). The Flow-Rate Ratio (FRR) at each region of flow-focusing microfluidic device is defined as the ratio of the flow-rate of the side streams to the flow-rate of the central stream. Thus, in the first region for microfluidic synthesis (FRR<sub>1</sub>), the FRR<sub>1</sub> represents the ratio of the water flow-rate (Q<sub>W</sub>) to the lipid flow-rate (Q<sub>LIP</sub>). For physicochemical characterization of the liposomes obtained in the microfluidic device, water for injection was introduced in the DNA inlet of the second region under same flow-rates used in the formation of lipoplexes. The total volumetric throughputs of the first region for liposome synthesis (Q<sub>T1</sub>) was investigated at 100 µL/min and 150 µL/min, and the FRR<sub>1</sub> varied from 10 to 16.

#### 5.3.4. Preparation of lipoplexes

The lipoplex assembly was carried out using HFF microfluidic devices and the conventional bulk mixing process under varying molar charge ratios (R<sub>±</sub>). R<sub>±</sub> represents the molar ratio of positive charges from the cationic lipid DOTAP to negative charges from the phosphate groups of pDNA (3 nmol/µg). For the bulk mixing process (107), the pDNA solution was added to the CL dispersion (2 mM), followed by up-and-down pipette mixing.

For the microfluidic processes, two microfluidic configurations were investigated for one-step preparation of lipoplexes. The first configuration comprised a single hydrodynamic flow-focusing region, in which the two adjacent aqueous streams containing the pDNA compressed the center stream of lipids dispersed in ethanol (Figure 5.S1 of supplementary material). As shown later, when using suitable concentration conditions for *in vitro* assays, this configuration resulted in the formation of lipid-DNA aggregates. The second microfluidic device comprised a two-stage configuration with two consecutive hydrodynamic focusing regions, as illustrated in Figure 5.1. The two-stage configuration was designed to allow the synthesis of liposomes in a first focusing region through the water-ethanol mixing. Then, the pre-formed liposome stream was split into two streams in order to focus a pDNA-containing stream in a second focusing region. The mixing between CLs and pDNA along the main

channel enabled the formation of lipoplexes. The lipoplex assembly region had a longer mixing channel to promote proper DNA condensation into the liposomal structures and to assure the stabilization of the electrostatic complexes, minimizing possible effects that the residence time would cause on lipoplex properties (Figure 5.1).

The total volumetric flow rate ( $Q_{T1}$  or  $Q_{Total}$ ) of each region in the two-stage microfluidic device is the sum of individual flow rates of center and side stream after the focusing region. Thus, for the liposome synthesis throughput in the first region,  $Q_{T1}$  is represented as  $Q_{T1} = Q_W + Q_{LIP}$ , with  $Q_W$  and  $Q_{LIP}$  being the volumetric flow rate of the water and lipid (in ethanol) streams, respectively. The total volumetric rate of the second region ( $Q_{Total}$ ) is represented as  $Q_{Total} = Q_{T1} + Q_{DNA}$ , with  $Q_{DNA}$  being the volumetric flow rate of the aqueous stream containing the pDNA. In the one-stage configuration (Figure 5.S1), the FRR refers to the pDNA/lipids flow rate in the two-stage configuration, the  $FRR_1$  refers to  $Q_W/Q_{LIP}$  ratio in the first focusing region, whereas in the second focusing region, the  $FRR_2$  refers to  $Q_{T1}/Q_{DNA}$  ratio. For the liposome synthesis in the two-stage configuration, we used  $Q_{T1}$  of 100 and 150  $\mu\text{L}/\text{min}$ , and  $Q_{Total}$  varied according to the  $FRR_1$  and to  $R_{\pm}$  used in the lipoplex assembly. To generate lipoplexes with varying  $R_{\pm}$ , we kept constant the concentration of the pDNA stream at 100  $\mu\text{g}/\text{mL}$  and varied its volumetric flow rate according to the desired  $R_{\pm}$ . Under different  $FRR_1$  and  $R_{\pm}$  conditions, the  $Q_{DNA}$  in  $\mu\text{L}/\text{min}$  was calculated from the following equation:

$$Q_{DNA} = 41.67 \frac{Q_{T1} \cdot C_{Lip}}{R_{\pm} \cdot C_{DNA}(FRR_1 + 1)} \quad (1)$$

in which  $C_{lip}$  and  $C_{DNA}$  are the concentrations of lipids (in mM) and DNA (in  $\mu\text{g}/\text{mL}$ ), respectively. The constant in the equation accounts unit conversion, DOTAP content (25 mol%), and concentration of negative charges in the plasmid (3 nmol of phosphate/ $\mu\text{g}$  of pDNA(108))

### 5.3.5. Zeta potential and size measurements

The physicochemical properties (zeta potential, size, and polydispersity) of liposomes and lipoplexes were analyzed using a Malvern Zetasizer Nano ZS (Malvern Instrument, UK). Hydrodynamic diameter and polydispersity index (Pdl) were determined by Dynamic Light Scattering (DLS) using the autocorrelation functions of CONTIN algorithm. The zeta potential was obtained by applying an electric field across samples in disposable folded capillary cells to estimate the electrophoretic mobility of the system. All the samples were analyzed at 0.2 mM three times for each replicate in ultrapure water.

### **5.3.6. Agarose gel electrophoresis**

Agarose gel electrophoresis (0.8%), containing ethidium bromide (0.5 µg/mL), was utilized to check the pDNA binding into the liposomal structures. Free pDNA and pDNA/CL lipoplexes (1 µg of pDNA) prepared by conventional and microfluidic methods were electrophoresed under 50V for 2h, and subsequently photographed using a UV transilluminator acquisition system.

### **5.3.7. Transmission Electron Microscopy**

Transmission electron microscopy of liposomes and lipoplexes were accessed by adding 10 µL of the sample onto a copper grid coated by formvar for 30 seconds. After air-drying, a negative staining was performed as follows. The TEM grid was exposed to a 10 µL droplet of a 1 wt/v% uranyl acetate solution (pH 4) for 10 s. Samples were examined by transmission electron microscopy (TEM) using LEO 906 transmission electron microscope (Carl Zeiss, Germany).

### **5.3.8. Transfection Protocol and Cytotoxicity**

Transfection efficiency of the lipoplexes prepared using microfluidic device was evaluated by flow-cytometry technique and compared to lipoplexes prepared by the conventional bulk procedure. Briefly, the cell cultures were incubated in 5% CO<sub>2</sub> humidified environment at 37 °C according to (109). For transfection, prostate cancer cell line (PC3) were seeded on 12-well plates at a density of 1·10<sup>5</sup> cells per well, according to (107). After 24h, cells were washed with PBS, followed by the addition of 400 µl per well serum- and antibiotic-free medium. The cells were then incubated with 100 µl of samples containing 1 µg of pDNA for 4 h. After the incubation, the transfection media was replaced with complete medium. After 24 h, the transfection efficiency was quantified based on the percentages of EGFP-positive cells determined by flow cytometry (FACS/Calibur Flow Cytometer, Becton Dickinson, Mansfield, MA).

Since liposomes prepared by dispersing lipids in alcohol exhibit a residual percentage of the organic solvent, cell viability assays were carried out to evaluate the cytotoxicity of these formulations. Lipoplexes prepared by microfluidic devices were compared to lipoplexes prepared by the bulk method with and without the addition of ethanol. For the cytotoxicity, the MTT ([3-(4,5- dimethylthiazol-2-yl)-2,5-diphenyltetrazolium bromide]) reduction assay was employed, detailed elsewhere (110) . Briefly, 1·10<sup>4</sup> human cervical cancer (HeLa) and PC3 cells were seeded onto 96-well microplates. Cells were treated with samples at increasing

pDNA concentrations from 10 µg/mL to 40 µg/mL for 4 h in transfection media (serum- and antibiotic-free medium). Then the transfection media were replaced by complete medium for 24 h. After this, the complete medium was replaced by 100 µL of fresh complete medium containing MTT (1 mg/mL) for 4 h, after which the medium was removed and replaced by 100 µL of ethanol per well. The absorbance of samples was measured at 570 nm in an ELX800 spectrophotometer (Biotek, USA). Results were presented as the percentage of viable cells, compared to control samples adding water for injection only instead of lipoplexes.

### **5.3.9. Statistical analysis**

All experiments were performed in independent triplicate and the measurements were repeated independently at least three times. The statistical significance of experiments was determined by Student's t-test and differences were considered significant for \* $p < 0.05$ . Data are presented as mean  $\pm$  standard deviation (SD).

## **5.4. Results and Discussion**

Many studies have been reported on the development of high-efficacy gene delivery systems, but few has attempted to the development of processes for lipoplex production with reduced number of steps. Usually, for the lipoplexes preparation via conventional bulk methods, the synthesis of liposomes requires a first step for the formation of vesicles that is followed by a second unit operation step for size reduction and homogenization. The pre-formed liposomes are then complexed with the genetic material to finally form the lipoplexes. Such multi-step processes not only involve a series of laborious operations but can also be infeasible for clinical trials where higher throughputs are required. Thereby, the primary technological motivation of this work was to develop and biologically evaluate a one-step microfluidic process to synthesize liposomal-based lipoplexes towards point-of-care platform for future use in gene therapy.

Firstly, a microfluidic configuration with a single hydrodynamic flow-focusing region was used, using the center stream of the lipids in ethanol and two aqueous adjacent streams containing the pDNA. Such microfluidic geometry was previously studied for the synthesis of liposomes for different applications, and for lipoplex assembly with pre-formed liposomes as well (41,31). Using a staggered herringbone micromixer, lipid nanoparticles with low polydispersity were previously synthesized by mixing two streams of lipids in ethanol and small interfering RNA (siRNA) in aqueous solution (55). Here, we hypothesized the self-

assembly of phospholipids could concomitantly occur with the pDNA electrostatic association to form lipoplexes with appropriate characteristics using microfluidic devices based on HFF mixing. Only under lower lipid concentrations ( $C_{LIP}$ ) conditions, lipoplexes could be properly analyzed by DLS and cumulant fitting techniques. The formation of lipoplexes under higher  $C_{LIP}$  resulted in sedimenting aggregates, which could be visualized in the focusing area where the two species are brought into contact to each other (Figure 5.1S, supplementary material). The influence of  $Q_T$  and FRR variations on lipoplex size and polydispersity was also evaluated as a function of  $C_{lip}$  (Figure 5.S2, supplementary material). Although it was possible to obtain lipoplexes whose properties could be considered suitable for transfection studies, the concentration was still a limiting step and the use of higher  $C_{LIP}$  showed to be infeasible particularly due to the precipitation of lipid agglomerates in the focusing area. In previous works (21,107), it has been shown that the lipid composition used here presented only lamellar phases in the presence of pDNA. In the one-stage configuration, the fast electrostatic association between the pDNA with phospholipid bilayer fragments, which are much less stable than vesicles (6), likely did not promote an adequate condensation of the pDNA into the structures, leading to the formation of lipid plus pDNA aggregates. To overcome such problem, the assembly of lipoplexes with a prior stage for the liposome formation was next investigated.

#### **5.4.1. Mixing behavior of the two-stage microfluidic configuration**

To verify the mixing behavior of the two-stage microfluidic device, the  $Q_{LIP}$  stream containing sulforhodamine B and  $Q_W$  and  $Q_{DNA}$  containing water for injection were examined through a fluorescent microscope, as shown in Figure 5.1. As expected, fluids were flowing in parallel after they met in both hydrodynamic focusing regions. Under the studied conditions, the maximum Reynolds number achieved was approximately 50 and only laminar flow was observed. Lower conditions of FRR values result in a wider center stream that requires a longer microchannel to ensure complete mixing under same volumetric throughputs. Conversely, higher FRR conditions generate a narrower center stream, resulting in a relatively high surface-to-volume ratio and the rapid depletion of the focused center stream, which was mainly driven by molecular diffusion in the normal direction to streamlines (29). At the end of the first region, it was expected that the lipids completely self-assemble into liposomes when the alcohol-water mixing is achieved, due to the reduced hydrophobicity of the media. Here, under the lowest focusing in the first region, FRR 10 (Figure 5.1b), both center and side streams were completely mixed at the end of the first region (data now shown).

#### 5.4.2. Effects of Flow Rate-Ratio ( $FRR_1$ ) and Volumetric Flow Rate ( $Q_{T1}$ ) in the first region on Liposome and Lipoplex Size

The influences of the parameters  $FRR_1$  and  $Q_{T1}$  on size and surface charge properties of liposomes and lipoplexes prepared in the two-stage configuration were evaluated. Liposomes synthesized under  $C_{Lip}$  25 mM and  $FRR$  higher than 25 would render a lipid concentration lower than 1 mM, limiting their use for *in vivo* studies or clinical applications. Furthermore, the  $C_{Lip}$  was maintained constant at 25 mM through the experiments since it produced CL with better conditions than those CL produced under higher  $C_{Lip}$  (34,41). The higher the focusing, the lower the lipid concentration of liposomes becomes; thereby it would be preferable to operate at low  $FRR$  conditions.

Figure 2 shows the hydrodynamic diameter and polydispersity index of CL using  $FRR_1$  of 10, 13 and 16, at  $Q_{T1}$  of 100 and 150  $\mu\text{L}/\text{min}$ . It is possible to observe that liposomes exhibited hydrodynamic diameters weighted by intensity in the range of 140 to 175 nm for both studied  $Q_{T1}$ . The polydispersity indexes of liposomes were significantly unaffected by  $FRR_1$  and  $Q_{T1}$  variations. Lipoplexes presented greater sizes compared to pure liposomes produced under the same  $FRR_1$  conditions. Since each  $FRR_1$  requires a different  $Q_{DNA}$  in the second region (according to Equation 1) and the lipoplex size was unaffected by  $FRR_1$  variation, the  $FRR_2$  seem to be of minor significance for lipoplex assembly. The increase in the lipoplex size compared to the liposomes is due to the rearrangement of the unilamellar structures (34) promoted by the DNA binding to the cationic lipids, forming multilamellar structures in which the nucleic acid is located between bilayers (15,107). These results corroborate previous studies on the liposome formation and lipoplex assembly using microfluidic devices. Using a similar microfluidic geometry based on the hydrodynamic flow-focusing technique (34), the CL size increased with flow velocities higher than 180 mm/s. In the two-stage configuration (Figure 5.2a), the higher flow velocity used was 148 mm/s, generating CL with hydrodynamic diameters smaller than 180 nm. Thereby, since physicochemical properties were unaffected in the studied range ( $FRR$  10 to 16), small  $FRR$  variations do not compromise the synthesis of CLs with diameters in the range of 160 nm.

Once the lipoplexes presented suitable physicochemical properties for *in vitro* transfection studies at both studied conditions of  $Q_{T1}$ , it is more convenient to operate the microfluidic process at 150  $\mu\text{L}/\text{min}$  for liposome synthesis due to the higher volumetric throughput, i.e. increased productivity. As mentioned earlier, the concentration is an important parameter for pharmaceutical applications of the obtained dispersions (34). Lower values of  $FRR$ , i.e. higher focusing conditions, generate final liposomal dispersions with

higher concentrations, achieving higher productivity in terms of lipid content. Thereby, we selected the  $FRR_1$  values of 10 and 13 to investigate the influence of the molar charge ratio of lipoplexes.

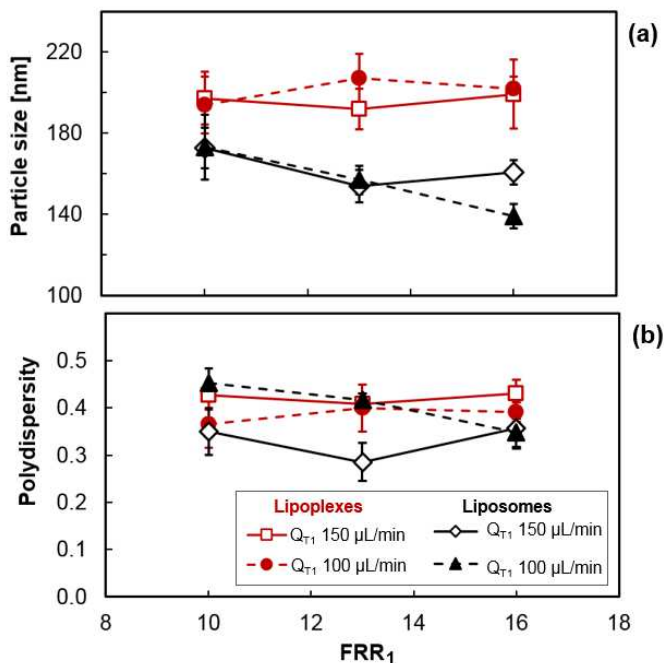


**Figure 5.2.** (a) Hydrodynamic diameter weighted by intensity and (b) polydispersity index of liposomes (CL) and lipoplexes obtained by the microfluidic device as a function of the flow rate ratio (FRR). Liposomes (black lines) and lipoplexes (red lines) were obtained at total volumetric throughputs in ( $Q_T$ ) of 100 and 150  $\mu\text{L/min}$ . Lipid and DNA concentrations in the inlet streams were 25 mM and 100  $\mu\text{g/mL}$ , respectively.  $FRR_1$  and  $Q_{T1}$  values refer to conditions in the first focusing region. The molar charge ratio ( $R_{\pm}$ ) of lipoplexes was constant at 6. Error bars represent the standard deviation of independent triplicates.

### 5.4.3. Effects of pDNA Content on Lipoplex Size

Having chosen the operational conditions of  $Q_{T1}$  of 150  $\mu\text{L/min}$  and  $FRR_1$  of 10 and 13 to generate liposomes in the first region, we next investigated the influence of the pDNA content in the lipoplexes, represented by  $R_{\pm}$ , on size and zeta potential of lipoplexes. It is known that lipoplexes usually achieve better biological activities when they are positively charged, to allow the electrostatic interaction with the negatively charged cell-surface, and small and homogeneous in size, to be better internalized and processed by cells (23).  $R_{\pm}$  is one of the most important parameters to be explored as it affects physicochemical and biological properties (21,107,58). In the two-stage configuration, depending on the FRR used in the first focusing region, the liposomes to be complexed with the pDNA in the second region present varying lipid concentrations. The higher the  $FRR_1$ , the lower the concentration

of liposomes becomes.

Figure 5.3 shows the hydrodynamic diameter and polydispersity index of lipoplexes with liposomes synthesized at two lipid concentration levels, 2.3 and 1.8 mM, by using FRR<sub>1</sub> of 10 and 13, respectively. In the second focusing area, the pDNA flow-rate varied according to the R<sub>±</sub> of lipoplexes and to the lipid concentration of the pre-formed liposomes. CLs and lipoplexes exhibited positive zeta potentials, whose values were significantly unaffected by the FRR<sub>1</sub> and Q<sub>T1</sub> variations (data not shown). Lipoplexes formed at FRR<sub>1</sub> 10 exhibited smaller sizes than those formed at FRR 13, whereas the polydispersity indexes (approximately 0.3) were nearly unaffected, which is in agreement with the results from Figure 5.2b.

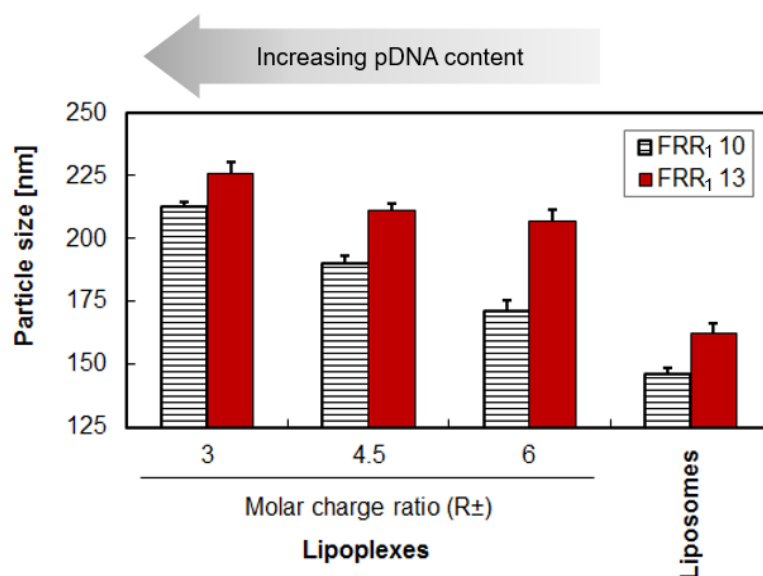


**Figure 5.4.** Effects of molar charge ratio (R<sub>±</sub>) on hydrodynamic diameter of lipoplexes generated by the two-stage microfluidic configuration. The pDNA flow rate in the second focusing region varied according to the R<sub>±</sub> of lipoplexes and flow-rate ratio (FRR of 10 and 13) of the previous liposome synthesis region. Properties of “pure” liposomes are shown for comparison. The amount of lipid in the samples was kept constant whereas the amount of DNA varied according to R<sub>±</sub>. Error bars represent the standard deviation of triplicates.

Under the studied R<sub>±</sub> conditions (3, 4.5, and 6), the average of the polydispersity index did not change significantly. With the increase in pDNA content (i.e., smaller R<sub>±</sub> values), the hydrodynamic diameter slightly increased. These results corroborate previous reports on the bulk-mixing formation of lipoplex and its physicochemical effects under varying pDNA content (58,57). It is known that the presence of genetic material in liposomal dispersions leads to the formation of multilamellar phases so that the increase in size of pDNA/CL complexes is due to the rearrangement of the vesicular conformation to

condensate the pDNA between lamellae, resulting in structures with higher number of stacked lipid bilayers or hexagonal architectures (15,53).

Since lipoplexes formed at  $Q_{T1}$  150  $\mu\text{L}/\text{min}$  and  $FRR_1$  10 not only presented smaller hydrodynamic diameters, but also had higher throughput and lipid concentration, these conditions were selected for further physicochemical and biological evaluations.

#### 5.4.4. pDNA-retaining ability and morphology of lipoplexes

Next, the DNA retardation assay was carried out to evaluate the ability of lipoplexes to retain the pDNA into the liposomal structures. Figure 5.5 shows the gel electrophoresis of the pDNA retardation assay of lipoplexes prepared by the microfluidic devices under varying  $R_{\pm}$ , at  $FRR$  10 and  $Q_{T1}$  150  $\mu\text{L}/\text{min}$ . It is possible to see that the free pDNA (control) migrated out of the well presenting its characteristics bands. At all the studied  $R_{\pm}$  conditions, the lipoplexes generated in the microfluidic device were able to completely retain the pDNA into the structures, since no free pDNA band is observed in the agarose gel. This is in good agreement with previous studies using this lipid composition and pDNA, in which lipoplexes obtained by bulk-mixing and microfluidic process with sequential steps were able to retain the pDNA at  $R_{\pm} \geq 1.5$  (41,21).

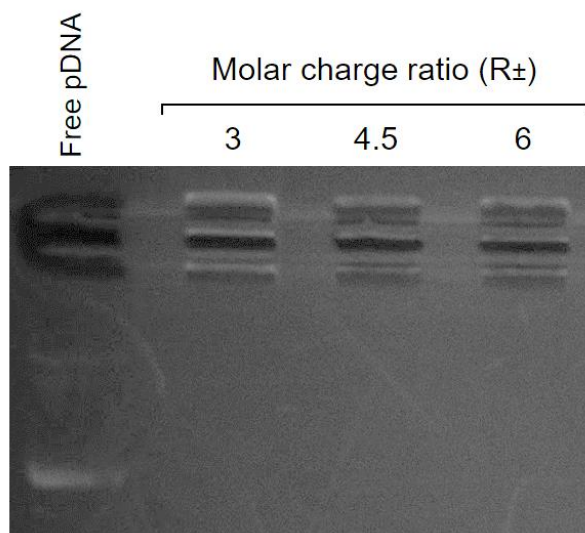


**Figure 5.5. Electrophoretic mobility retardation assay.** Lipoplexes were generated by the microfluidic device with two-stage configuration. 1<sup>st</sup> lane: free pDNA; 2<sup>nd</sup> to 4<sup>th</sup>: lipoplexes under molar charge ratios from 3 to 6, respectively, using 0.5  $\mu\text{g}$  of DNA per well. The operational conditions were average volumetric throughput ( $Q_{T1}$ ) of 150  $\mu\text{L}/\text{min}$  and flow rate ratio ( $FRR_1$ ) of 10.

The morphological characterization of the liposomes and lipoplexes prepared by the two-stage configuration was performed by means of TEM, presented in Figure 5.6.

Liposomes and lipoplexes exhibited similar relatively small and homogeneous particle sizes, which is in agreement with the DLS results. It is possible to observe a defined area surrounding the vesicles showing to the unilamellar characteristic of liposomes.

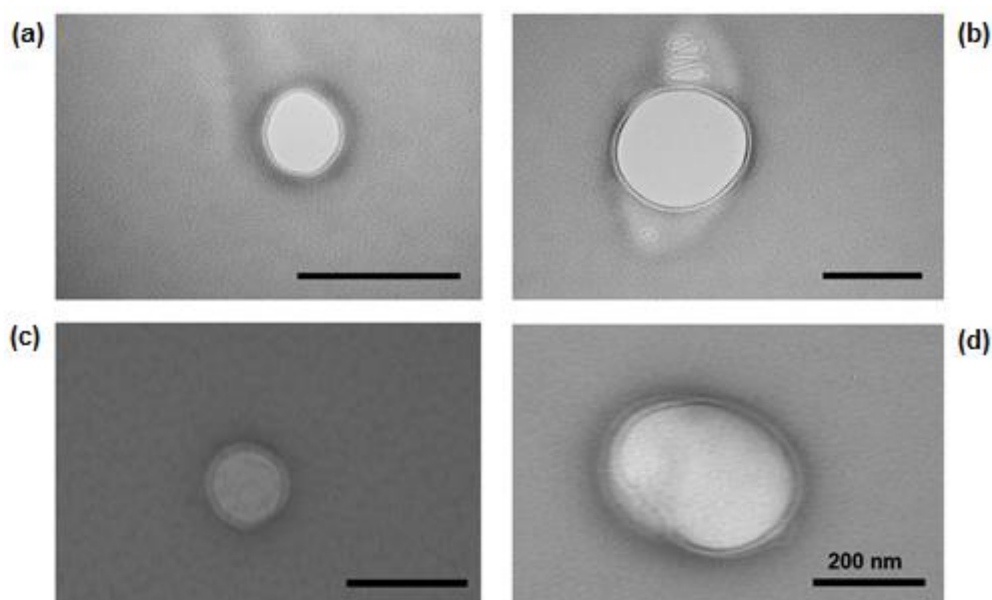


**Figure 5.6.** Transmission electron microscopy (TEM) images of (a and b) “pure” liposomes and (c and d) lipoplexes prepared by the two-stage microfluidic device under average volumetric throughput ( $Q_{T1}$ ) of 150  $\mu\text{L}/\text{min}$  and flow rate ratio ( $\text{FRR}_1$ ) of 10. Scale bars indicate 200 nm.

#### 5.4.5. *In vitro* evaluation of cytotoxicity and transfection efficacy of lipoplexes

Liposomes prepared by processes based on the dispersion of the lipid mixture in an alcoholic phase present a residual amount of the alcohol in the final formulation that can be toxic to cells. Thereby we evaluated cytotoxicity of the formulations on Hela and PC3 cells using the MTT assay. Approximately 10% (v/v) of ethanol was added to extruded liposomes prepared by the thin film method to simulate the amount of ethanol present in liposomes when produced at  $\text{FRR}_1$  10 (highest concentration of ethanol in the studied conditions). It is possible to observe in Figure 5.7 that Hela and PC3 cells exhibited a small decrease in cell viability compared to the control of cells treated with water for injection only. Cells treated with lipoplexes prepared by the two-stage microfluidic device and by bulk procedures with or without ethanol presented significantly similar levels of cytotoxicity (approximately 80% of viable cells). The addition of 10% of ethanol in extruded liposomes prepared by bulk process did not affect significantly the cell viability. Therefore, additional post-processing steps for removal of the ethanol in the lipoplexes can be obviated for gene delivery purposes.

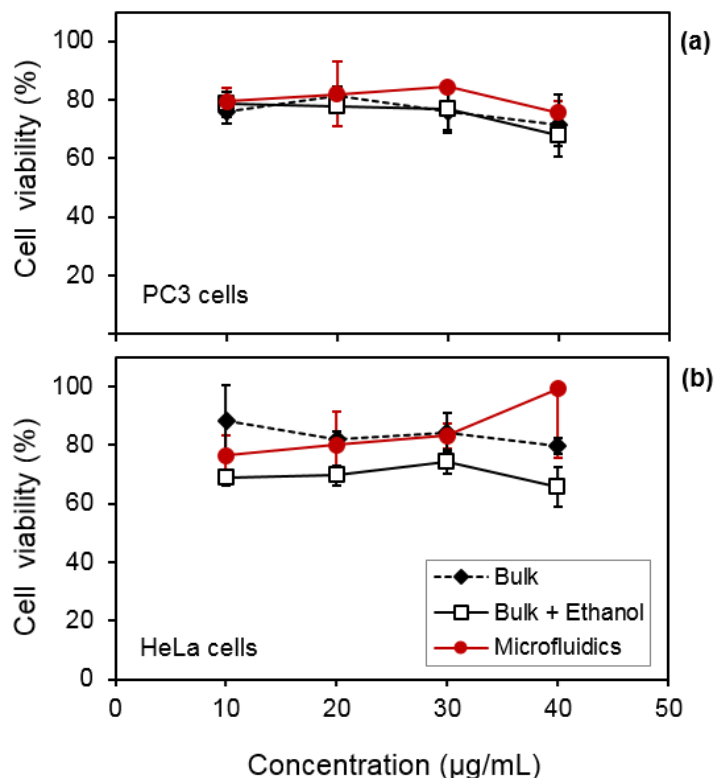


**Figure 5.7.** Cell viability assay on **(a)** prostate cancer cells (PC3) and **(b)** human cervical cancer (HeLa) cells of lipoplexes obtained by bulk and microfluidic processes. The presence of ethanol in the microfluidic lipoplexes was simulated by adding 10% of ethanol in extruded liposomes prepared by bulk process (Bulk + Ethanol). Cells treated with water for injection were used as the control.

Having evaluated the cytotoxic effects of lipoplexes, the level of transfection efficiency was next quantified by determining the percentage of cells that expressed the GFP by means of flow cytometry technique. Figure 5.8 shows the transfection efficiency of the lipoplexes generated by the two-stage microfluidic device were *in vitro* examined in PC3 cells. Lipoplexes prepared in sequential steps by the conventional bulk mixing process were shown for comparison. Lipoplexes prepared by conventional and microfluidic processes exhibited significantly similar transfection levels. This highlights the feasibility of microfluidic devices based on HFF mixing to prepare lipid-based gene nanocarriers with substantially reduced number of steps compared to conventional bulk procedures.

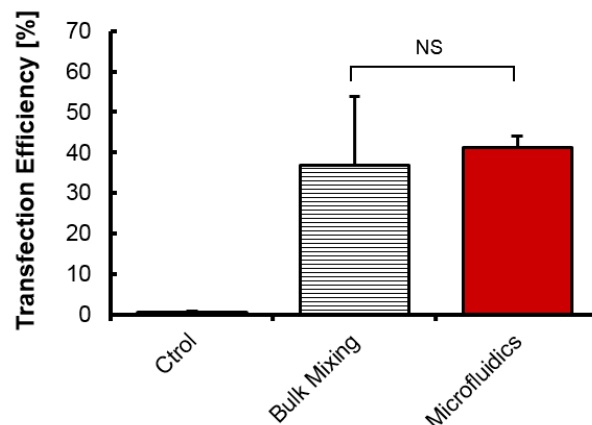


**Figure 5.8.** *In vitro* efficacy on the transfection of prostate cancer cells PC3 with lipoplexes prepared by conventional bulk mixing and microfluidic processes. Cells were transfected with eGFP-encoding pDNA and analyzed by measuring the eGFP-positive cells by flow cytometry. Cells without treatment were used as control. Lipoplexes were obtained at molar charge ratio ( $R_{\pm}$ ) of 3, average volumetric throughput ( $Q_{T1}$ ) of 150  $\mu\text{L}/\text{min}$  and flow rate ratio ( $FRR_1$ ) of 10. Each value represents the standard deviation of at least four replicates. \*  $p < 0.05$  was considered statistically significant. NS, not significant.

## 5.5. Conclusions

In this work, for the first time, it has been employed an integrated, continuous-flow microfluidic device with two distinct regions for the one-step preparation of lipoplexes with suitable physicochemical properties and biological activity for gene therapy applications. Process parameters were investigated in order to prepare liposomes and lipoplexes with higher lipid concentration and volumetric throughputs. It was possible to use a low-cost technique to fabricate the microfluidic devices that successfully generated lipoplexes and liposomes, besides the roughness of microchannel features differed from master molds prepared in clean-room procedures. The microfluidic process developed here generated lipoplexes whose transfection efficiency was similar to those obtained via the bulk-mixing process, considerably reducing the number of manual operations and required equipment.

## 5.6. Acknowledgments

The authors gratefully acknowledge the financial support of the São Paulo Research Foundation – FAPESP, Brazil (Grants No. 2012/23143-9, 2013/05868-9 and 2013/14925-6). The microfluidic devices were partially constructed at the Microfabrication Laboratory (LMF) of the Brazilian Nanotechnology National Laboratory (LNNano).

## 5.7. Supplementary information

In the one-stage configuration (Figure 5.1S), the phospholipid assembly in bilayers simultaneously occurs with the association and condensation of the pDNA into the structures, which would in turn generate lipid structures with distinct characteristics than those ones complexed with pre-formed liposomes. In this configuration, we first investigated the concentration of the species in the central and adjacent streams. The pDNA concentration in water varied from 17 to 70  $\mu\text{g/mL}$ , whereas the lipid concentration in ethanol ( $C_{\text{lip}}$ ) varied from 6.5 to 50 mM. The total volumetric flow rate ( $Q_T$ ) and Flow Rate Ratio (FRR) was maintained constant at 150  $\mu\text{L/min}$  and 10 respectively. As can be observed in Figure 1Sb, the use of  $C_{\text{lip}}$  higher than 12.5 lead to the formation of large aggregates and precipitates in the focusing area. This corroborates the dynamic light scattering analysis, in which lipoplexes produced at  $C_{\text{lip}}$  higher than 12.5 mM generated very polydisperse systems, with the presence of large and/or sedimenting aggregates, what impaired a proper cumulant analysis by the equipment software (poor data quality).

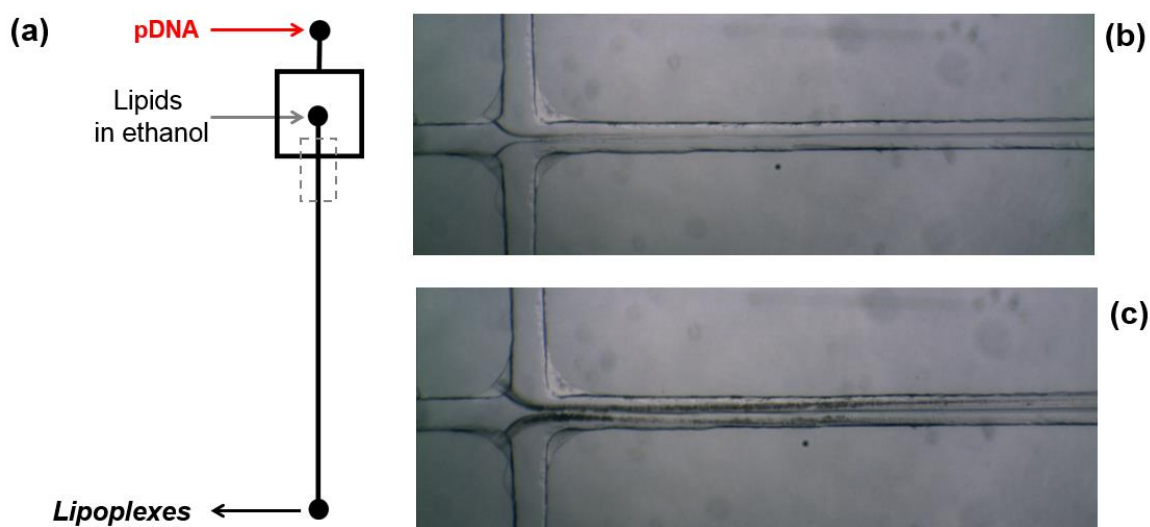


**Figure 5.1S.** (a) Representation of the one-stage microfluidic device for the formation of lipoplexes with a single hydrodynamic flow-focusing region. Hydrodynamic flow-focusing visualized through a stereo microscope operating at lipid concentration in the central stream of (b) 6.5 mM and (c) 12 mM. All channels were approximately 80- $\mu\text{m}$  wide and 70- $\mu\text{m}$  deep.

To investigate the influence of  $Q_T$  and FRR on lipoplexes formation we used  $C_{lip}$  12.5 mM. Figure 5.2Sa shows that the hydrodynamic diameter and the polydispersity index of lipoplexes are significantly unaffected by the FRR variation in the range from 7 up to 24. Under  $Q_T$  variations, as can be seen in Figure 5.2Sb, the polydispersity of lipoplexes was not dependent on the  $Q_T$  employed, and the hydrodynamic diameter slightly reduced with increasing  $Q_T$ . The decrease in size with increasing  $Q_T$  is likely caused by the reduced mixing region between the species when they are brought into contact at high throughputs (111), which renders less favorable conditions for the formation of precipitates at the focusing area. Although some conditions of this microfluidic process exhibited suitable characteristics for transfection studies, it was not possible to obtain lipoplexes at higher concentrations. Since the required pDNA concentration of lipoplexes for *in vitro* studies was fixed at 20  $\mu\text{g/mL}$  (see methodology),  $C_{LIP}$  lower than 12.5 mM produced diluted lipoplexes in most of the FRR conditions, which are not suitable for biological assays.

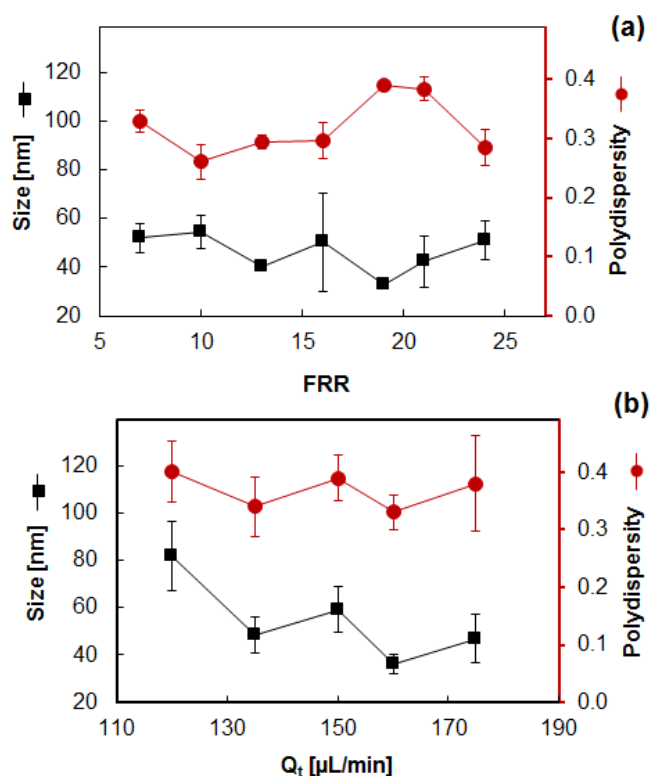


**Figure 5.2S.** Hydrodynamic diameter (square symbols) and polydispersity index (circle symbols) of lipoplexes generated by the one-stage microfluidic device as a functions of **(a)** Flow Rate Ratio (FRR) and **(b)** Total volumetric rate ( $Q_T$ ). Lipoplexes were produced at a lipid concentration in the central stream ( $C_{LIP}$ ) of 12.5 mM. The molar charge ratio of lipoplexes ( $R_{\pm}$ ) was maintained constant at 6. Error bars represent the standard deviation of triplicates.

We hypothesized that the lipoplex formation in the one-stage configuration would occur with the interactions between the pDNA and the phospholipid bilayer fragments, which are presumably formed as soon as the water and alcohol are brought into contact to each other. We have previously shown that the lipid composition used in this work presented only lamellar phases in the presence of pDNA. Thereby, the low stability of phospholipid bilayer fragments and the lamellar organization nature of the lipid mixture likely caused the formation of instable and large lipoplexes, resulting in precipitation in the focusing area. When using lipid nanoparticles for the delivery of siRNA, structural differences and type of microfluidic mixing are likely the main reason why it has been possible to generate nanoparticles with controllable sizes. Additional studies are currently being developed in order to elucidate the colloidal arrangement of lipid nanoparticles and genetic materials such as pDNA and siRNA.

## 6. Conclusões

Este trabalho visou ao desenvolvimento tecnológico de plataformas microfluídicas para a formação de lipossomas e seus complexos com DNA para aplicações em terapia gênica. De modo geral, foi possível contribuir para a elucidação de fenômenos envolvidos no processo de formação de lipossomas, como os efeitos proporcionados pela presença de etanol na autoagregação dos lipídeos derivatizados com polímero em estruturas vesiculares e micelares, bem como as organizações estruturais observadas durante a formação de lipoplexos, cujos resultados físico-químicos e estruturais puderam ser correlacionados aos ensaios de transfecção *in vitro*. De forma mais específica, foi possível concluir que:

- Os dispositivos microfluídicos, além de serem plataformas miniaturizadas de baixo consumo de energia, apresentaram condições hidrodinâmicas de mistura mais convenientes para a formação de lipoplexos em condições de alto carregamento de pDNA. Isso, por sua vez, permitiu a formação de lipoplexos de diâmetros menores e menor número de bicamadas lipídicas sobrepostas, resultando em repostas de transfecção *in vitro* mais eficientes em condições de alto carregamento de pDNA;
- Lipoplexos obtidos pelos processos microfluídico e *bulk* em proporções de pDNA diferentes de  $R \pm 1,5$  exibiram propriedades físico-químicas, estruturais e biológicas similares, o que indica que o tipo de mistura somente interferiu na interação eletrostática e na organização estrutural em condições próximas ao ponto de neutralidade de cargas, sob as condições estudadas;
- Apesar do processo *bulk* ser facilmente implementado em laboratórios para a complexação entre carreadores catiônicos e material genético, as plataformas microfluídicas permitem amplificar a escala de produção de forma automatizada por meio da paralelização de dispositivos, dentre outras alternativas;
- Com o emprego de dispositivos microfluídicos com associações de focalizações hidrodinâmicas em série e pseudo-paralelo, foi possível produzir lipossomas protegidos estericamente com o polímero PEG utilizando fosfolipídios derivatizados, visando aumentar o tempo de circulação dos lipossomas para administrações sistêmicas;
- As configurações microfluídicas em série e pseudo-paralelo foram capazes de produzir lipossomas em condições de focalização similares aos dispositivos de

focalização única, porém com formulações finais de concentrações lipídicas mais altas devido às associações de entradas múltiplas em cada dispositivo;

- A presença de etanol, utilizado para dispersar os lipídeos na produção dos lipossomas derivatizados com PEG, acarreta na formação de estruturas micelares formadas pelo fosfolipídio derivatizado PEG-PE, na composição lipídica empregada. Consequentemente, durante a formação de lipossomas na configuração microfluídica em série, a formação de vesículas em escala nanométrica ocorreu concomitantemente à formação dessas estruturas menores;
- Uma vez que a formação de estruturas micelares é considerada indesejável, a utilização da associação de focalizações em pseudo-paralelo se mostra mais interessante para aplicações na produção de lipossomas derivatizados pois os efeitos da presença do solvente orgânico são minimizados;
- Foi possível empregar técnicas para a fabricação dos moldes de réplica de microcanais de PDMS mais simples e de menor custo em comparação às técnicas convencionais de microfabricação que requerem o uso de sala limpa e outros equipamentos específicos;
- Graças a integração de regiões distintas para a formação de lipossomas e a posterior complexação com pDNA, lipoplexos com características adequadas para aplicações em terapia gênica foram obtidos em um único dispositivo microfluídico de fluxo contínuo;
- Os lipoplexos obtidos em dispositivo único de duas regiões apresentaram níveis de transfecção equivalentes aos complexos obtidos por processos convencionais multietapas, reduzindo drasticamente o número de etapas geralmente necessárias para a formação de lipossomas de tamanhos reduzidos e seus lipoplexos.

## 7. Perspectivas de Trabalhos Futuros

Através da pesquisa apresentada nesta tese, uma variedade de investigações experimentais pode ser vislumbrada para a continuação de pesquisas futuras, principalmente, referentes ao desenvolvimento de processos microfluídicos e nanopartículas para a formação de sistemas carreadores de material genético para aplicações em terapia gênica. Dessa forma, os tópicos seguintes são sugeridos como sugestões para trabalhos futuros:

### 7.1. Formação de complexos pseudo-ternários multifuncionais

Apesar de obterem êxito em diversas aplicações em terapia gênica em estudos *in vitro* e *in vivo*, os LCs podem apresentar relativa baixa eficiência de transfecção, uma vez que, isoladamente, não possuem especificidade para atuarem ora no tráfego extracelular, ora no tráfego intracelular (112). Diversos estudos exploram estratégias para a formação de nanocarreadores multifuncionais com diferentes domínios, a fim de aumentar a eficiência de transfecção via múltiplos mecanismos de entrega gênica, com a associação de diferentes adjuvantes (13). O uso de peptídeos com sequências específicas para o direcionamento nuclear (NLS) permite o transporte do pDNA até o núcleo celular, aumentando a eficiência de entrega gênica (113). Para a formação dos complexos pseudo-ternários, os complexos binários de pDNA/NLS são primeiramente formados com carga superficial resultante negativa ou próxima à neutralidade, para então serem complexados com os lipossomas catiônicos formados, na maioria das vezes, pelo processo de hidratação do filme seco seguido por múltiplas extrusões (113).

Dessa forma, baseados nas arquiteturas desenvolvidas nos estudos das associações de focalizações em série e paralelo (Capítulo 4), a formação de complexos pseudo-ternários seria factível utilizando duas focalizações hidrodinâmicas que escoassem paralelamente em diferentes microcanais, seguidas por uma região de contato entre as duas correntes e mistura mais eficiente, similar ao segundo estágio de *loops* do dispositivo estudado no Capítulo 5. Nessa associação de microcanais de mistura paralelos, seria possível realizar as etapas de formação de lipossomas concomitante a de complexos binários de pDNA/NLS, cujas correntes se convergiriam para um subsequente canal de mistura com vórtices.

## 7.2. Formação de lipossomas com peptídeos ancorados na superfície

No Capítulo 4, foi possível obter lipossomas utilizando lipídeos derivatizados com PEG cujas propriedades podem ser consideradas adequadas para aplicações em terapia gênica. Com o uso de lipídeos derivatizados com PEG, diferentes funcionalizações no terminal do polímero podem ser realizadas, possibilitando que a entrega do pDNA seja sítio-específica. Dentre as diversas interações moleculares que podem mediar a adesão celular de sistemas carreadores, muitos estudos focaram na utilização de peptídeos que ativem o conjunto de receptores de superfície celular de integrinas, especialmente os baseados na sequência dos três aminoácidos: arginina, glicina e aspartato (RGD), conforme ilustra a Figura 7.1. As integrinas  $\alpha_v\beta_3$  são seletivamente expressadas em várias células tumorais e endoteliais, que constituem vasos sanguíneos tumorais, e são os receptores predominantes dos peptídeos RGD (114). Como os receptores de integrinas reconhecem o RGD como sequência primária (embora outras conformações possam modular a afinidade, como peptídeos cíclicos e lineares, por exemplo), a funcionalidade do RGD é geralmente mantida após etapas de processamentos e esterilização, as quais podem causar a sua desnaturação. Com a funcionalização dos nanocarreadores com peptídeos RGD é possível que a entrega gênica seja sítio-específica (*targeted delivery*), resultando em transfecções *in vitro* e *in vivo* mais eficientes.

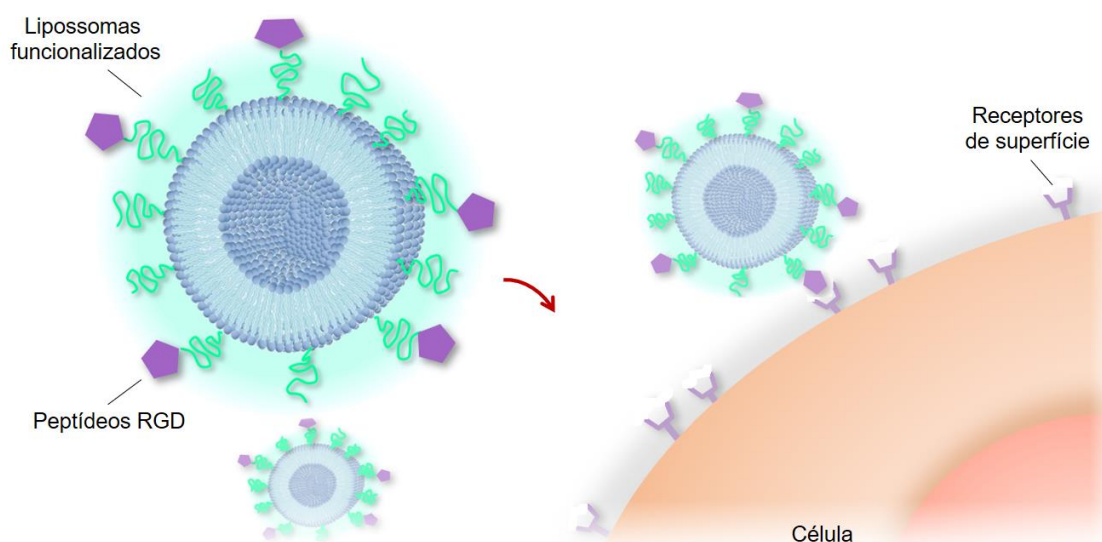


**Figura 7.1.** Figura ilustrativa dos lipossomas funcionalizados com lipídeos contendo o polímero polietilenoglicol e peptídeos com sequência RGD. Os peptídeos RGD favorecem interações com o conjunto de receptores de superfície de integrinas  $\alpha_v\beta_3$ , comumente expressadas em células tumorais e endoteliais.

Normalmente, os processos convencionais de obtenção de nanocarreadores lipídicos ancorados com peptídeos requerem basicamente três etapas principais: (i) formação das vesículas; (ii) redução e homogeneização de tamanho por extrusão; e (iii) incubação do lipídeo derivatizado contendo o peptídeo com os lipossomas pré-formados (37). Para a formação de lipossomas funcionalizados, a última fase ocorre através da incubação das micelas do lipídeo derivatizado com as vesículas, em que o lipídeo derivatizado se insere na bicamada lipídica afim de atingir estados de energia entropicamente mais favoráveis que na organização micelar (89). Dessa forma, utilizando a geometria desenvolvida para a formação de lipoplexos em dispositivo de duas regiões (Capítulo 5), a formação dos lipossomas poderia ser realizada na primeira etapa do dispositivo, seguida pela etapa de inserção do lipídeo derivatizado com o peptídeo RGD nas bicamadas dos lipossomas formados anteriormente.

### **7.3. Estudos biológicos de lipoplexos obtidos por dispositivos microfluídicos**

No Capítulo 3, sob determinadas condições, os lipoplexos obtidos pelos dispositivos microfluídicos apresentaram diversas características distintas daqueles obtidos pelo processo *bulk*. Foi observado que as diferentes organizações estruturais resultaram em diferentes respostas de transfecção *in vitro*. Partindo do conhecimento adquirido com os estudos dos lipoplexos formados em altas condições de carregamento e considerando o emprego de peptídeos funcionalizados mencionados acima, estudos interessantes poderiam ser conduzidos a fim de avaliar os fenômenos celulares envolvidos no processo de transfecção *in vitro*. Tempos de transfecção variados e ensaios de citotoxicidade celular poderiam contribuir na elucidação das diferentes respostas de transfecção aliadas a cinéticas de internalização e expressão da proteína de interesse. Para avaliar o impacto do escape endossomal dos lipossomas, as transfecções poderiam ser realizadas na presença de cloroquina, uma base fraca que promove o rompimento do endossomo e liberação do seu conteúdo. É possível ainda investigar a capacidade de direcionamento dos peptídeos RGD e sua interação com a superfície celular (*cell binding*) na presença de fluoróforos com interação seletiva ao peptídeo RGD, que permite a quantificação por citometria de fluxo de células associadas ao peptídeo. O tráfego intracelular também poderia ser avaliado diretamente por meio de técnicas de microscopia confocal, utilizando plasmídeos e lipídeos marcados com o fluoróforos.

Como etapa mandatória para a transposição de testes *in vitro* para futuros ensaios clínicos, sugere-se ainda avaliar a eficiência de transfecção dos lipoplexos obtidos por

dispositivos microfluídicos em modelos *in vivo* com camundongos. Os ensaios seriam realizados a fim de compreender os mecanismos terapêuticos dos lipoplexos e avaliar a potencialidade dos vetores lipossomais derivatizados com PEG para aumentar o tempo de circulação dos complexos.

#### **7.4. Estudos de fluidodinâmica computacional de configurações microfluídicas**

Uma vez que as geometrias propostas apresentam diferenças de escoamento hidrodinâmico significativas em comparação às geometrias previamente estudadas na literatura, as propriedades de escoamento e a interferência das variáveis operacionais de fluxo poderiam ser melhor exploradas por meio de estudos de fluidodinâmica computacional, investigando principalmente os perfis de concentração etanol-água nas geometrias. Para o desenvolvimento das simulações empregando o software *COMSOL Multiphysics*, os modelos matemáticos desconsiderariam a não-linearidade na viscosidade das misturas, assumindo que essa consideração não apresentaria impacto significativo nos resultados de perfil de concentração para efeitos de comparação.

Como visto no Capítulo 5 (material suplementar), quando correntes aquosas com pDNA e alcoólicas com lipídeos se tocam na região de focalização hidrodinâmica, há a formação de agregados lipídeos sedimentáveis, formados provavelmente devido à forte e rápida interação entre cargas, gerando partículas lipídicas com alta polidispersidade. Dessa forma, foi desenvolvido o dispositivo de duas regiões distintas para a formação de lipossomas numa etapa anterior a complexação com DNA. Nesse sentido, uma outra alternativa promissora a ser explorada foi desenvolvida por nosso grupo de pesquisa no âmbito da dissertação de mestrado da Amanda da Costa e Silva de Noronha Pessoa, que versou sobre o desenvolvimento de processos microfluídicos para a formação de nanopartículas de quitosana. Devido a rápida reação entre o agente reticulante e a quitosana, assim como com as partículas lipídicas, foi observada a formação de precipitados/aglomerados na região de contato entre as correntes. Esse problema foi então superado utilizando uma corrente aquosa central no dispositivo de focalização hidrodinâmica, a qual era comprimida por duas correntes laterais distintas, uma contendo a quitosana e a outra contendo o agente reticulante; dessa forma, o contato entre as espécies envolvidas foi conduzido de forma mais gradual, o que permitiu uma reticulação mais controlada para a formação de nanopartículas. Uma desvantagem dessa abordagem se refere a diluição das formulações lipossomais ocasionada pela corrente aquosa central.

Assim, por meio de estudos de fluidodinâmica computacional, propõe-se realizar a otimização das vazões de escoamento dessas correntes a fim de minimizar os efeitos diluição e otimizar as condições de mistura. A formação dos lipoplexos se daria, por sua vez, com a mistura entre as correntes alcoólica lateral e a aquosa central; com a difusão da corrente aquosa em direção às correntes laterais, o pDNA negativamente carregado interagiria eletrostaticamente com os lipídeos catiônicos já com os lipossomas recém-formados na região adjacente. Os resultados teóricos de fluidodinâmica aliados aos resultados experimentais de formação de lipoplexos permitiriam conhecer a correlação dos efeitos de variáveis de mistura e de organização coloidal do sistema.

## 8. Referências

- 1 Lentz, T.B.; Gray, S.J.; et al. Viral vectors for gene delivery to the central nervous system. **Neurobiology of Disease**, v. 48, n. 2, p. 353–64, 2011.
- 2 Elzoghby, A.O.; Samy, W.M.; et al. Protein-based nanocarriers as promising drug and gene delivery systems. **Journal of Controlled Release**, v. 161, n. 1, p. 38–49, 2012.
- 3 Roots Analysis **Gene Therapy Market**. 2015.
- 4 Nayerossadat, N.; Ali, P.; et al. Viral and nonviral delivery systems for gene delivery. **Advanced Biomedical Research**, v. 1, n. 1, p. 27, 2012.
- 5 Balazs, D.A.; Godbey, W. Liposomes for Use in Gene Delivery. **Journal of Drug Delivery**, v. 2011, p. 1–12, 2011.
- 6 Lasic, D.D. Spontaneous Vesiculation and Spontaneous Liposomes. **Journal of Liposome Research**, v. 9, n. 1, p. 43–52, 1999.
- 7 ELOUAHABI, A.; RUYSSCHAERT, J. Formation and Intracellular Trafficking of Lipoplexes and Polyplexes. **Molecular Therapy**, v. 11, n. 3, p. 336–347, 2005.
- 8 Whitesides, G.M. The origins and the future of microfluidics. **Nature**, v. 442, n. 7101, p. 368–73, 2006.
- 9 Sackmann, E.K.; Fulton, A.L.; et al. The present and future role of microfluidics in biomedical research. **Nature**, v. 507, n. 7491, p. 181–9, 2014.
- 10 Agirre, M.; Ojeda, E.; et al. New insights into gene delivery to human neuronal precursor NT2 cells: a comparative study between lipoplexes, nioplexes and polyplexes. **Molecular Pharmaceutics**, p. 150925144355008, 2015.
- 11 Lasic, D.D. Applications of Liposomes. v. 1, p. 491–519, 1995.
- 12 Balmayor, E.R.; Azevedo, H.S.; et al. Controlled Delivery Systems: From Pharmaceuticals to Cells and Genes. **Pharmaceutical Research**, v. 28, n. 6, p. 1241–1258, 2011.
- 13 Shan, Y.; Luo, T.; et al. Gene delivery using dendrimer-entrapped gold nanoparticles as nonviral vectors. **Biomaterials**, v. 33, n. 10, p. 3025–3035, 2012.
- 14 Nikcevic, G. Improved transfection efficiency of cultured human cells. **Cell Biology International**, v. 27, n. 9, p. 735–737, 2003.
- 15 Ma, B.; Zhang, S.; et al. Lipoplex morphologies and their influences on transfection efficiency in gene delivery. **Journal of Controlled Release**, v. 123, n. 3, p. 184–194, 2007.

- 16 Rosada, R.S.; Torre, L.; et al. Protection against tuberculosis by a single intranasal administration of DNA-hsp65 vaccine complexed with cationic liposomes. **BMC Immunology**, v. 9, n. 1, p. 38, 2008.
- 17 Mozafari, M.R. LIPOSOMES: AN OVERVIEW OF MANUFACTURING TECHNIQUES. **Drug Delivery**, v. 10, n. October, p. 711 – 719, 2005.
- 18 Felgner, P.L.; Gadek, T.R.; et al. Lipofection: a highly efficient, lipid-mediated DNA-transfection procedure. **Proceedings of the National Academy of Sciences of the United States of America**, v. 84, n. 21, p. 7413–7417, 1987.
- 19 Perrie, Y.; Gregoriadis, G. Liposome-entrapped plasmid DNA: Characterisation studies. **Biochimica et Biophysica Acta - General Subjects**, v. 1475, n. 2, p. 125–132, 2000.
- 20 la Torre, L.G. de; Rosada, R.S.; et al. The synergy between structural stability and DNA-binding controls the antibody production in EPC/DOTAP/DOPE liposomes and DOTAP/DOPE lipoplexes. **Colloids and Surfaces B: Biointerfaces**, v. 73, n. 2, p. 175–184, 2009.
- 21 Balbino, T.A.; Gasperini, A.A.M.; et al. Correlation of the Physicochemical and Structural Properties of pDNA/Cationic Liposome Complexes with Their in Vitro Transfection. **Langmuir**, v. 28, n. 31, p. 11535–11545, 2012.
- 22 Debus, H.; Beck-Broichsitter, M.; et al. Optimized preparation of pDNA/poly(ethylene imine) polyplexes using a microfluidic system. **Lab on a Chip**, v. 12, n. 14, p. 2498, 2012.
- 23 Pozzi, D.; Amenitsch, H.; et al. How lipid hydration and temperature affect the structure of DC-Chol–DOPE/DNA lipoplexes. **Chemical Physics Letters**, v. 422, n. 4-6, p. 439–445, 2006.
- 24 Hsieh, A.T.-H.; Hori, N.; et al. Nonviral gene vector formation in monodispersed picolitre incubator for consistent gene delivery. **Lab on a Chip**, v. 9, n. 18, p. 2638, 2009.
- 25 Morille, M.; Passirani, C.; et al. Progress in developing cationic vectors for non-viral systemic gene therapy against cancer. **Biomaterials**, v. 29, p. 3477–3496, 2008.
- 26 Kuo, J.S.; Chiu, D.T. Controlling mass transport in microfluidic devices. **Annual review of analytical chemistry (Palo Alto, Calif.)**, v. 4, p. 275–296, 2011.
- 27 Bettinger, C.J.; Borenstein, J.T. Biomaterials-based microfluidics for engineered tissue constructs. **Soft Matter**, v. 6, n. 20, p. 4999, 2010.
- 28 Spoorthi, G.; Thakur, R.S.; et al. Process intensification in PSA processes for upgrading synthetic landfill and lean natural gases. **Adsorption**, v. 17, n. 1, p. 121–133, 2011.
- 29 Jahn, A.; Stavis, S.M.; et al. Microfluidic mixing and the formation of nanoscale lipid vesicles. **ACS Nano**, v. 4, n. 4, p. 2077–2087, 2010.
- 30 Lo, C.T.; Jahn, A.; et al. Controlled self-assembly of monodisperse niosomes by microfluidic hydrodynamic focusing. **Langmuir**, v. 26, n. 11, p. 8559–8566, 2010.

- 31 Jahn, A.; Vreeland, W.N.; et al. Controlled Vesicle Self-Assembly in Microfluidic Channels with Hydrodynamic Focusing. **Journal of the American Chemical Society**, v. 126, n. 9, p. 2674–2675, 2004.
- 32 Jahn, A.; Vreeland, W.N.; et al. Microfluidic directed formation of liposomes of controlled size. **Langmuir**, v. 23, n. 11, p. 6289–6293, 2007.
- 33 Zook, J.M.; Vreeland, W.N. Effects of temperature, acyl chain length, and flow-rate ratio on liposome formation and size in a microfluidic hydrodynamic focusing device. **Soft Matter**, v. 6, p. 1352, 2010.
- 34 Balbino, T.A.; Aoki, N.T.; et al. Continuous flow production of cationic liposomes at high lipid concentration in microfluidic devices for gene delivery applications. **Chemical Engineering Journal**, v. 226, p. 423–433, 2013.
- 35 Otten, A.; Köster, S.; et al. Microfluidics of soft matter investigated by small-angle X-ray scattering. **Journal of Synchrotron Radiation**, v. 12, n. 6, p. 745–750, 2005.
- 36 Chee, G.K.; Kang, X.; et al. Delivery of polyethylenimine/DNA complexes assembled in a microfluidics device. **Molecular Pharmaceutics**, v. 6, n. 5, p. 1333–1342, 2009.
- 37 Chen, H.; Zhao, Y.; et al. Co-delivery strategies based on multifunctional nanocarriers for cancer therapy. **Current drug metabolism**, v. 13, n. 8, p. 1087–1096, 2012.
- 38 Koh, C.G.; Zhang, X.; et al. Delivery of antisense oligodeoxyribonucleotide lipopolyplex nanoparticles assembled by microfluidic hydrodynamic focusing. **Journal of Controlled Release**, v. 141, n. 1, p. 62–69, 2010.
- 39 Endres, T.; Zheng, M.; et al. Optimising the self-assembly of siRNA loaded PEG-PCL-IPEI nano-carriers employing different preparation techniques. **Journal of Controlled Release**, v. 160, n. 3, p. 583–591, 2012.
- 40 Ho, Y.P.; Grigsby, C.L.; et al. Tuning physical properties of nanocomplexes through microfluidics-assisted confinement. **Nano Letters**, v. 11, n. 5, p. 2178–2182, 2011.
- 41 Balbino, T.A.; Rodrigues, A.; et al. Microfluidic devices for continuous production of pDNA/ cationic liposome complexes for gene delivery and vaccine therapy. **Colloids and Surfaces B: Biointerfaces**, v. 111, p. 203–210, 2013.
- 42 Simonelli, F.; Maguire, A.M.; et al. Gene Therapy for Leber's Congenital Amaurosis is Safe and Effective Through 1.5 Years After Vector Administration. **Molecular Therapy**, v. 18, n. 3, p. 643–650, 2010.
- 43 Hollander, A.I. den; Roepman, R.; et al. Leber congenital amaurosis: Genes, proteins and disease mechanisms. **Progress in Retinal and Eye Research**, v. 27, n. 4, p. 391–419, 2008.
- 44 Keswani, R.; Su, K.; et al. Efficient in vitro gene delivery by hybrid biopolymer/virus nanobiovectors. **Journal of Controlled Release**, v. 192, p. 40–46, 2014.
- 45 Köping-Höggård, M.; Tubulekas, I.; et al. Chitosan as a nonviral gene delivery system.

- Structure-property relationships and characteristics compared with polyethylenimine in vitro and after lung administration in vivo. **Gene therapy**, v. 8, n. 14, p. 1108–1121, 2001.
- 46 Jesus, M.B. de; Zuhorn, I.S. Solid lipid nanoparticles as nucleic acid delivery system: Properties and molecular mechanisms. **Journal of Controlled Release**, v. 201, p. 1–13, 2015.
  - 47 Toledo, M.A.S.; Janissen, R.; et al. Development of a recombinant fusion protein based on the dynein light chain LC8 for non-viral gene delivery. **Journal of Controlled Release**, v. 159, n. 2, p. 222–231, 2012.
  - 48 McCarthy, H.O.; McCaffrey, J.; et al. Development and characterization of self-assembling nanoparticles using a bio-inspired amphipathic peptide for gene delivery. **Journal of Controlled Release**, v. 189, p. 141–149, 2014.
  - 49 Rehman, Z. ur; Zuhorn, I.S.; et al. How cationic lipids transfer nucleic acids into cells and across cellular membranes: Recent advances. **Journal of Controlled Release**, v. 166, n. 1, p. 46–56, 2013.
  - 50 Muñoz-Úbeda, M.; Misra, S.K.; et al. Why is less cationic lipid required to prepare lipoplexes from plasmid DNA than linear DNA in gene therapy? **Journal of the American Chemical Society**, v. 133, n. 45, p. 18014–18017, 2011.
  - 51 Candiani, G.; Pezzoli, D.; et al. Bioreducible Liposomes for Gene Delivery: From the Formulation to the Mechanism of Action. **PLOS ONE**, v. 5, n. 10, p. e13430, 2010.
  - 52 Masotti, A.; Mossa, G.; et al. Comparison of different commercially available cationic liposome–DNA lipoplexes: Parameters influencing toxicity and transfection efficiency. **Colloids and Surfaces B: Biointerfaces**, v. 68, n. 2, p. 136–144, 2009.
  - 53 Ewert, K.K.; Evans, H.M.; et al. A columnar phase of dendritic lipid-based cationic liposome–DNA complexes for gene delivery: Hexagonally ordered cylindrical micelles embedded in a DNA honeycomb lattice. **Journal of the American Chemical Society**, v. 128, n. 12, p. 3998–4006, 2006.
  - 54 Barreleiro, P.C.A.; May, R.P.; et al. Mechanism of formation of DNA-cationic vesicle complexes. **Faraday Discussions**, v. 122, p. 191–201, 2003.
  - 55 Belliveau, N.M.; Huft, J.; et al. Microfluidic Synthesis of Highly Potent Limit-size Lipid Nanoparticles for In Vivo Delivery of siRNA. **Molecular therapy. Nucleic acids**, v. 1, p. e37, 2012.
  - 56 Muñoz-Úbeda, M.; Rodríguez-Pulido, A.; et al. Gene vectors based on DOEPC/DOPE mixed cationic liposomes: a physicochemical study. **Soft Matter**, v. 7, n. 13, p. 5991, 2011.
  - 57 Balbino, T.A.; Correa, G.S.C.; et al. Physicochemical and in vitro evaluation of cationic liposome , hyaluronic acid and plasmid DNA as pseudo-ternary complexes for gene delivery. v. 484, p. 262–270, 2015.

- 58 Muñoz-Úbeda, M.; Misra, S.K.; et al. How does the spacer length of cationic gemini lipids influence the lipoplex formation with plasmid DNA? physicochemical and biochemical characterizations and their relevance in gene therapy. **Biomacromolecules**, v. 13, n. 12, p. 3926–3937, 2012.
- 59 Naher, S.; Orpen, D.; et al. Effect of micro-channel geometry on fluid flow and mixing. **Simulation Modelling Practice and Theory**, v. 19, n. 4, p. 1088–1095, 2011.
- 60 Oliveira, C.L.P. & Pedersen, J.S. (2015). SuperSAXS. Disponível em: <https://social.stoa.usp.br/crislpo/supersaxs-package>.
- 61 Gasperini, A.A.M.; Puentes-Martinez, X.E.; et al. Association between cationic liposomes and low molecular weight hyaluronic acid. **Langmuir**, v. 31, n. 11, p. 3308–17, 2015.
- 62 Oliveira, C.L.P.; Gerbelli, B.B.; et al. Gaussian deconvolution: a useful method for a form-free modeling of scattering data from mono- and multilayered planar systems. **Journal of Applied Crystallography**, v. 45, n. 6, p. 1278–1286, 2012.
- 63 Caillé, A. X-Ray Scattering by Smectic-A Crystals. **CR Acad Sci Paris Sér B**, v. 274, p. 891, 1972.
- 64 Zhang, R.; Suter, R.M.; et al. Theory of the structure factor of lipid bilayers. **Physical Review E**, v. 50, n. 6, p. 5047–5060, 1994.
- 65 Pozzi, D.; Marchini, C.; et al. Mechanistic understanding of gene delivery mediated by highly efficient multicomponent envelope-type nanoparticle systems. **Molecular Pharmaceutics**, v. 10, n. 12, p. 4654–4665, 2013.
- 66 Dalgleish, D.G.; Hallett, F.R. Dynamic light scattering: applications to food systems. **Food Research International**, v. 28, n. 3, p. 181–193, 1995.
- 67 Murphy, R.M. Static and dynamic light scattering of biological macromolecules: what can we learn? **Current Opinion in Biotechnology**, v. 8, n. 1, p. 25–30, 1997.
- 68 Balbino, T.A.; Correa, G.S.C.; et al. Physicochemical and in vitro evaluation of cationic liposome, hyaluronic acid and plasmid DNA as pseudo-ternary complexes for gene delivery. **Colloids and Surfaces A: Physicochemical and Engineering Aspects**, v. 484, p. 262–270, 2015.
- 69 Misra, Santosh K, Muñoz-Úbeda, Mónica, Datta, Sougata, Barrán-Berdón, Ana L, Aicart-Ramos, Clara, Castro-Hartmann, Pablo, Kondaiah, Paturu, Junquera, Elena, Bhattacharya, Santanu, Aicart, E. Effects of a Delocalizable Cation on the Headgroup of Gemini Lipids on the Lipoplex-Type Nanoaggregates Directly Formed from Plasmid DNA. **Biomacromolecules**, v. 14, p. 3951–3963, 2013.
- 70 Kesharwani, P.; Gajbhiye, V.; et al. A review of nanocarriers for the delivery of small interfering RNA. **Biomaterials**, v. 33, n. 29, p. 7138–7150, 2012.
- 71 Casadei, B.R.; Domingues, C.C.; et al. Direct visualization of the action of triton X-100 on giant vesicles of erythrocyte membrane lipids. **Biophysical Journal**, v. 106, n. 11, p.

2417–2425, 2014.

- 72 Michelon, M.; Mantovani, R.A.; et al. Structural characterization of  $\beta$ -carotene-incorporated nanovesicles produced with non-purified phospholipids. **Food Research International**, v. 79, p. 95–105, 2016.
- 73 Chou, T. Current Application of Lipid- and Surfactant-based Vesicles for Cosmetics : A Review. p. 1035–1044, 2015.
- 74 Bally, M.B.; Harvie, P.; et al. Biological barriers to cellular delivery of lipid-based DNA carriers. **Advanced Drug Delivery Reviews**, v. 38, n. 3, p. 291–315, 1999.
- 75 Suk, J.S.; Xu, Q.; et al. PEGylation as a strategy for improving nanoparticle-based drug and gene delivery. **Advanced Drug Delivery Reviews**, 2015.
- 76 Pattni, B.S.; Chupin, V. V.; et al. New Developments in Liposomal Drug Delivery. **Chemical Reviews**, p. 150526165100008, 2015.
- 77 Patil, Y.P.; Jadhav, S. Novel methods for liposome preparation. **Chemistry and Physics of Lipids**, v. 177, p. 8–18, 2014.
- 78 Hood, R.R.; DeVoe, D.L. High-Throughput Continuous Flow Production of Nanoscale Liposomes by Microfluidic Vertical Flow Focusing. **Small**, p. n/a–n/a, 2015.
- 79 Hood, R.R.; DeVoe, D.L.; et al. A facile route to the synthesis of monodisperse nanoscale liposomes using 3D microfluidic hydrodynamic focusing in a concentric capillary array. **Lab on a chip**, v. 14, n. 14, p. 2403–9, 2014.
- 80 Swaay, D. van; deMello, A. Microfluidic methods for forming liposomes. **Lab on a Chip**, v. 13, n. 5, p. 752, 2013.
- 81 Sekhon, B.S.; Kamboj, S. Microfluidics Technology for Drug Discovery and Development - An Overview. **International Journal**, v. 2, n. 1, p. 804–809, 2010.
- 82 Mijajlovic, M.; Wright, D.; et al. Microfluidic hydrodynamic focusing based synthesis of POPC liposomes for model biological systems. **Colloids and Surfaces B: Biointerfaces**, v. 104, p. 276–281, 2013.
- 83 Hood, R.R.; Shao, C.; et al. Microfluidic synthesis of PEG- and folate-conjugated liposomes for one-step formation of targeted stealth nanocarriers. **Pharmaceutical Research**, v. 30, n. 6, p. 1597–1607, 2013.
- 84 Hood, R.R.; Kendall, E.L.; et al. Microfluidic Formation of Nanoscale Liposomes for Passive Transdermal Drug Delivery. p. 1–4, 2013.
- 85 Costa, A.P.; Xu, X.; et al. Liposome Formation Using a Coaxial Turbulent Jet in Co-Flow. **Pharmaceutical Research**, v. 33, n. 2, p. 404–416, 2016.
- 86 Hood, R.R.; Vreeland, W.N.; et al. Microfluidic remote loading for rapid single-step liposomal drug preparation. **Lab on a Chip**, p. 3359–3367, 2014.

- 87 Ginn, B.T.; Steinbock, O.; et al. Polymer Surface Modification Using Microwave-Oven-Generated Plasma. p. 8117–8118, 2003.
- 88 Wi, R.; Oh, Y.; et al. Formation of liposome by microfluidic flow focusing and its application in gene delivery. **Korea Australia Rheology Journal**, v. 24, n. 2, p. 129–135, 2012.
- 89 Marsh, D. Handbook of Lipid Bilayers, 2a. edição, Boca Raton, FL. **CRC press**, p. 1145, 2013.
- 90 Ingólfsson, H.I.; Andersen, O.S. Alcohol's Effects on Lipid Bilayer Properties. **Biophysical Journal**, v. 101, n. 4, p. 847–855, 2011.
- 91 Lukyanov, A.N.; Torchilin, V.P. Micelles from lipid derivatives of water-soluble polymers as delivery systems for poorly soluble drugs. **Advanced Drug Delivery Reviews**, v. 56, n. 9, p. 1273–1289, 2004.
- 92 Edwards, K.; Johnsson, M.; et al. Preparations of Small Unilamellar Liposomes. **Biophysical Journal**, v. 73, n. 1, p. 258–266, 1997.
- 93 Evans, D.F.; Wennerstrom Hakan **The colloidal domain: where physics, chemistry, biology, and technology meet**. Wiley-VCH, 2a. edição, p. 672, 1999.
- 94 Myers, D. **Surfaces, interfaces, and colloids: principles and applications**. John Wiley and Sons, 1999.
- 95 Pradhan, P.; Guan, J.; et al. A facile microfluidic method for production of liposomes. **Anticancer Research**, v. 28, n. 2 A, p. 943–947, 2008.
- 96 Mintzer, M. a; Simanek, E.E. Nonviral Vectors for Gene Delivery. **Chemical Reviews**, v. 109, n. 979, p. 259–302, 2008.
- 97 Schuster, B.S.; Ensign, L.M.; et al. Particle tracking in drug and gene delivery research: State-of-the-art applications and methods. **Advanced Drug Delivery Reviews**, v. 91, p. 70–91, 2015.
- 98 Tian, H.; Chen, J.; et al. Nanoparticles for gene delivery. **Small (Weinheim an der Bergstrasse, Germany)**, v. 9, n. 12, p. 2034–44, 2013.
- 99 Allen, T.M.; Cullis, P.R. Liposomal drug delivery systems: From concept to clinical applications ☆. **Advanced Drug Delivery Reviews**, v. 65, n. 1, p. 36–48, 2013.
- 100 Wang, H.; Liu, Y.; et al. Multifunctional TiO<sub>2</sub> nanowires-modified nanoparticles bilayer film for 3D dye-sensitized solar cells. **Optoelectronics and Advanced Materials, Rapid Communications**, v. 4, n. 8, p. 1166–1169, 2010.
- 101 Mortazavi, S.M.; Mohammadabadi, M.R.; et al. Preparation of liposomal gene therapy vectors by a scalable method without using volatile solvents or detergents. **Journal of Biotechnology**, v. 129, n. 4, p. 604–613, 2007.
- 102 Weisman, S.; Hirsch-lerner, D.; et al. Nanostructure of Cationic Lipid-Oligonucleotide

Complexes. **Biophysical Journal**, v. 87, n. 1, p. 609–614, 2004.

- 103 Feng, Q.; Sun, J.; et al. Microfluidics-mediated assembly of functional nanoparticles for cancer-related pharmaceutical applications. **Nanoscale**, v. Advance Ar, 2016.
- 104 Faustino, V.; Catarino, S.O.; et al. Biomedical microfluidic devices by using low-cost fabrication techniques: A review. **Journal of Biomechanics**,
- 105 Tian, W.-C.; Finehout, E. **Microfluidics for Biological Applications**. Springer, 2009.
- 106 Belliveau, N.M.; Huft, J.; et al. Microfluidic assembly of lipid-based oligonucleotide nanoparticles. **Journal of Controlled Release**, v. 12, n. 3, p. 62–69, 2012.
- 107 Balbino, T.A.; Sera, J.M.; et al. Microfluidic Assembly of pDNA/Cationic Liposome Lipoplexes with High pDNA Loading for Gene Delivery. **Langmuir**, v. 32, p. 1799–1807, 2016.
- 108 Boussif, O.; Lezoualc'h, F.; et al. A versatile vector for gene and oligonucleotide transfer into cells in culture and in vivo: Polyethylenimine. **Proc. Natl. Acad. Sci. USA**, v. 92, n. August, p. 7297–7301, 1995.
- 109 Jesus, M.B. de; Radaic, A.; et al. Inclusion of the Helper Lipid Dioleoyl-Phosphatidylethanolamine in Solid Lipid Nanoparticles Inhibits Their Transfection Efficiency. **Journal of Biomedical Nanotechnology**, v. 10, n. 2, p. 355–365, 2014.
- 110 Sln, N.; Radaic, A.; et al. Factorial Design and Development of Solid Lipid. **Journal of Nanoscience and Nanotechnology**, v. 14, n. xx, p. 1–8, 2014.
- 111 Ismagilov, R.F.; Stroock, A.D.; et al. Experimental and theoretical scaling laws for transverse diffusive broadening in two-phase laminar flows in microchannels. **Applied Physics Letters**, v. 76, n. 2000, p. 2376–2378, 2000.
- 112 Scholz, C.; Wagner, E. Therapeutic plasmid DNA versus siRNA delivery: Common and different tasks for synthetic carriers. **Journal of Controlled Release**, v. 161, n. 2, p. 554–565, 2012.
- 113 Rosada, R.S.; Silva, C.L.; et al. Effectiveness, against tuberculosis, of pseudo-ternary complexes: Peptide-DNA-cationic liposome. **Journal of Colloid and Interface Science**, v. 373, n. 1, p. 102–109, 2012.
- 114 Huang, Y.; Wang, X.; et al. Systemic Administration of siRNA via cRGD-containing Peptide. **Scientific Reports**, v. 5, p. 1–15, 2015.

## Anexo I. Licença de publicação de artigo na tese

Autorização da *America Chemical Society* para a inclusão do artigo publicado em *Langmuir*, 2016, 32 (7), 1799–1807, na tese de doutorado.

 **Copyright Clearance Center**

 **RightsLink®**

[Home](#) [Create Account](#) [Help](#)

 **ACS Publications**  
Most Trusted. Most Cited. Most Read.

**Title:** Microfluidic Assembly of pDNA/Cationic Liposome Lipoplexes with High pDNA Loading for Gene Delivery

**Author:** Tiago A. Balbino, Juliana M. Serafin, Antonio A. Malfatti-Gasperini, et al

**Publication:** Langmuir

**Publisher:** American Chemical Society

**Date:** Feb 1, 2016

Copyright © 2016, American Chemical Society

[LOGIN](#)  
If you're a [copyright.com](#) user, you can login to RightsLink using your [copyright.com](#) credentials. Already a [RightsLink](#) user or want to [learn more?](#)

### PERMISSION/LICENSE IS GRANTED FOR YOUR ORDER AT NO CHARGE

This type of permission/license, instead of the standard Terms & Conditions, is sent to you because no fee is being charged for your order. Please note the following:

- Permission is granted for your request in both print and electronic formats, and translations.
- If figures and/or tables were requested, they may be adapted or used in part.
- Please print this page for your records and send a copy of it to your publisher/graduate school.
- Appropriate credit for the requested material should be given as follows: "Reprinted (adapted) with permission from (COMPLETE REFERENCE CITATION). Copyright (YEAR) American Chemical Society." Insert appropriate information in place of the capitalized words.
- One-time permission is granted only for the use specified in your request. No additional uses are granted (such as derivative works or other editions). For any other uses, please submit a new request.

[BACK](#)[CLOSE WINDOW](#)

Copyright © 2016 [Copyright Clearance Center, Inc.](#) All Rights Reserved. [Privacy statement.](#) [Terms and Conditions.](#) Comments? We would like to hear from you. E-mail us at [customer@copyright.com](mailto:customer@copyright.com)